Title
TRANSPARENT HEAT-MIRROR MATERIALS AND DEPOSITION TECHNOLOGY

Authors
Lampert, CM.
Seltowitz, S.

Publication Date
1982-07-01

Lawrence Berkeley Laboratory
UNIVERSITY OF CALIFORNIA

ENERGY & ENVIRONMENT DIVISION

Papers selected from the proceedings of the International Society of Optical Engineering (SPIE) Conference on Optical Coatings for Energy Efficiency and Solar Applications and the Conference on Optical Thin Films, Los Angeles, CA, January 25-29, 1982

TRANSPARENT HEAT-MIRROR MATERIALS AND DEPOSITION TECHNOLOGY

July 1982

ENERGY AND ENVIRONMENT DIVISION

Prepared for the U.S. Department of Energy under Contract DE-AC03-76SF00098

DISCLAIMER

LBL-15258
EEB-W-82-12
W-134

Papers selected from the proceedings of the International Society for Optical Engineering (SPIE) Conference on Optical Coatings for Energy Efficiency and Solar Applications and the Conference on Optical Thin Films, Los Angeles CA, January 25-29, 1982.

TRANSPARENT HEAT-MIRROR MATERIALS AND DEPOSITION TECHNOLOGY

compiled by:

Carl M. Lampert
Materials and Molecular Research Division and
Energy and Environment Division

and

Stephen Selkowitz
Energy and Environment Division

Lawrence Berkeley Laboratory
University of California
Berkeley CA 94720 USA

July 1982

This work was supported by the Assistant Secretary for Conservation and Renewable Energy, Office of Building Energy Research and Development, Building Systems Division of the U.S. Department of Energy under Contract No. DE-AC03-76SF00098.

INTRODUCTION

This work consists of selected papers on architectural coatings from two seminars held by the International Society for Optical Engineering (SPIE) January 25 - 29, 1982 in Los Angeles, California. The papers were selected from Optical Coatings for Energy Efficiency and Solar Applications, Vol. 324, edited by C.M. Lampert and Optical Thin Films, Vol. 325, edited by R.I. Seddon. All papers are reproduced by permission of the authors and SPIE. Full proceedings can be purchased from SPIE, PO Box 10, Bellingham, WA 98227-0010 USA.

This collected work represents a sampling of the research and development interest in transparent heat-mirror films for mainly architectural uses. The heat-mirror coatings discussed range from single-layer semiconductors to dielectric/metal/dielectric multilayers. New ternary compounds and nitride films are also introduced. Properties of heat mirrors deposited on glass and polyester substrates are discussed. The final section deals with large-scale processing, which is the link between research and development and mass production. Details of large physical-vapor deposition, chemical-vapor deposition, and roll-coating systems are presented.

TRANSPARENT HEAT-MIRROR MATERIALS

and

DEPOSITION TECHNOLOGY

Contents

Durable innovative solar optical materials—the international challenge

Carl M. Lampert
Materials and Molecular Research Division and Energy Efficient Buildings Program
Lawrence Berkeley Laboratory, University of California
1 Cyclotron Road, Bldg. 62-235, Berkeley, California 94720

Abstract

A variety of optical coatings are discussed in the context of solar energy utilization. Well known coatings such as heat mirrors, selective absorbers, and reflective films are covered briefly. Emphasis is placed on the materials limitations and design choices for various lesser known optical coatings and materials. Physical and optical properties are detailed for protective antireflection films, fluorescent concentrator materials, holographic films, cold mirrors, radiative cooling surfaces, and optical switching films including electrochromic, thermochromic, photochromic, and liquid crystal types. For many of these materials research is only now being considered, and various design and durability issues must be addressed.

Introduction

Optical coatings play a vital role in solar energy conversion. A number of well known coatings can be classified as heat mirrors, selective absorbers and reflective materials. But there remain numerous less known films and materials that have significant consequence to solar energy development. The deployment of such films in active and passive solar energy conversion, photovoltaic, energy efficient windows, and mixed designs offers improvement in efficiency and allows new designs to be introduced. It is the function of this study to expand the horizon of innovation by considering new materials, concepts, and techniques that can manipulate solar energy as a form of heat, light, and electrical power. Specific coatings and materials will be covered under individual sections. Such materials are not without shortcomings. The solution to materials science and design problems is the responsibility of a number of scientists and engineers working in many countries and various fields. It is their commitment that will further this technology.

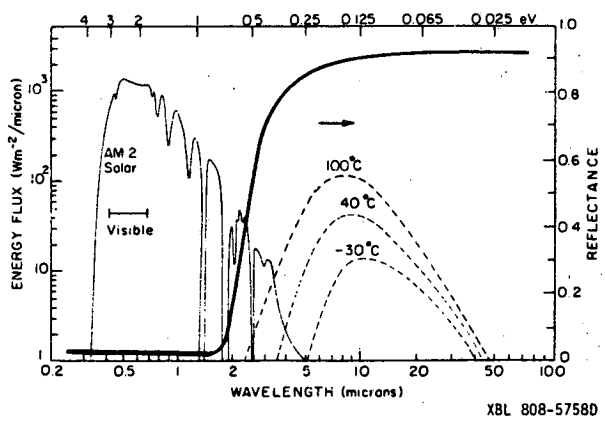

Figure 1. Spectrum of solar radiation (airmass 2) shown with three blackbody spectral distributions (-30°C, 40°C, 100°C). Superimposed is the idealized selective reflectance of a heat mirror or solar-selective absorber.

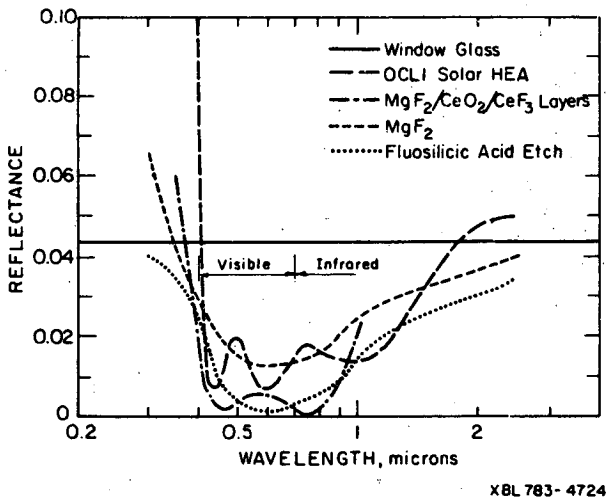

Figure 2. Reflectance of various antireflection treatments for glass.

Transparent conductive films

Transparent conductive coatings can be utilized for four major applications in solar energy conversion. They can be used as low-emittance coatings for windows and solar collectors, as electrodes for photovoltaic and photoelectrochemical cells, and as active elements in heterojunction and oxide photovoltaics. The use of heat mirrors for architectural windows[1,2,3] and for solar collectors[4,5,6] is dicussed extensively elsewhere. The relationship between the solar spectrum, blackbody spectra, and idealized selective reflectors is shown in Figure 1. Heat mirrors fall into two classes based on design: single-layer doped semiconductors, and metal/dielectric interference films. Examples of the former are SnO_2:F, In_2O_3:Sn, Cd_2SnO_4, and CdO. Illustrative systems of the latter might be based on TiO_2/metal, Al_2O_3/metal, or ZnS/metal alternations. Photovoltaics and photoelectrodes can utilize only single-layer materials having high electrical conductivity. Several reviews cover the properties of doped transparent semiconductors.[7,8,9]

Active materials research areas center around deposition processes and materials microstructural-property relationships. Development of cost-effective techniques to deposit such films on glass and plastic film materials is of major concern.[10] Eliminating post-annealing treatments, to increase conductivity, would reduce expense. Improvement in chemical dip coating processes and understanding of hydrolysis (CVD) chemistry as it relates to film properties through deposition parameters are important research areas. Further development of plasma-assisted physical vapor deposition (PVD) is critical to room-temperature deposition on thin plastic film substrates. Lower deposition temperatures along with near-atmospheric pressures should be utilized for refined coating processes. An understanding of doping and defect properties in semiconductor films is necessary, with emphasis on durability and stability. There is also room for basic materials research of new binary and ternary compounds including boride, nitride, oxide, and carbide systems which may be better suited to simple deposition. Existing high-rate, large-scale deposition techniques for heat mirrors should be examined carefully for cost-effectiveness.

Solar absorbers

Solar absorber research is dominated by studies on selective surfaces and paints. Absorbers for solar collectors have been one of the most active research fields in solar coatings in the last few years. This work has produced a better understanding of one of the most popular coatings, black chrome. Its chemistry, microstructure, degradation lifetime, and thermal limitations have been explored in detail.[11,12] Studies of chemical conversion and native oxide coatings have uncovered new absorbers. The development of stick-on solar absorber foils has allowed versatility in solar designs.[13] The study of high-temperature selective absorbers is quite challenging. Large-scale, high-temperature conversion requires an absorber material which will remain stable and have consistant properties under high solar flux and cyclic temperature extremes. One promising coating is the refractory metal-oxide, graded-index coating in which simple materials composition variation is responsible for the graded optical index. The development of a selective spray-on or dip paint is also an area of active research. The challenge is to find a binder material that is devoid of infrared absorption bands within the region of the absorber's blackbody operating temperature response. This binder must be sufficiently strong to withstand the operational environment. Spraying or dipping techniques also must be optimized to assure consistancy and uniformity of properties.

Reflector materials

Reflector materials for solar energy uses fall into two distinct categories: front-surface and back-surface. They also differ according to method of deposition of the metallic aluminum, silver, or alloy layer and whether the host material is flexible. Front-surface mirrors suffer from abrasion, atmospheric corrosion, and delamination. A protective, durable overcoating material is required. For second-surface mirrors produced by the wet chemical process there is a lack of understanding of the various interfacial chemical reactions. For example, certain mirrors degrade rapidly while others last for several years. For both types of reflectors an understanding of the stability between metal/polymer and metal/glass mirrors is a significant issue. Dirt and dust can be responsible for considerable decline of efficiency of reflector surfaces. Techniques to limit dusting and washing of surfaces need to be devised. Many of these concerns were addressed at a recent solar materials workshop.[14]

Antireflective and protective overcoatings

Antireflective coatings, if designed with proper compounds, can also serve as durable overcoating materials. For photovoltaics some polymeric and elastomeric protective coatings can be effective antireflective materials if the coating is thin enough, although protective coatings are generally used in thick-film form. Popular protective materials are silicones, fluorocarbons, halocarbons, and acrylic resins. One major need is to develop a coating that serves both protective and antireflective functions. Some polymers having a low refractive index (n) can antireflect glass (n = 1.5) and other high-index plastics. Dispersions of fluorinated ethylene propylene (n = 1.34) can be used for this purpose. Polyvinyl fluoride (n = 1.46) can be antireflected by dipping in acetophenon. Graded-index films present a versatile range of coatings having refractive indices that are not readily found. Fluorosilicic acid can give a graded-index,

antireflective coating to glass. (See Figure 2.) It primarily roughens the surface by etching out small pores, in nonsilica regions.[16,15] Silica coatings deposited from sodium silicate or collodial silica can be used for acrylic, polycarbonate, and several glasses. A film for polyethylene terephthalate (polyester) and glass materials has been devised.[17,18] The coating is made from a steam-oxidized aluminum film; this processing causes a needle-like structure of aluminum hydroxide [AlO(OH)] to form. A polyester film treated in this fashion can serve in glazing applications where solar transmission must be optimum.[19] (See Figure 3.) Inorganic thin films have been used for a wide range of single and multiple interference coating applications. Compounds such as MgF_2, CeO_2 CeF_2, SiO, SiO_2, and TiO_2 in various combinations have been used for antireflection applications. Other than the traditional PVD techniques, a number of oxides can be dip-coated onto optical substrates. Coatings of hot hydrolysed metal alkoxides can be polycondensed, forming oxides of Al, In, Si, Ti, Fr, Sn, Pb, Ta, Cr, Fe, Ni, Co, and some rare earths.[20] A similar method known as the sol-gel process has formed mixed TiO_2-SiO_2 antireflective films on silicon[21] and black chrome. Diamond-like (i - Carbon) transparent coatings have been used for antireflective films. They are formed from plasma decomposition of hydrocarbons and ion beam deposition.[22] Coatings of about n = 1.9 can be made which are suited to photovoltaics.

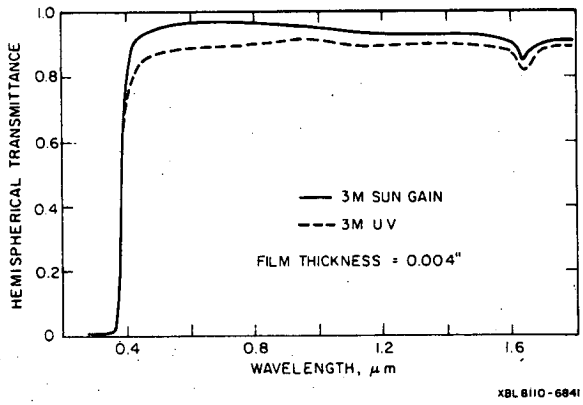

Figure 3. Hemispherical transmission of antireflected 3M Sungain polyester film compared to uncoated substrate.

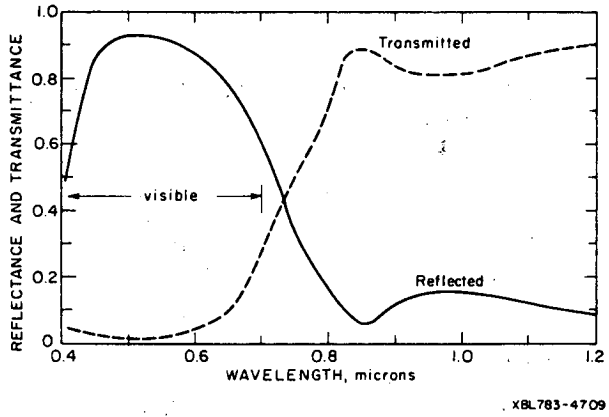

Figure 4. Spectral transmittance for OCLI greenhouse cold mirror.

Cold-mirror and spectral splitting coatings

Cold-mirror coatings are selective transmission films having optical properties directly opposite to those of the heat mirror. Cold mirrors exhibit high reflectance in the visible region and transmit highly in the infrared. Generally such coatings are all-dielectric, for example ZnS/MgF_2 and TiO_2/SiO_2 hard-layer films.[23] These coatings are useful for separating light and heat and might be utilized in a combined thermal-photovoltaic system. Another application for these films is for greenhouses.[24] Plants require only a range of wavelengths 0.3 - 0.75 microns; the remainder of the solar spectrum is unused. This extra portion can be separated as heat and used to warm the greenhouse. A baffle-type greenhouse utilizing both cold-mirror and reflective coatings is illustrated in Figure 4.

Spectral splitting coatings are used to separate the solar spectrum into various bands of wavelengths. These bands are matched to a particular photovoltaic response.[25] A system might consist of a series of cold mirrors where the transition from reflecting to transmitting moves to longer wavelengths for each sucessive spectral splitting cell. In this way the solar spectrum could be partitioned from high to low energies. A series of heat mirrors could also be used, but the solar spectrum would be partitioned from low to high energy as the heat-mirror transition wavelength became shorter.

Fluorescent concentrator materials

The principle of fluorescent concentrators consists of a transparent plate which has been doped with fluorescent dye molecules. Incident light corresponding to the fluorescent absorption will be captured and emitted isotropically. Due to the index of refraction difference between the plate and surrounding media, a large fraction of light will be trapped and transmitted to the edges of the plate by total internal reflection. By silvering some of the edges, a greater amount of light can be funneled to a favored edge where tuned photovoltaics, for example, may be placed. The amount of light guided in a plate to that lost by transmission out of the sheet, according to $G=(n^2-1)^{1/2}/n$, is 75% for a sheet with n = 1.5. By using multiple plates various portions of the solar spectrum can be utilized. For each level of collector plate a higher absorption level is used so the innermost plate absorbs the highest energy. With the use of a backup mirror reemitted energy can be absorbed by lower-energy fluorescent levels. (See Figure 5.) The advantages of using a fluorescent plate for concentration are that the concentration ratio is high (10 -100), the concentrator works even in low insolation or diffuse sky conditions, and no tracking of the sun is required.

Also, there is less heat dissipation in photovoltaic systems and high efficiency at low insolation levels. For thermal collectors using fluorescent concentrators, efficiencies of 42-59% have been estimated. For purely photovoltaic conversion overall efficiency of 32% for a four-plate system has been calculated.[26,27]

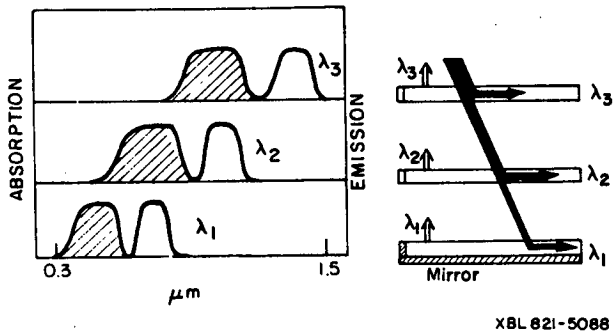

Figure 5. Fluorescent concentrator design showing hypothetical absorption and emission spectra.

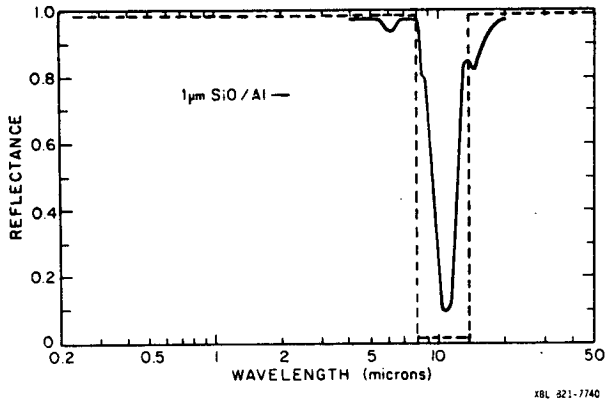

Figure 6. Spectral reflectance of 1 micron SiO/Al film for radiative cooling.[19] Idealized properties are shown by broken line.

Materials for fluorescent concentrators have favored polymethyl methacralate (PMMA) for converting wavelengths shorter than 1 micron. Good materials for the infrared need to be devised as glazings for cover plates. Fluorescent dyes need to be custom tailored for solar collectors as they have been for lasers. The dyes should have high quantum efficiency and low self-absorption with absorption and emission spectra well separated in energy. Many existing dyes have overlapping spectra. Dyes need to be chemically resistant to UV decomposition. New materials can be used such as ligands containing rare earth ions and mixed organic systems with nonradiative energy transfer between different molecules. The types of fluorescent materials used for experimentation fall into the category of rare-earth doped laser glass and laser dyes. Rhodamine 6G in PMMA has W_a = 525 nm W_e = 575nm and ED2 Ne-doped glass has W_a = 500-900nm W_e = 1060nm. A dye-doped fluorescent thin film could also be devised as a substrate coating. This design could minimize reabsorption by the dye. Furthermore, a broader coverage in tailoring the dye emission spectrum can be obtained by mixing dye materials in such a way that one emission band corresponds to the absorption band of another. Rhodamine 6G and Coumarin 6 dyes have been used in this fashion.[28]

Radiative cooling materials

The earth naturally cools itself by radiative transfer through high-transmission windows in the atmosphere to the cold troposhere. This effect is most noticeable on clear nights. A significant atmospheric window occurs from 8-13 microns wavelength. One could conceivably design an upward-facing surface which would emit over this wavelength range. A material would have to have high reflectance for 0.3-50 microns, excluding the 8-13 microns region. In the 8-13 micron region the material would have to have a very low reflectance or high emittance. It is theoretically possible for such a surface to reach 50 °C below ambient, with typical temperatures about 15 °C below ambient. Temperatures below the dew point should be avoided.

Materials used for radiative cooling include SiO/Al (see Figure 6) and polymer-coated metals. Polymers such as polyvinylchloride (PVC), polyvinylfluoride (PVF, Tedlar), and poly-4-methylpentene(TPX) have been suggested.[29] A radiative cooling device can also consist of two separate materials, a selective cover and an emitter. Infrared emitters are easy to find, but the selective cover is a challenge. Materials like polyethylene with coatings of Te or dispersions of TiO_2 have been experimented with. The overall field of radiative cooling has just recently regained interest. Materials need to be designed that not only satisfy the optical requirements but are also resistant to weathering and solar degradation. For the materials investigated thus far, the emittance of the coatings need to be optimized to take full advantage of the 8-13 micron window. Finally, methods of coupling these surfaces with heat-transfer media need to be devised.

Optical shutter materials

Optical shutter materials or devices can be used for energy-efficient windows or other passive solar uses. An optical shutter offers a drastic change in optical properties under the influence of light, heat, or electrical field or by their combination. The change can be, for example, a transformation from a material that is highly solar transmitting to one which is reflecting either totally or partly over the solar spectrum. A lesser choice might be a film which converts from highly transmitting to highly absorbing. In application an optical shutter coating could control the flow of light and/or heat in and out of a

building window, thus performing an energy management function. Depending upon design such a coating device could also control light and thermal levels for lighting, heating, and cooling functions. Generally, this idea represents future research and design areas. Phenomena of interest to optical shutters are electrochromic, photochromic, thermochromic, and liquid crystal processes.

Electrochromic devices

Electrochromism is exhibited by a large number of materials both inorganic and organic. The electrochromic effect is of current research interest mainly because of its application to electronic display devices. However, the use of electrochromic devices for windows has been addressed.[30] The electrochromic effect, in essence, is a material which exhibits intense color change due to the formation a colored compound. This compound is formed from an ion insertion reaction induced by an instanteous applied electric field. The reaction might follow: $MO_x + yA^+ + ye \leftrightarrow A_yMO_x$.

There are three categories of electrochromic materials: transition metal oxides, organic compounds, and intercalated materials. The materials which have gained the most research interest are WO_3, MoO_3, and IrO_x films. These compounds, among other transition metal oxides, are the subject of a timely review.[31] Organic electrochromics are based on the liquid viologens, anthraquinones, diphthalocyanines, and tetrathiafulvalenes. With organics, coloration of a liquid is achieved by an oxidation-reduction reaction, which may be coupled with a chemical reaction. Intercalated electrochromics are based on graphite and so are not useful for window applications.

A solid-state window device can be fabricated containing the elements shown in Figure 7: transparent conductors (TC), an electrolyte or fast-ion conductor (FIC), counter electrode (CE), and electrochromic layer (EC). Much research is needed to develop a usable panel, better electrochromic materials with high cycle lifetimes, and short response times. Certainly fast-ion conductors and electrolytes also require study.

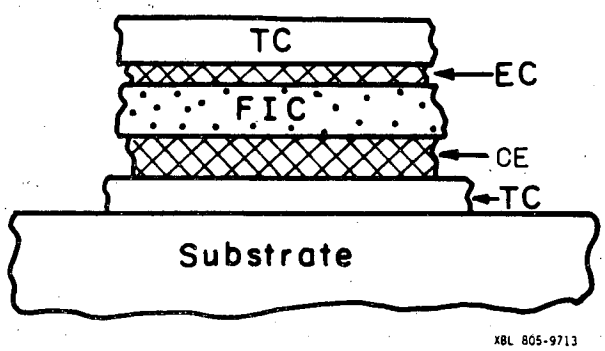

Figure 7. Model of solid-state electrochromic cell.

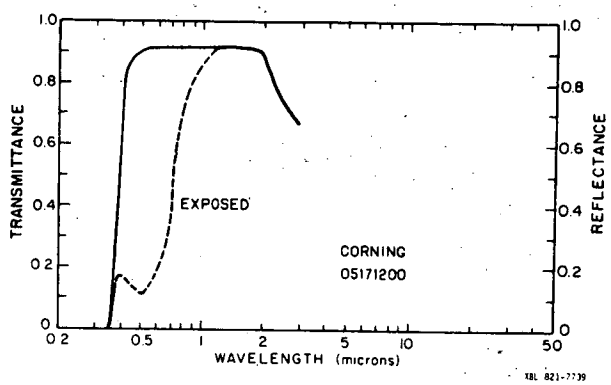

Figure 8. Example of spectral transmittance for photochromic glass showing light and dark responses.

Photochromic materials

Photochromic materials change their optical properties or color with light intensity. Generally, photochromic materials are energy-absorptive. Basically, the phenonemon is the reversible change of a single chemical species between two energy states, having different absorption spectra. This change in states can be induced by electromagnetic radiation. Photochromic materials have been reviewed.[32,33] Probably the best known is photochromic glass used in eyeglasses and goggles. Photochromic materials are classified as organics, inorganics, and glasses. Within the organics are stereoismers, dyes, and polynuclear aromatic hydrocarbons. The inorganics include ZnS, TiO_2, Li_3N, HgS, HgI_2, HgCNS, and alkaline earth sulfides and titanates, with many of these compounds requiring traces of heavy metal or a halogen to be photochromic. Glasses that exhibit photochromism are Hackmanite, Ce, and Eu doped glasses (which are ultraviolet sensitive), and silver halide glasses (which include other metal oxides). The silver halide glasses color by color-center formation from an AgCl crystalline phase. The typical response for a photochromic glass is shown in Figure 8.

For windows, development work is needed to ultilize commercially available silver halide glasses. Other deposition of such glasses as film compounds requires more research for possible utilization as films and suspensions in polymeric materials.

Reversible thermochromic materials

Many thermochromic materials are used as nonreversible temperature indicators, but for an optical shutter one can consider only the reversible materials, although their actual cyclic lifetime is limited by nonreversible secondary reactions. Organic materials such as spiropyrans, anils, polyvinyl acetal resins, and hydrozides are examples of thermochromism. Inorganic materials include HgI_2,AgI, Ag_2HgI_4, Cu_2,HgI_4, $SrTiO_3$ Cd_2P_3Cl, and Copper, Tin, and Cobalt, complexes. Research areas are fairly wide open; some work is suggested on compounds which exhibit both photo and thermochromism.[34] Identification of limiting reactions, development of film materials, and polymeric and glassy dispersions are necessary.

Liquid crystals

Liquid crystals are actively used for electronic and temperature displays. The greatest part of research has gone into these areas. Liquid crystals can be in one of three structural organic mesophases: smectic, nematic, or twisted nematic (cholesteric). The most widely used is the twisted nematic.[35] From a materials standpoint liquid crystals are based on azo-azoxy, esters, biphenyls, and Schiff bases. Also passive liquid crystal films can be solidified into solid films by polymerization, giving preset optical properties. A liquid crystal in the form of a light valve could be used to modulate transmittance and reflectance of light entering the cell. Unlike the electrochromic device, a liquid crystal would require continuous power to stay reflective. Both cost and fabrication must be considered for large-area optical shutters.

Holographic and interferometric films

Holography consists of the recording of two reflected, coherent beams inteferometrically from a physical object. An analogous technique using interferometric noncoherence could be used to construct thin films which are light-concentrating, reflecting or redirecting in a wavelength-selective manner. As a hologram requires coherent light (a laser) to reconstruct the image, this analogous method could utilize a noncoherent light source like the sun. The holographic phase and amplitude pattern needed for solar uses could be generated by computer, once given a mathematical model of the spatial distribution required.

Holographic recording materials [36] can be photographic emulsions (phase and amplitude holograms), photo polymers, thermoplastic xerography, and dichromatic gelatin, which are useable for all phase-only holography.

Acknowledgement

This work was supported by the Assistant Secretary for Conservation and Renewable Energy, Office of Buildings and Community Systems, Buildings Division of the U.S. Department of Energy under Contract No. W-7405-ENG-48.

References

1. Lampert, C. M., "Heat Mirror Coatings for Energy Conserving Windows," Solar Energy Materials, Vol. 6, pp. 1-42. 1981.

2. Selkowitz, S., "Transparent Heat Mirrors for Passive Solar Heating Applications", Proceedings of the Third Passive Solar Conference, San Jose, CA. Jan. 1979.

3. Rubin, M., Creswick, R., and Selkowitz, S., "Transparent Heat Mirror for Windows: Thermal Performance", Proceedings of the Fifth National Passive Solar Conference, Amherst, MA. Oct. 1980.

4. Goodman, R. D., and Menke, A. G., "Effect of Cover Plate Treatment on Efficiency of Solar Collectors," Solar Energy, Vol. 17, p. 207. 1975.

5. Apfel, J. H., "Optical Coatings for Collection and Conservation of Solar Energy," J. Vac. Science and Technology, Vol. 12, p. 1016. 1975.

6. Jarvinen, P.O., "Heat Mirrored Solar Energy Receivers," J. Energy, Vol. 2, p. 95. March/April 1978.

7. Haacke, G., "Transparent Conducting Coatings," Ann. Rev. Mat. Sci., Vol. 7, p. 73. 1977.

8. Baum, V. A., and Sheklein, A.V., "Choice of Materials for Selective Transparent Insulation," Geliotekhnika, Vol. 4, p. 50. 1968.

9. Vossen, J. L., "Transparent Conducting Films," Physics of Thin Films, Vol. 9, p. 1. 1977.

10. Lampert, C.M., "Materials Chemistry and Optical Properties of Transparent Conducting Thin Films for Solar Energy Utilization," The Vortex of the American Chemical Society, Vol. 42, No. 10, p. 12. Dec. 1981.

11. Lampert, C. M., "Coatings for Enhanced Photothermal Energy Collection I & II," Solar Energy Materials, Vol. 1, p. 319 and Vol. 2, p. 1. 1979.

12. Angnihotri, O.P., and Gupta, B.K., Solar Selective Surfaces, Wiley Interscience, New York. 1981.

13. Lampert, C. M., "Metal Foils for Direct Application of Absorber Coatings on Solar Collectors," Plating and Surface Finishing, Vol. 67, pp. 52 - 56. 1980.

14. Lind, M. A., ed.,"Proceedings of the Second Solar Reflective Materials Workshop" (Feb. 12 - 14, 1980, San Francisco, CA), in Solar Energy Materials, Vol. 3, pp. 1-346. Dec. 1980.

15. Pastirik, E. M., and Keeling, M. C., "A Low Cost, Durable Antireflective Film for Solar Collectors," Proceedings of the IEEE 13th Photovoltaic Spectrum Conference, Washington, D.C., June 5-8, 1978. p. 620.

16. Jurison, J., Peterson, R. E., and Mar, H. Y. B., "Principles and Applications of Selective Solar Coatings," J. Vac. Science and Technology, Vol. 12, p. 101. Sept/Oct. 1975.

17. Lee, P.K., and Debe, M. K., "Measurement and Modeling of the Reflectance-Reducing Properties of Graded Index Microstructured Surfaces," Photo. Science and Engineering, Vol. 24, p. 211. July/Aug. 1980.

18. Lampert, C. M., "Microstructure and Optical Properties of High Transmission Coatings for Plastics," to be published in 1982.

19. Rubin, M., and Selkowitz, S., "Thermal Performance of Windows Having High Solar Transmittance, Proceedings of the Sixth National Passive Solar Conference, Portland, OR. Sept 8-10, 1981.

20. Dislich, H., and Hussman, E., "Amorphous and Crystalline Dip Coatings Obtained From Organometallic Solutions: Procedures, Chemical Processes and Products," Thin Solid Films, Vol. 77, pp. 129-139. 1981.

21. Brinker, C. J., and Harringston, M.S., "Sol-gel Derived Antireflective Coatings for Silicon," Solar Energy Materials, Vol. 5, pp. 159-172. 1981.

22. Vora, H., and Moravec, T. J., "Structural Investigation of Thin Films of Diamondlike Carbon," J. Appl. Phys., Vol. 52, p. 6151. 1981.

23. Kienel, G., and Dachselt, W., "Cold Light Mirrors," Ind. Res. and Development, Vol. 22, p. 135. Jan. 1980.

24. Winegarner, R., "Greenhouse Selective Baffle Collector," Proceedings of ISES, American Section, pp. 33-36. June 1977.

25. Bennett, A., and Olsen, L. C., "Analysis of Multiple-Cell Concentrator/Photovoltaic Systems," Proceedings of IEEE Photovolt. Spect. Conference, p. 868. 1978.

26. Goetzberger, A., and Grenbel, W., "Solar Energy Conversion with Fluorescent Collectors," Appl. Phys., Vol. 14, p. 123. 1977.

27. Goetzberger, A., and Wittwer, V. "Fluorescent Planar Collector-Concentrators: A Review," Solar Cells. Vol. 4, p. 3. 1981.

28. Weber, W. H., and Lambe, J., "Luminescent Greenhouse Collector for Solar Radiation," Appl. Opt., Vol. 15, p. 2299. Oct. 1976.

29. Granqvist, C. G., "Radiative Heating and Cooling with Spectrally Selective Surfaces," Appl. Opt., Vol. 20, p. 2606-2615. Aug. 1981.

30. Lampert, C.M., "Thin Film Electrochromic Materials for Energy-Efficient Windows," Lawrence Berkeley Laboratory Report, LBL-10862. Oct. 1980.

31. Dautremont-Smith, W.C., "Transition Metal Oxide Electrochromic Materials and Displays: A Review," Display Technology and Appl. Jan and April 1982.

32. Brown, G. H., and Shaw, W.G., "Phototropism," Rev. Pure Appl. Chem., Vol. 11, pp. 2-32. 1961.

33. Exelby, R. and Grinter, R., "Phototrophy or Photochromism", Chem. Rev. Vol. 64, p. 247-260. 1964.

34. Day, J.H., "Chromogenic Materials," Ency. of Chemical Techn., J. Wiley, New York, 1977.

35. Sherr, S., Electronic Displays, Wiley Interscience, NY. 1979.

36. Smith, H. M.,"Holographic Recording Materials," Topics in Applied Physics, Vol. 20, Springer-Verlag, Berlin. 1977.

Low emissivity and solar control coatings on architectural glass

Wolf-Dieter Dachselt, Wolf-Dieter Münz, Michael Scherer
Department of large-scale coating systems, Leybold-Heraeus GmbH
Wilhelm-Rohn-Str. 25, D-6450 Hanau, Federal Republic of Germany

Abstract

Methods of depositing thin films on glass using the vacuum coating technic have been developed to impede the transfer of heat through glass thus reducing the energy costs for room heating or air conditioning. Heat reflecting so-called low emissivity coatings permit a maximum amount of daylight to pass through, but then block the heat that is generated when light strikes an object (greenhouse effect). They are composed of metals like silver or copper sandwiched in selected oxide films or they are transparent semi-conducting mono-films. Double glazed insulating units with coated glass achieve k-values in the order of magnitude 1,8 to 1,5 Watts per squaremeters and degree Kelvin. Maximum available transmittance values at lambda = 550 nm are 85% (single pane), maximum reflectance values are 93% measured at lambda = 8 µm. The corresponding emissivities are around 0,1. The investigated low-e films are stable within 1% concerning transmittance and sheet resistance changes when exposed to elevated temperatures in air of up to 150°C. Solar control films used to keep out sunheat are sputtered in a reactive gasatmosphere on the base of titanium, stainless steel or chromium. Reflectance values of 32% are achieved at a transmission of e.g. 8%. The shading coefficient b is about 0,27. Large-scale production equipment for sputter deposition of the cited films is introduced.

Introduction

From the entire energy consumption all over the world 45% are used for the climatisation of buildings during heating or air conditioning. In countries and zones with warm climate and long hours of sunshine the fuel saving when cutting air conditioning costs by less sunheat getting into the rooms is of major importance. By coating glass panes with solar control films heat is prevented to get into the rooms. In colder or moderate climate zones insulating glass windows are used, which are coated with heat reflecting so-called low emissivity films retaining the heat inside the rooms. For a positive overall energy balance additionally the highest possible transmission for the incident radiation in the visible and near infrared wavelength range is required. Film systems for both applications are developed which can be sputter deposited under vacuum in large-scale production equipment.

Optical and thermal properties of glass windows

Entire radiation energy balance

From the incident solar energy 98% are contained in a wavelength range between 200 nm and 2500 nm. Window glass shows for this wavelength range a transmission of about 87%.

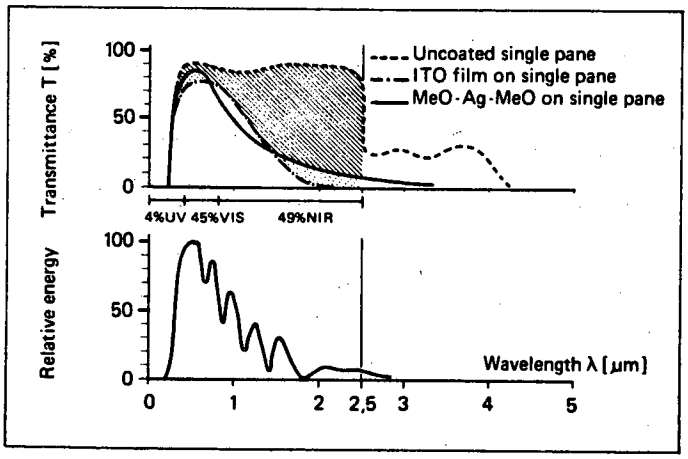

Figure 1. Spectral transmittance of uncoated and coated glass for sunlight and daylight and spectral energy distribution of the sun radiation.

The heat radiation energy emitted from heat sources inside of rooms is to 98% in the wavelength range between 3 µm and 30 µm. This far infrared heat radiation is absorbed and reradiated of up to 89% from the glass.

Resulting from these properties of a glass pane the short-wave sunlight and the daylight radiation pass through the glass into the rooms where it is absorbed from the walls and interior objects. The in the sense of heat technology nearly black objects emit the absorbed energy as long-wave heat radiation. The major portion of the generated heat is blocked by the glass. Thus window panes act like solar collectors being transparent for short-wave radiation and opaque for long-wave radiation.

In figure 1 the spectral transmittance of an uncoated single glass pane is shown

together with the spectral distribution of the sun radiation energy in the wavelength range between 300 nm and 2800 nm.

Single glazed panes and solar control coatings

The heat isolation effect of window panes is determined by the coefficient of heat transmission (k-value), which defines the passing through quantity of heat per unit area and degree Kelvin. It is a function of the surface heat transfer coefficent of the roomside glass surface $\alpha(i)$, the surface heat transfer coefficient at the outside glass surface $\alpha(a)$ and the heat conductivity $\alpha(g)$ of the glass. The formula for the reciprocal k-value (heat transfer resistance) is given by

$$\frac{1}{k} = \frac{1}{\alpha_i} + \frac{1}{\alpha_g} + \frac{1}{\alpha_a} \quad \left[\frac{m^2\ K}{W}\right] \qquad (1)$$

During heat transfer from the building interior to the glass pane 58 % heat are transmitted by radiation and 42 % are transmitted by convection. The heat transfer at the outer pane surface is convection induced by 82 % and radiation induced by 18 %. [1] Means to improve the heat isolation effect of a single pane are to reduce the convection at the outside by venetian blinds and to reduce the radiation share by infrared reflecting coatings at the roomside. The sun protection effect defined as the reduction of the total radiation transport from the outside to the inside is achieved by decreasing the glass transmittance. A suitable mean is depositing a reflective film on the glass surface which also partially increases the absorption, because a unilaterally the reflection increasing solar control film may disturb for instance the traffic and settlements adjacent to the building glazed with the coated glass. The solar control film efficiency is specified by the shading coefficient b, which is defined as the ratio of the relative energy transport through the coated glass pane to the relative energy transport through a 3 mm thick uncoated glass pane. The relative energy transport value of uncoated glass is 87 %.

Insulating glass and low-e coatings

The k-value of a two pane insulating glass unit is 3 W/m^2k. It is approximately half of the k-value of an uncoated single glass.

The heat transfer resistance 1/k is dependent on the heat transfer coefficients $\alpha(i)$ (inner glass pane surface), $\alpha(a)$ (outer glass pane surface), $\alpha(g1)$, $\alpha(g2)$ (glass panes one and two) and $\alpha(12)$ (transmission from pane 1 to pane 2). It is given by:

$$\frac{1}{k} = \frac{1}{\alpha_i} + \frac{1}{\alpha_{g1}} + \frac{1}{\alpha_{g12}} + \frac{1}{\alpha_{g2}} + \frac{1}{\alpha_a} \quad \left[\frac{m^2\ K}{W}\right] \qquad (2)$$

The heat transmission coefficient $\alpha(12)$ is a function of the emissivities $\varepsilon(1S)$ and $\varepsilon(2S)$ of the two glass panes.

The heat transfer from the roomside to the inner pane of the double glass is the same as with the single glass pane. The absorbed heat of the inner pane of the insulating unit is transmitted to the outer glass pane by 67 % by radiation.

Therefore the isolation effect of an insulating glass unit against heat loss of the inner rooms is improved by considerably decreasing radiation exchange between the two glass panes of the insulating unit.

This can be achieved by coating the number two or/and number three surface of the insulating glass unit with a low emissivity film, which reduces the emissivity of the glass surface from 0,8 to 0,1. The k-value of a coated insulating glass unit is a function of the emissivity and consequently diminishes from 3 W/m^2K to 1,8 W/m^2K, or to 1,6 W/m^2K when both inner surfaces are coated.

The solar collector effect of a twin glass is only little improved by coating because the transmission for sunlight is diminished.

Solar control films can be combined used with low emissivity films in insulating glass units, thus superimposing both effects.

Experimental results of new developments

Solar control films

Sputter deposited solar control films on glass panes are mainly composed of semi-trans-

parent metal films of Al, Cr, Ni, Ti or stainless steel. To meet the additional requirements of appropriate film hardness and chemical stability, especially when using monolithic glass as substrate, it has proven useful not to deposit the pure metals but partially oxidized metal or metal alloy films, metal carbides or metal nitrides, containing a metal excess. By changing the share of the free metal it is possible to vary the ratio of reflection by absorption in certain limits, keeping the transmission constant.

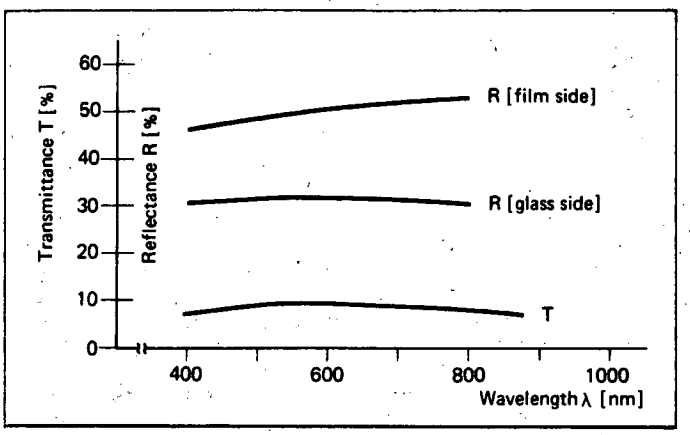

Figure 2. Measured transmittance and reflectance of a solar control film on single glass pane (film on titanium basis).

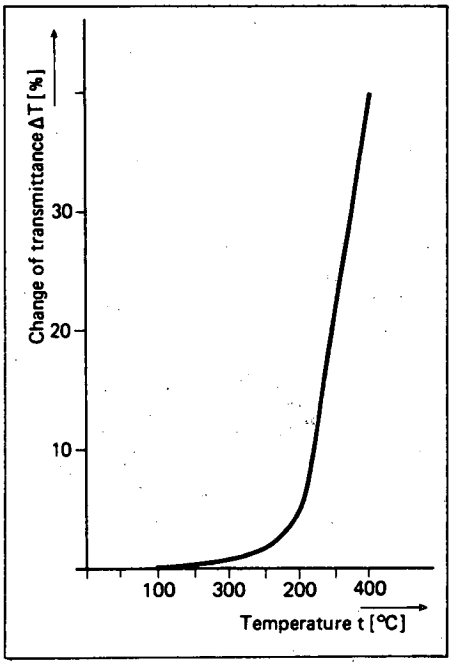

Figure 3. Step-stress-temperature test of a solar control film on glass (heating time between 50 °C steps 1 h), transmittance measured at λ= 550 nm.

Based on the titanium a relatively hard and sufficiently chemically resistant single layer film of a reflectance conform to the market requirements was developed. The film appears metallic when viewed in reflection and grey when viewed in transmission. The figure 2 shows the measured transmittance and reflectance of this solar control film on a single glass pane versus the wavelength from 400 nm to 850 nm. The film was reactively sputtered from a titanium target. The transmittance at λ = 550 nm is 8 %, the reflectance from the coated side is 47 % and from the glass side 32 %. The absorption of this film is approximately 45 %. From these values a shading coefficient b of 0,36 can be derived, assuming a temperature difference of 10 °C between the outside and inside room temperature. This means the incident radiation can be reduced by more than 50 %.

As a measure for the film durability the change of film transmittance and film sheet resistance was taken dependent upon temperature influence during longer storing in atmosphere and during a stepp-stress-test, which means stepwise elevation of the temperature by steps of 50 °C each after one hour storing time at constant temperature. The transmittance

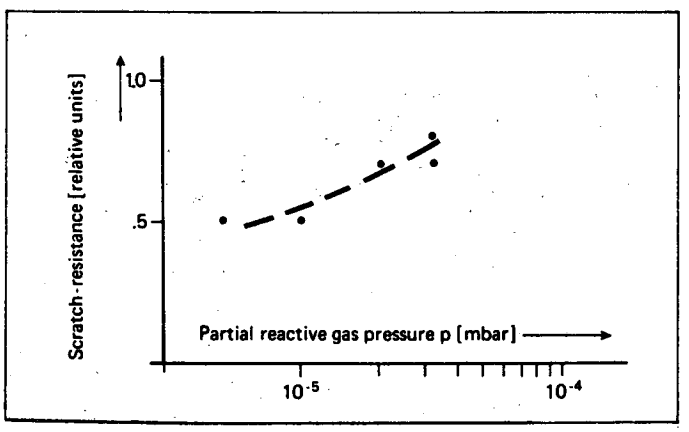

Figure 4. Solar control film hardness versus partial pressure of reactive sputter gases.

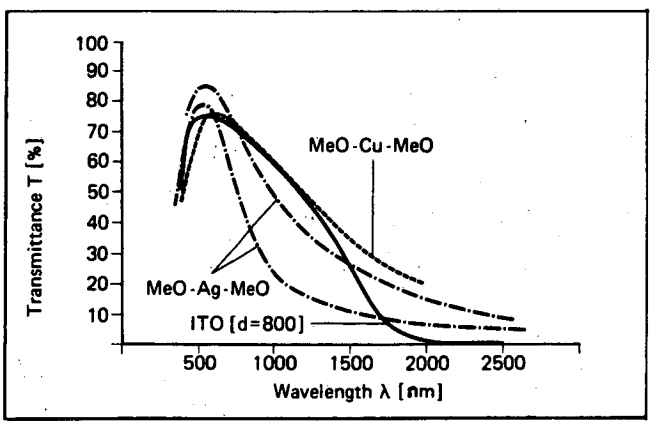

Figure 5. Measured transmittance of sputter deposited low-e MeO-Me-MeO and ITO films.

changes ΔT shown in figure 3 versus temperature remain below 1 % to temperatures of 150 °C.

The hardness of the demonstrated solar control film is dependent on the partial pressure of the reactive components of the sputter gas. Figure 4 shows the scratch resistance in relative units as a function of the reactive gas components partial pressure. The composition of the solar control film of a single layer film allows a relatively simple construction and design of a high performance in-line sputter system, considering particularly the number of cathodes, gas supply and lock design.

Low emissivity coatings

Sputter deposited thin films to reduce the heat radiation exchange between two panes in an insulating glass unit consist either of a film sequence metaloxide-metal-metaloxide or of semi-conducting oxidefilms. The low emissivity is caused by the metallic components or a metallic structure of the semiconducting oxide. The metaloxide films serve to enhance the metal film adhesion and to increase the film transmittance in the visible range in coincidence with the human eyes' maximum sensitivity range. The wider the transmitted wavelength range of light is the more neutral looks the coated glass in transmission. Selected metals for this metal film are gold, silver and copper. Possible oxides for the sandwiched low-e coatings are titaniumoxide, bismuthumoxide, tinoxide, indiumtinoxide or zincoxide.

The measured transmittance of several metaloxide-metal-metaloxide low-e coatings on a single glass pane is shown in figure 5 and the measured far infrared reflectance is shown in figure 6. Using silver as metallic intermediate film maximum transmittance values in the range 83-85 % are achieved. The far infrared reflectance is about 93 % and the film emissivity is 0,1 corresponding to a sheet resistance of 9 Ω. Replacing the silver film by a copper film, the maximum transmittance values in the visible are in the range 70-74 %. The far infrared reflectance is about 88 % and the emissivity corresponds to a k-value of a coated double glass without special gas filling of 1,8 W/m^2K.

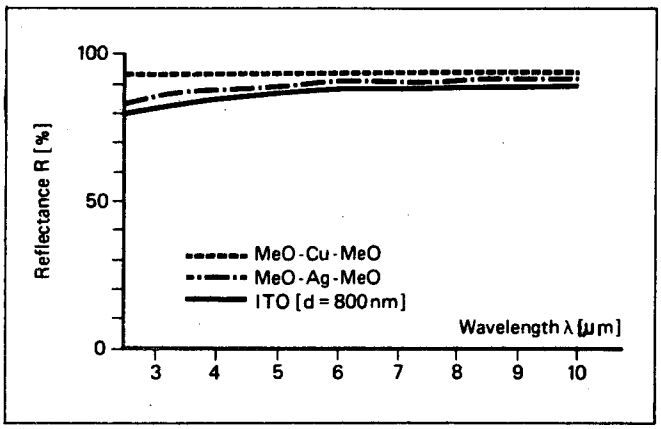

Figure 6. Measured far infrared reflectance of sputter deposited low-e MeO-Me-MeO and ITO films on single glass.

Figure 5 also shows the measured transmittance of an 800 nm thick ITO-film. The ITO-film was sputter deposited on room temperature substrates using a dc-magnetron provided with a specially prepared and manufactured target. A comparison of the different transmittance curves in figure 5 up to wavelength 2500 nm results in silver containing low-e coatings show the highest transmittance at λ = 550 nm with 85 % and, considering the entire near infrared wavelength range from 800 nm to 2500 nm, larger transmitted sun radiation energy shares than ITO-films. A similar good total balance of energy transmission with a slightly lower transmission value for sunlight in the near infrared shows the copper containing film.

These properties of the metal containing low-e coatings are resulting in more positive values of the overall heat balance of even southside and westside windows in a building than shown by ITO-coated double glazed units. These facts are demonstrated in figure 1, where the measured spectral transmittance of a silver containing sandwiched low-e film and an ITO-film is inserted in the spectral transmission curve of sun radiation through glass. The sputter conditions like reactive gas partial pressure, gas flow and sputter rate are closely related to the low-e film stability. The hardness of the films is strongly influenced by the fact, whether the films during deposition are in close contact with the

gaseous plasma or not. For harder films like solar control films a so-called "hot plasma" (close contact) is necessary. Copper or silver containing low-e coatings need a so called "cold plasma" (little contact with the plasma) to prevent oxidizing effects during film deposition.

Aging tests with low-e coatings concerning changes of the transmittance versus temperature and resistivity changes have been accomplished by the same procedures (step-stress-test, storing at elevated temperature) as described with solar control films. Below 150 °C no changes of more than 1,0 % of transmittance in the visible range and sheet resistance do occur.

In-line sputter systems for the production of solar control and low-e coatings under vacuum.

Substrates to be coated with solar control films or low-e films are mainly tempered or non-tempered flat glass in cut or standard sizes of up to 3,18 by 6 m, or curved glass pieces in standardized sizes of larger quantities as for instance automobile moon lights and sun roofs. A large-scale production machine for economic manufacturing of coated glass has to be capable of putting through large quantities of glass at short cycles with least possible rejects.

A machine design allowing sputter deposition of either low-e films or, with slightly modified machine outline, of solar control films shows figure 7. A schematic plant drawing is shown in figure 8.

Figure 7. Load lock in-line sputter system for glass coating.

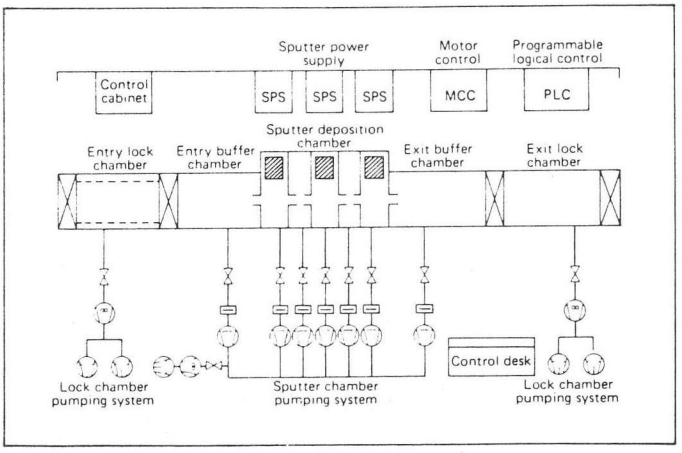

Figure 8. Schematic drawing of a typical architectural glass coating system with three coating zones.

The throughput for coated flat glass related to 3 shifts per day and 6000 hours per year is dependent upon the layer system and machine equipment, between 5 and 30 million square feet, and for curved automobile glass in the range of 600 000 till 800 000 pieces per year.

The plant is designed as a modular fully automatically operating load lock in-line sputter system. The basic equipment comprises an entrance lock chamber, a sputter chamber with entry buffer zone, sputter station and exit buffer zone and an exit lock chamber, assembled in-line and separated by lock valves. By inserting additional chamber modules, isolated by flap valves from each other, to transfer process steps of longer duration to shorter in parallel running single process steps, the machine cycle time is shortened and the troughput consequently increased.

Flat glass substrates are frameless transported by rollerways with the utmost possible utilisation of the available loading area per cycle. The transport is discontinuous in all process chambers except the sputter chamber, where the substrates are continuously moved, passing beyond the sputter cathodes. The speed is adjustable. As the entire film deposition process is vacuum operated the substrates are brought from atmosphere into the vacuum in the entrance load lock chamber. For better design and film adhesion some preliminary treatments like glow discharge cleaning or heating is done in the entrance lock chamber before passing on the substrate into the sputter chamber.

In the sputter chambers the individual layers of the desired film system are simultaneously sputter deposited on a continuously moving substrate. The different process parameters and machine functions are individually controlled, adjusted and monitored to achieve the optimum described film properties.

The sputter gas atmosphere of the individual sputter cathodes is composed of up to four different gas components of precisely controled flow and determined partial pressure and concentration. The sputter cathode targets are manufactured and fixed to the cathode base plate following special techniques. It turned out that a constant sputter rate can be maintained over hours just by controlling the dc power supplies' voltage and current, without closed loop rate control.[2] The achieved thickness uniformity across a pane width of 3,18 m and a depth of 6 m, is in the magnitude of $\pm$ 1 %, excluding a marginal zone of 10 cm.

The cross contamination between the parallel operated sputter cathodes with reference to the partial gas pressure is below 0,5 % when processing flat glass pieces and using a thoroughly calculated and designed configuration of slot-type locks between the individual sputter zones.

The low-e films and solar control films sputter deposited using the described technology are durable enough to pass a smooth washing process in a glass washing machine. When assembling double pane insulating glass units with the coating on the number three surface, the two panes can be bonded together without removing the coating along the edges under the bonding zone.

When coating curved automobile glass the glass transport is accomplished by using special holding plates loaded into frames with shieldings around the curved glass backsides to prevent coating by backsputtering. The design of the lock valves is adapted to the special glass shape.

For further informations especially on batch-type glass coaters, simpler in-line systems and state of the art process technics reference is made to previous publications.[3]

Conclusions

When coating the number 3 surface of an insulating glass unit with a silver or copper film sandwiched in metaloxide films the coefficient of heat transmission k is reduced from 3 W/m^2K (uncoated glass) to 1,8 W/m^2K.

Metaloxide-silver-metaloxide films have 72-78 % transmittance in the visible wavelength range (insulating glass unit), a moderate transmittance in the near infrared to 2500 nm and a low emissivity of 0,1. Similar values are shown by semi-conducting tinoxide or ITO-films of sufficient thickness.

Solar control films based on partially reactive sputtered titanium decrease the incident solar radiation by more than 50 % (shading coefficients of 0,4-0,2/). At a transmittance of 8 % reflectance values in the range 40-20 % can be adjusted with corresponding changing absorption values in the range 52-72 %. Both kinds of layer systems can be sputter deposited onto large substrate sizes of up to 3,18 m x 6 m by means of the vacuum technic in large scale production equipment.

Acknowledgements

The outhor wishes to thank Gonde Dittmer and Wolf-Dieter Muenz of Leybold Heraeus GmbH for helpful discussions.

References

1. Dittmer, G.; Coating Architectural Glass, GLASS (Monthly J. of the Europ. Glass Ind.), Vol. 58, No. 10, pp. 363-369, 1981

2. Kienel, G.; Optical Layers Produced By Sputtering, Thin Solid Films, Vol. 77, No. 1/2/3 pp. 213-224, 1981

3. Gläser, H.J.; Verfahren zur Beschichtung von Fensterscheiben mit Sonnen- und Wärmeschutzschichten, Glastechn. Ber. Vol. 53, Nr. 9, pp 245-258, 1980

4. Kienel, G; B. Meyer and W.D. Münz; Moderne Beschichtungstechnologien von Architekturglas, Vakuum Technik, Bd. 30, Heft 5, S. 236-246, 1981

Materials for transparent heat mirror coatings

G. Haacke
Chemical Research Division, American Cyanamid Company
Stamford, Connecticut 06904

Abstract

Transparent heat mirrors can be constructed from single- or multi-layer coatings. For single-layer mirrors wide-band-gap semiconductors are the best available materials. The required fundamental semiconductor properties are reviewed and experimental data of binary and ternary compounds discussed.

Introduction

The wavelength-selective control of light transmission through transparent enclosures is an accepted means of energy conservation. Research is also in progress to exploit this principle in energy conversion, i.e., in solar heat collectors. Basically, the control can be accomplished in two ways - partial absorption (tinted glass) or reflection (transparent heat mirrors).

Low cost and simple manufacture have contributed to the widespread use of tinted glass in architectural glazing, automobile windows and protective equipment. Tinted glass, however, has the disadvantage of re-emitting part of the absorbed energy and is unsuitable for solar heat collector covers or light bulb envelopes. For these reasons, emphasis is shifting increasingly to transparent heat mirrors and should accelerate as improvements in cost, durability and performance come along.

Heat mirror classification and applications

Transparent heat mirrors can be divided into different classes characterized by their application or construction. Considering applications, two groups exist: 1. mirrors which transmit visible light and in the ideal case reflect over the total infrared heat spectrum (Class 1), 2. mirrors transmissive to visible and near-infrared light and reflective only beyond the near-infrared transmission cut-off (Class 2). Class 1 contains all present applications related to energy conservation and personal protection and, thus, includes architectural glass coatings to reduce air conditioning requirements[1], light bulb envelopes[2], furnace windows[3], welder and laser goggles, astronaut helmets. The Class 2 heat mirrors comprise solar heat collector covers and window coatings for the passive solar heating of buildings. Some of these applications are still in an early development stage.

The construction of transparent heat mirrors provides another means for classification. Three approaches have been considered. In two cases, a transparent substrate is needed which is either covered by a single-layer or a multi-layer coating. The third system, conducting microgrids, does not necessarily depend on a substrate.

Conducting microgrids[4] are electromagnetic filters which in their simplest form consist of a metal wire mesh. The grids transmit short-wavelength radiation and reflect infrared light if wire diameter and mesh openings are properly chosen. To be effective in the optical spectrum the wire diameter must be submicron size and the mesh openings in the order of a few microns. Herein lies the major disadvantage of these filters. They are difficult to produce in freely suspended wire form and also as photoetched thin film grids on large area substrates.

In comparing single- and multi-layer heat mirrors, both are viable candidates for commercial products. It would seem that for economical reasons single-layer systems are the preferred choice. This is true in principle, but many current architectural coatings consist of more than one film to achieve optical properties not yet obtainable with a single layer. When, for example, a complete infrared cut-off is desired (Class 1) metal films are needed which may require additional films to alter the visible reflection and provide mechanical protection[5].

Of the transparent heat mirror applications listed earlier, coatings on architectural glass and sodium lamp envelopes are made on a commercially significant scale. The architectural coatings add aesthetic appeal to the windows and this fact may be of more importance to some users than optimal heat reflector performance. Frequently, today's commercial coatings do not have the highest possible infrared reflectance; some leading glass manufacturers quote the total solar energy reflectance of their best products in the

30-40% range. Considering that approximately 50% of the solar radiation is in the infrared, higher reflectivities would reduce air conditioning requirements below existing levels.

In contrast, heat mirror coatings for solar collector covers must meet more stringent performance specifications. They need to be highly transmissive (>90%) over the solar spectrum up to 2.5 μm and highly reflective beyond this wavelength. These requirements arise primarily from economic considerations but also from the existence of a competing technology, selective absorber surfaces[6]. Cost and optical properties of available Class 2 heat reflectors still have to be optimized to become competitive on a large scale. Progress in this area may come from wide-band-gap semiconductor coatings which are the main subject of this paper.

Semiconductor heat mirror coatings

The unique transparent heat mirror properties of semiconductors are based on the existence of a forbidden energy gap in their band structure and the possibility to generate in these materials free electrons or holes by doping. The energy gap E_g is an intrinsic materials parameter that provides for a spectral region of high optical transmission. In an undoped, purified semiconductor, E_g determines a wavelength λ_g at which transmission changes into absorption due to interband transitions of the intrinsic charge carriers. If E_g is measured in electron volts λ_g, given in μm, can be calculated according to $\lambda_g = 1.23/E_g$. It follows, for example, that semiconductors with E_g less than 1.6 eV are opaque to all visible light. Band gaps larger than 3 eV are needed for complete transparency over the visible spectrum. However, E_g's as small as 2.5 eV are acceptable in many applications because thin films of such materials show only a slight bluish to greenish tint.

Pure, wide-band-gap semiconductors do not reflect much infrared light. Their infrared reflectivity, however, can be raised to high levels by creating free charge carriers by doping. The carriers, for example electrons, are excited by infrared light to intraband transitions resulting in infrared reflectivity. A good understanding of the relationships between the optical properties and basic materials parameters can be gained by applying Drude's free electron theory to semiconductors[7]. It follows that a plasma wavelength λ_p exists at which the infrared reflectivity drops steeply. We have $\lambda_p > \lambda_g$ whereby the wavelength interval between λ_p and λ_g defines the transparency region of a heat mirror.

The position of λ_p is given by the free electron concentration N and shifts to shorter wavelengths with increasing N. In metals N is large enough to have λ_p in the visible or ultraviolet part of the spectrum. In semiconductors N needs to be in the 10^{20} -10^{21} cm^{-3} range to bring λ_p to the near infrared. Besides the position of the plasma edge two additional properties determine the performance of an infrared reflector: the slope of the reflectivity increase at λ_p toward longer wavelengths and the highest obtainable reflectivity. Both are characterized by a quality factor Q_R which should be as large as possible. Q_R is in effect the product of plasma frequency and electron relaxation time and is given by the Drude theory as

$$Q_R = \sqrt{\frac{N \cdot \mu^2 \cdot m^*}{\varepsilon_o \varepsilon} - 1} \qquad 1.$$

Here, μ is the electron mobility, m* the effective mass, ε_o the vacuum dielectric constant and ε the dielectric constant of the semiconductor. We see that N, μ, m* should be large and ε small. While m* and ε are intrinsic materials parameters which cannot be changed for a given semiconductor, suitable film preparation techniques can be used to maximize μ. The electron concentration can be maximized by doping but provides limited flexibility when λ_p is specified.

It should be recognized that free charge carriers are also responsible for light absorption. The absorption α increases with N and λ according to

$$\alpha \sim \frac{N}{\mu} \cdot \lambda^2 \qquad 2.$$

The effect is undesirable for transparent heat reflectors in solar collectors where α reduces the solar transmission through the cover plate, especially in the red and near-infrared. Again, some alleviation is possible by maximizing the mobility. On the other hand, if it were possible to develop a highly doped semiconductor coating for architectural glazing with λ_p close to the visible, the resulting free carrier absorption would impart a pleasing green-to-bluish color to the window. It is by no means certain, however, that in a semiconductor doping can shift λ_p so far to shorter wavelengths. To obtain

$\lambda_p \sim 0.7\text{-}0.8$ μm a carrier concentration between 10^{22} and 10^{23} cm^{-3} is needed, an order of magnitude more than has been achieved to date. Attempts to dope higher in some wide-band-gap semiconductors have resulted in the formation of new phases.

The known semiconductors with useful transparent heat mirror properties all contain either one or more of three elements located next to each other in the periodic table, i.e., cadmium, indium, tin. Initially, only the binary compounds CdO, SnO_2 and In_2O_3 were recognized; cadmium oxide is of limited utility because it is moisture sensitive. Recently, ternary wide-band-gap semiconductors were found which also have attractive heat mirror properties; they are Cd_2SnO_4, $CdSnO_3$ and $CdIn_2O_4$.

Binary Semiconductors

The fundamental semiconductor properties of these compounds have been reviewed recently[8]. Here, we summarize the transparent heat mirror performance of tin oxide and indium oxide. Published optical transmission and infrared reflectance curves for SnO_2 are shown in Figure 1. The full-line curves were measured on a spray coated film, doped with fluorine[2]. The

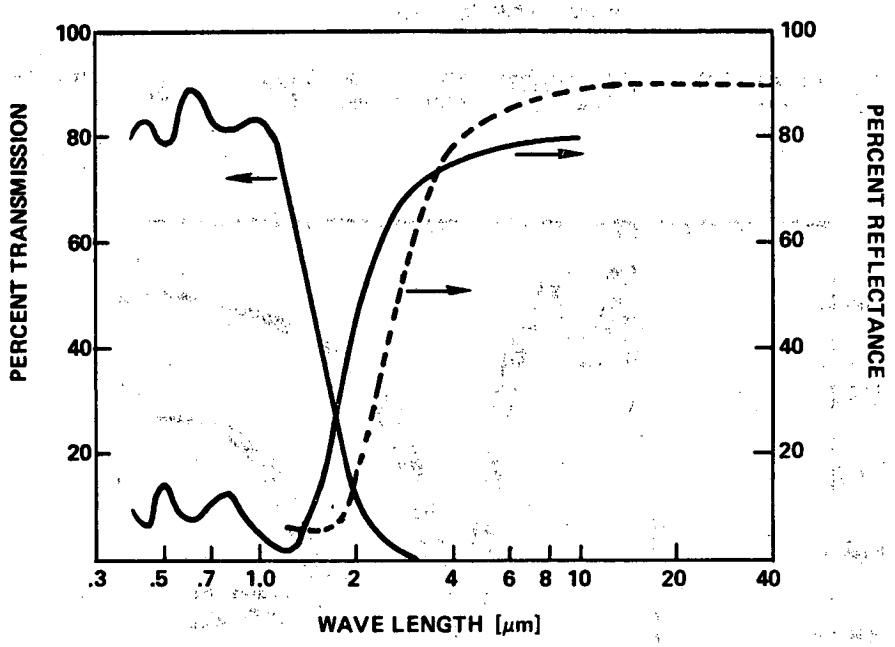

Figure 1. Spectral transmission and reflection of SnO_2 films; full line curves after Reference 2, broken curve after Reference 9.

sample had $6 \cdot 10^{20}$ cm^{-3} free electrons with 20 cm^2/Vs mobility. These optical and electrical properties have been considered typical for good-quality SnO_2 films. Recently, however, higher mobilities and infrared reflectivities were reported[9]. The broken curve in Figure 1 was taken from Reference 9; it was measured on a spray coated, fluorine doped SnO_2 film with $N = 3.5 \cdot 10^{20}$ cm^{-3} and $\mu = 46$ cm^2/Vs. Unfortunately, optical transmission data were not given so a complete assessment of this film as transparent heat mirror is not possible.

Typical transparent heat mirror data for indium oxide films are drawn in Figure 2. The curves were measured on two tin-doped films prepared by spray deposition[10]. The films are of equal thickness (0.3 μm) but have different electron concentrations. The effect of carrier absorption - given by expression 2. - on the transmission can be clearly seen. The shift of the plasma reflection edge toward shorter wavelengths with increasing electron concentration, predicted by the Drude theory, is also obvious.

Ternary semiconductors

Cadmium orthostannate Cd_2SnO_4 was the first ternary wide-band-gap semiconductor to show useful transparent heat mirror properties[11]. Along with optimized In_2O_3 it is still the material with the highest reported solar transmission and infrared reflectivity. Its electrical and optical properties are very sensitive to the preparation conditions. Optimal properties are obtained in films prepared by RF sputtering in oxygen and subjected to a post-deposition heat treatment[12]. Figure 3 shows typical transmission and reflection curves for a film prepared under optimized conditions after heat treatment (20 min., 670°C).

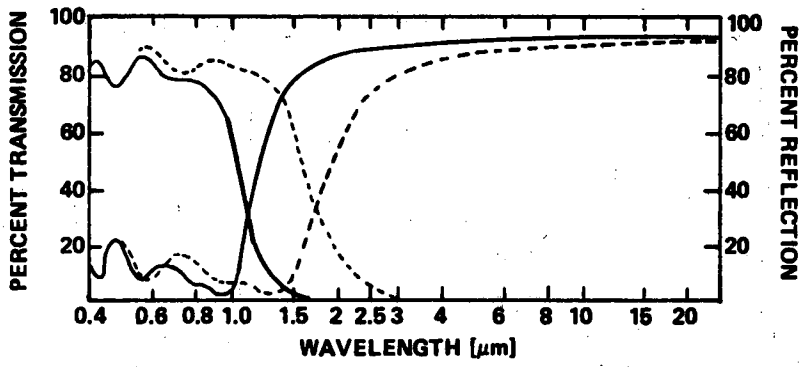

Figure 2. Spectral transmission and reflection of two In_2O_3 films, after Reference 10. Full line: $N = 1.3 \cdot 10^{21}$ cm^{-3}; broken line: $N = 3 \cdot 10^{20}$ cm^{-3}.

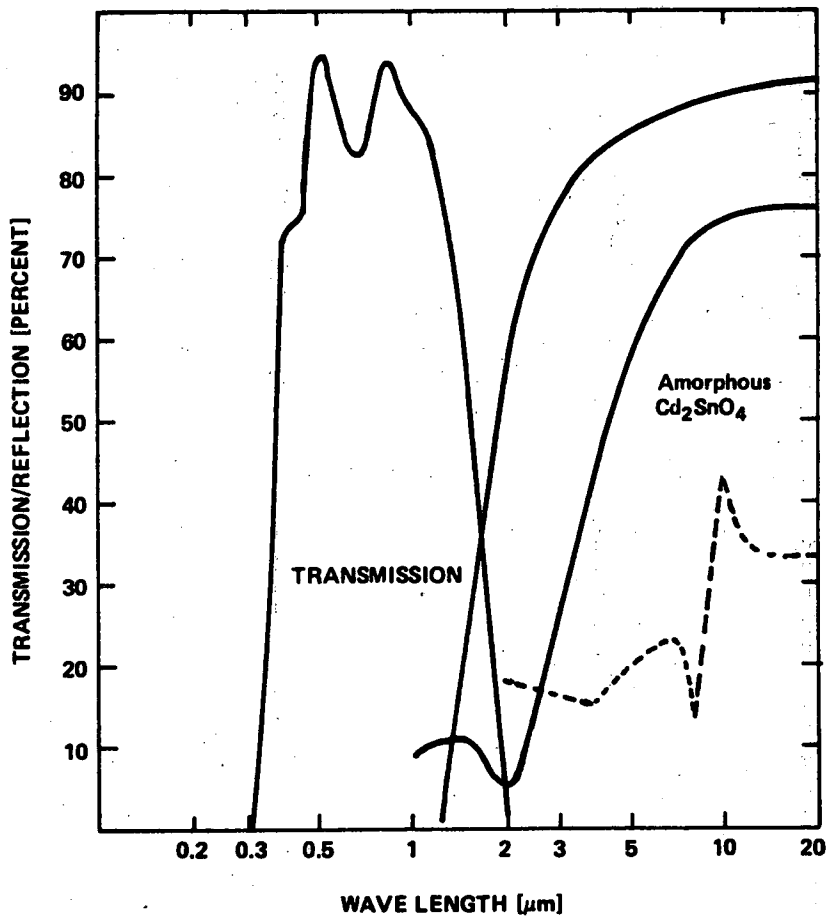

Figure 3. Spectral transmission and reflection of Cd_2SnO_4 films; full lines: after heat treatment; broken line: infrared reflectivity before heat treatment.

The figure also shows the infrared reflectivity of the same film before heat treatment when the free electron concentration is two orders of magnitude lower and also the mobility is smaller. The third reflectivity curve of Figure 3 was measured on an amorphous film and demonstrates that the reflectivity of amorphous coatings is inferior to those of polycrystalline samples.

The Cd_2SnO_4 films can also be deposited onto plastic substrates and have good adhesion. Since the plastic cannot be exposed to a high temperature heat treatment, the sputter coating must be carried out under reducing conditions in an Ar/O_2 plasma. Transmission and reflectivity are then smaller than when prepared in a two-step process. This can be seen in Figure 4 which presents the transmission and reflection spectra of a Cd_2SnO_4-coated Lexan substrate.

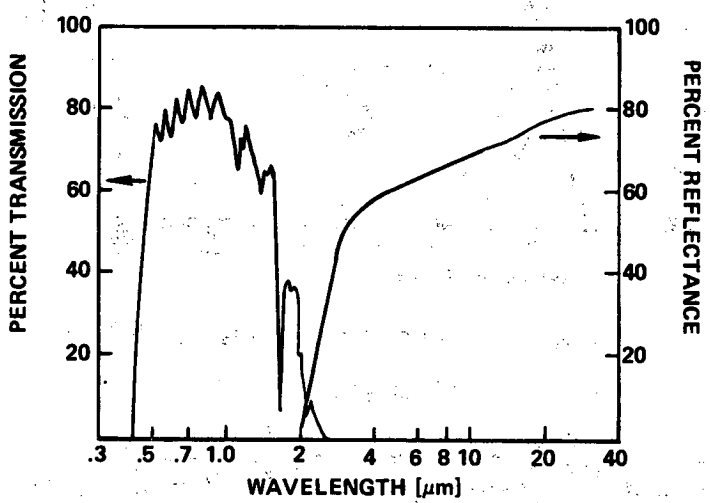

Figure 4. Spectral transmission and reflection of a polycarbonate substrate coated with Cd_2SnO_4.

The optical and electrical properties of the cadmium metastannate $CdSnO_3$ are similar to those of tin oxide. Electrical conductivities near 1000 $ohm^{-1}cm^{-1}$ have been obtained in contrast to Cd_2SnO_4 films in which we have measured conductivities as high as 6800 $ohm^{-1}cm^{-1}$. The transmission and reflection of $CdSnO_3$ films prepared to date are also lower than for Cd_2SnO_4 films of equal thickness.

A third ternary material has attractive heat mirror properties, $CdIn_2O_4$. This compound crystallizes in the spinel structure[13] and forms a light green powder when synthesized by calcining stoichiometric mixtures of the binary oxides. Thin films have been prepared only recently. They were RF sputtered from a hot-pressed powder target which yields transparent conductors with properties similar to those of Cd_2SnO_4. Complete characterization of RF sputtered cadmium indate has not yet been carried out. The information obtained thus far indicates that $CdIn_2O_4$ has the same tendency as Cd_2SnO_4 to form secondary phases (CdO, In_2O_3) during sputtering and that the film composition is critically dependent on the deposition conditions. Electrical conductivities in the 3000-4500 $ohm^{-1}cm^{-1}$ range have been measured on samples which are not considered optimized. Significant further improvements may be possible.

Representative optical spectra of $CdIn_2O_4$ are shown in Figure 5. It is encouraging that one of the samples reaches 93% infrared reflectivity, equal to the best Cd_2SnO_4 coatings. The X-ray diffraction pattern of this particular coating shows some In_2O_3 besides the major $CdIn_2O_4$ spinel phase. The sample with the lower infrared reflectivity (broken curve) is according to XRD analysis single-phase $CdIn_2O_4$. The differences in the optical properties of the two specimens cannot be explained by different electron concentrations or mobilities. Rather, the data suggest that under certain conditions the presence of a second phase may have a beneficial effect on the infrared reflectivity of these films. Clearly, more work is required to explain these observations.

Conclusions

Wide-band-gap semiconductors are promising candidates for transparent heat mirror applications. Further development is justified to optimize their optical properties and reduce fabrication costs. For applications requiring complete infrared cut-off, the challenge remains to shift the plasma reflection edge to the visible-infrared boundary.

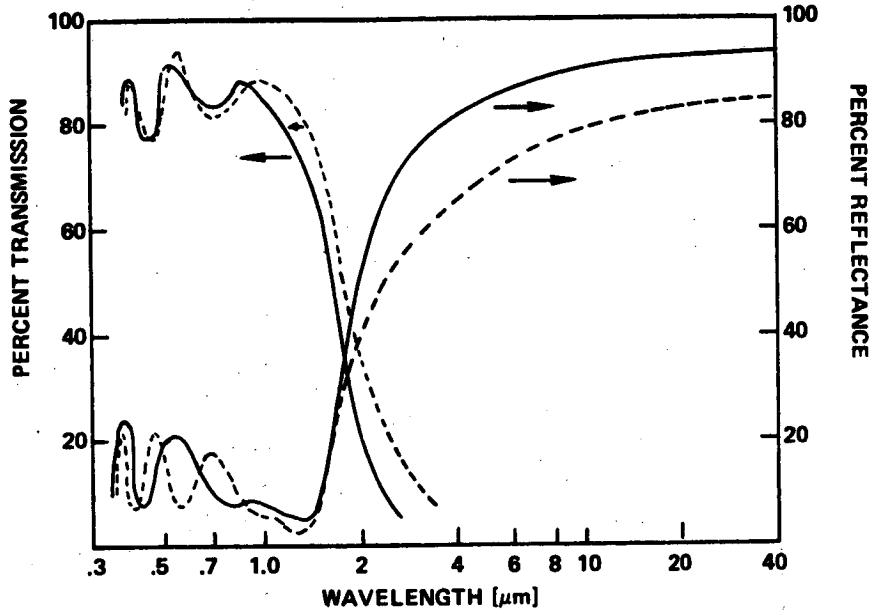

Figure 5. Transmission and reflection spectra of two $CdIn_2O_4$ films on silica.

References

1. R. Groth and W. Reichelt, Gold Bull. 7, 62 (1974).
2. R. Groth and E. Kauer, Philips Tech. Rev. 26, 105 (1965).
3. H. Kautz, "Heat Protection Glasses," Düsseldorf: Verlag Stahleisen (1960).
4. C. M. Horwitz, Opt. Commun. 11, 210 (1974).
5. J. C. C. Fan, F. J. Bachner, G. H. Foley and P. M. Zavracky, Appl. Phys. Lett. 25, 693 (1974).
6. C. M. Lampert, Solar Energy Materials 2, 1 (1979).
7. R. Groth, E. Kauer and P. C. v.d. Linden, Z Naturforschg. 17a, 789 (1962).
8. G. Haacke, Ann. Rev. Mat. Sci. 7, 73 (1977).
9. F. Simonis, M. v.d. Leij and C. J. Hoogendoorn, Solar Energy Materials 1, 221 (1979).
10. H. Köstlin, R. Jost and W. Lems, Phys. Stat. Sol. 29a, 87 (1975).
11. G. Haacke, Appl. Phys. Lett. 30, 380 (1977).
12. G. Haacke, W. E. Mealmaker and L. A. Siegel, Thin Solid Films 55, 67 (1978).
13. M. Skribljak, S. Dasgupta and A. B. Biswas, Acta Cryst. 12, 1049 (1954).

Optical properties of transparent heat mirrors based on thin films of TiN, ZrN, and HfN

Björn Karlsson, Carl G. Ribbing
Department of Solid State Physics, Institute of Technology, Uppsala University
Box 534, S-751 21 Uppsala, Sweden

Abstract

Calculations of the transmittance and reflectance between 0.35 μm and 10 μm of semitransparent films of TiN, ZrN and HfN have been performed. The calculations are based on recently reported optical constants. They show that these compounds can be used as transparent heat-mirrors. These materials show considerable higher emittance than the noble-metals but comparable or higher visible transmittance. It is also shown that the transmittance can be increased by the technique of induced transmission.

Introduction

Numerous investigations have been presented concerning transparent heat-reflectors. These filters which by definition combine visible transparency with high IR-reflectance have been prepared from doped semiconductors, thin metal films or metal-based multi-layers[1]. The principle difference between these materials in this application is that the transmittance of the doped semiconductors occurs above its plasma-energy, while the transmittance of the metallic films occurs below its plasma energy. Therefore the semiconductors used in this application can be rather thick while the metallic films have to be very thin. The transmittance of the thin metal film is the result of an interaction between the reflections from the first and second surface of the film. If the film is thin enough, the contribution to the reflected amplitude from the second surface will be in opposite phase to the reflected amplitude from the first surface and strong enough to partly cancel the first surface reflection, which enhances the transmittance of the film.

The metals which can be used in these cases are restricted to noble-metals and Al otherwise too high internal absorptance reduces the transparency[2]. The transition metals Fe, Ni, Cr etc. show a very modest selectivity and are not used unless a grey, sun-screening effect is desired[2]. The optical background to these facts is that the metal films desired to give high visible transmittance and low absorptance must possess low values of the real part of the refractive index over the visible spectrum. Physically it means the visible range has to belong to the relaxation region of a free-electron like metal. It is therefore obvious that the transition metals do not fulfil the requirements since they do not have any free-electron like region. The metals which are free-electron like are the noble metals, Al and some others like the alkali-metals, which, however, do not have a technical interest in this case. It has recently been shown that the nitrides of Ti, Zr and Hf have an extended free-electron region corresponding to a plasma-energy $\hbar\omega_p \sim 7$ eV and a relaxation energy $\hbar/\tau \sim 0.3$ eV [3]. The main difference between these values and the corresponding parameters for the noble metals is the substantially higher relaxation energy, which together with the higher effective electron mass imply a ten times lower electron mobility in these nitrides than in the noble-metals. In this report the possibility of using nitrides of Ti, Zr and Hf as transparent heat-mirrors is demonstrated by the reflectance- and transmittance-spectra for thin films, calculated from recently published optical constants[3,4,5]. It is proposed that these nitrides which are very durable, with excellent temperature- and wear-resistance, chemically inert and adhere well to glass are promising alternatives to the soft, wear-sensitive noble metals in applications of selective transmission.

Optical properties of TiN, ZrN and HfN

A number of measurements on the optical properties of TiN[6-11] and a few on ZrN[7,12] and HfN[13] have been reported. Most of them present reflectance spectra and the real- and imaginary parts of the dielectric constant calculated from the bulk reflectance. Very few give detailed data for the real and imaginary part of the refractive index, n and k. The n- and k-values used in our calculation were derived from Kramers-Krönig analysis of the reflectance-spectrum for CVD-coated TiN, ZrN and HfN[3] and of reactively sputtered TiN[4]. The bulk reflectances of these materials are shown in figure 1. A prominent feature is the high and constant IR-reflectance and the sharp edge in the visible due to a screened plasma resonance. The optical constants derived from this spectra are shown in figure 2 and figure 3. It can generally be stated that the higher the reflectance is above the knee and the deeper the reflectance minimum is, the lower is the n-values in the visible and the higher is the transmittance of the thin film. The optical constants used for TiN are valid for the sputtered film. The CVD-TiN has a higher IR-reflectance and a deeper minimum than the sputtered sample, but in spite of that, data for the sputtered film were used, mainly

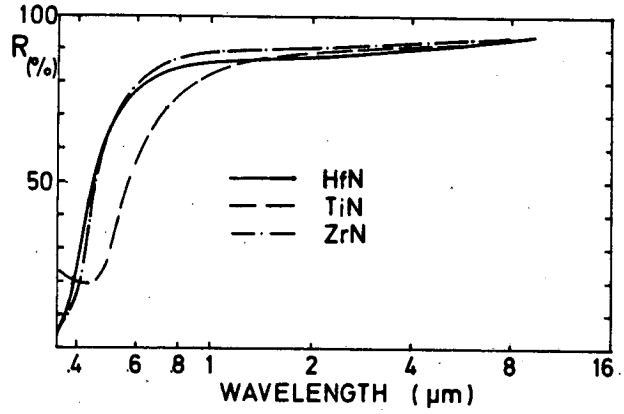

Fig. 1. Spectral reflectance of CVD, ZrN and HfN[3] and of sputtered TiN[4].

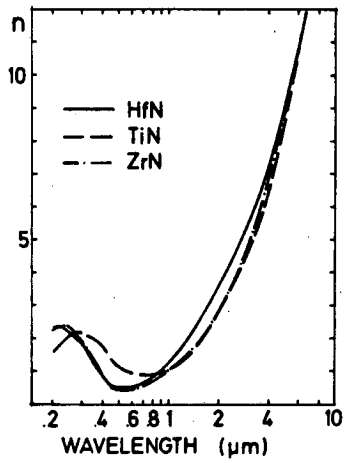

Fig. 2. Real part of the refractive index of TiN[4], ZrN[3] and HfN[3].

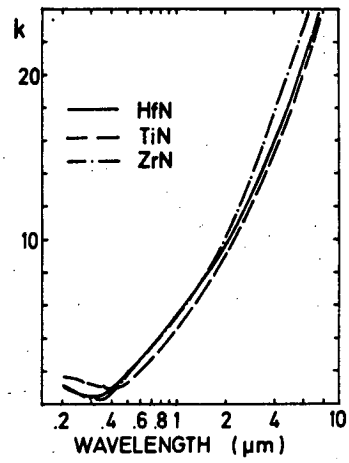

Fig. 3. Imaginary part of the refractive index of TiN[4], ZrN[3] and HfN[3].

because these data were derived in a more reliable Kramers-Krönig analysis. The refractive index for both types of films were calculated by K-$\bar{K}$ analysis. For the CVD-samples the extrapolation was taken from literature-data, while in the case of the sputtered film, the extrapolation was adjusted to independently measured n and k for some wavelengths. Another reason for using the data from the sputtered films is that this film is more related to a possible semitransparent film both with respect to thickness and way of preparation. The n-values in the visible which are critical for the transmittance of TiN agree well with data of Chassaing[10] derived from his published dielectric constant. His n-values show the same dispersion in the visible as ours, but are at most 0.2 higher. This can also be observed in his bulk reflectance-spectrum which show a lower NIR-reflectance and shallower reflectance-minimum than ours. The ZrN-data show good agreement with n and k reported by Knozp and Goretzki[12]. Their lower values of n and k indicate higher transmittance-values for thin films than our data give. The only known reference on HfN[13] could not be used for comparison since its optical constants were derived from reflectance measurements on a powder-pressed sample with much lower reflectance than our samples.

Transmittance and reflectance of single films

The spectral transmittance and reflectance of these nitride-films were calculated by use of a conventional matrix-method[14], where the indata are n, k and the thickness of the film. The films are assumed to be coated on a non-absorbing glass with the refractive index $n_s = 1.5$. In the calculations the backside of the glass is supposed to give contributions to R and T by multiple-reflections, but without interference effects. This implies that the values in the visible for the system goes towards T = 0.922 and R = 0.078 when the filmthickness goes to zero. Figures 4, 5 and 6 present the spectral reflectance and transmittance as a function of thickness for these films.

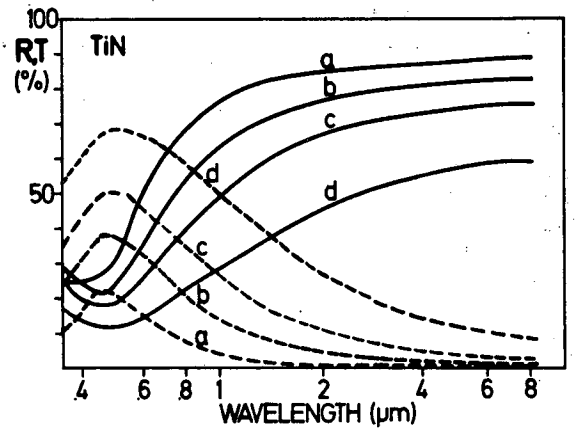

Fig. 4. Spectral reflectance and transmittance of TiN-films of thicknesses a-500 Å, b-300 Å, c-200 Å and d-100 Å.

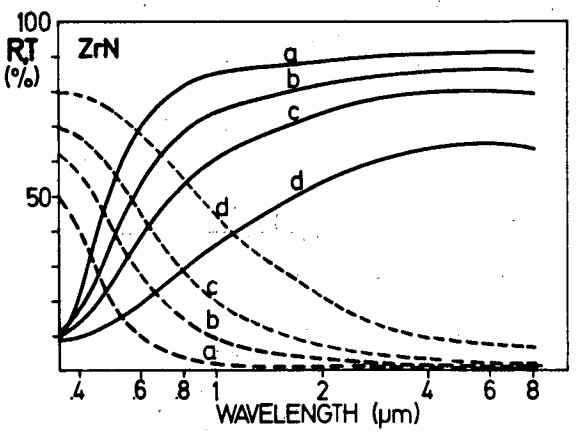

Fig. 5. Spectral reflectance and transmittance of ZrN-films of thicknesses a-500 Å, b-300 Å, c-200 Å and d-100 Å.

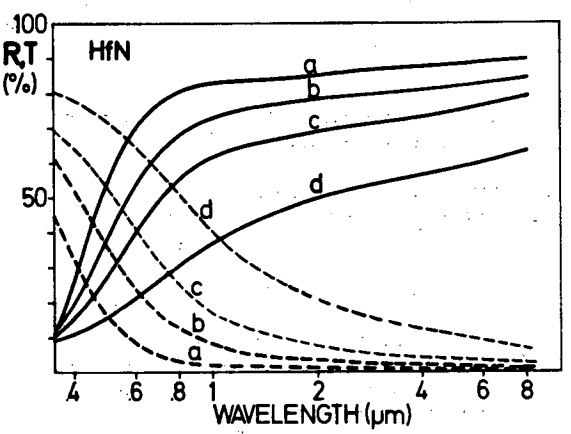

Fig. 6. Spectral reflectance and transmittance of HfN-films of thicknesses a-500 Å, b-300 Å, c-200 Å and d-100 Å.

The transmittance of these nitrides is surprisingly high. The spectral behaviour for HfN and ZrN are similar as expected from their bulk-reflectance. These transmittance-curves increase slowly with decreasing wavelength towards a maximum in the lower limit of the visible range. The bulk TiN has a reflectance-knee in the middle of the visible and has correspondingly a transmittance maximum at these wavelengths. If the spectral dependence of the transmittance of these nitrides is compared to that of the noble metals, TiN is most similar to Au while HfN and ZrN are similar to Ag.

The main difference between these compounds and the noble metals is the significantly lower IR-reflectance of the nitrides, which is due to their relatively low mobility. The precision of the IR-data are supposedly lower than the visible data because of the method of calculating n and k. The Kramers-Krönig method is very sensitive to small inaccuracies of the reflectance-measurement in the IR, where the denominator in the K-K integral assumes low values[15]. The IR-data of these compounds are also critically dependent on the quality of the samples, since impurities drastically affect the scattering-rate and thus the

relaxation-time. Such effects are pronounced in these compounds which often contain a large number of vacancies[16]. Correspondingly the scatter in the reported data of the electrical resistivity is very high[16]. The resistivity of the TiN used in this investigation is as low as 25 μΩ cm [4] which probably makes it difficult to prepare thin films of TiN with significantly better IR-performance than reported here. It has been reported, however, resistivities of ZrN as low as 7 μΩ cm [17].

Figure 7 presents integrated values of the reflectance and the transmittance over the solar spectrum and the sensitivity curve of the human eye and it also gives the room-temperature emittance as calculated from the IR-reflectance. The details in these integrations are given elsewhere[2]. It is noted here that T_{eye} for HfN is very similar to the same parameter for the best one of the noble metals: Au[18], while T_{eye} of TiN and ZrN stay even higher. The average solar transmittances of the nitrides are higher than those of Ag, Au and Cu for the same thicknesses. The reason for the high transmittance of the nitrides is their relatively low visible reflectance compared to the noble metals, which the latter

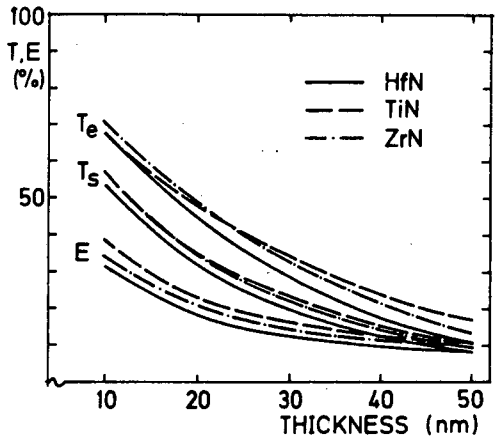

Fig. 7. Solar-transmittance, eye-transmittance and room-temperature emittance of thin films of TiN, ZrN and HfN.

cannot compensate by their very low internal absorptance. It must of course be noted that the emittance of these compounds is high compared to that of the noble metals. The noble metals would be superior if the transmittance is plotted as a function of emittance.

Multi-layer performance

In order to investigate the possibilities of increasing the transmittance of these compounds by the technique of induced transmission[19] they were assumed to be anti-reflected by one dielectricum or embedded between two dielectrica. The refractive index of the dielectricum was in all calculations assumed to be $n_o = 2.4$ without dispersion. This value represents in a good way ZnS, which is often used in this kind of applications[1]. A high value of the refractive index of the dielectricum is desired since it is known that the average solar- and eye-transmittances increase with increasing refractive index of the applied dielectricum[18]. The integrated parameters for these 3 nitrides are for the case of a single dielectricum given in figure 8. The thickness of the dielectricum has always been optimized for the actual nitride-thickness and application. Since the dielectricum is assumed to be non-absorbing it does not affect the IR-reflectance or equally the emittance.

Figure 9 shows the integrated optical parameters for triple-layer coatings, where the nitride is embedded between dielectrica of optimized thickness for each application and nitride-thickness. Both figure 8 and figure 9 underline the surprisingly high transmittance of these compounds. The transmittance of ZrN is higher than that of TiN and HfN when anti-reflected. This is mainly due to its lower value of the real part of the refractive index and the correspondingly lower internal absorptance.

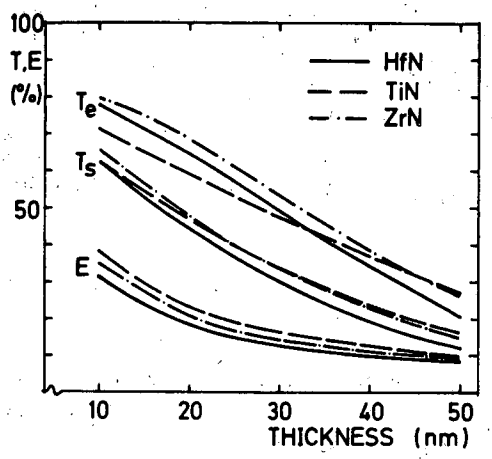

Fig. 8. Solar-transmittance, eye-transmittance and room-temperature emittance for thin films of TiN, ZrN and HfN coated with a dielectricum (n=2.4) of optimized thickness. The thickness of the dielectricum is typically 250 - 350 Å.

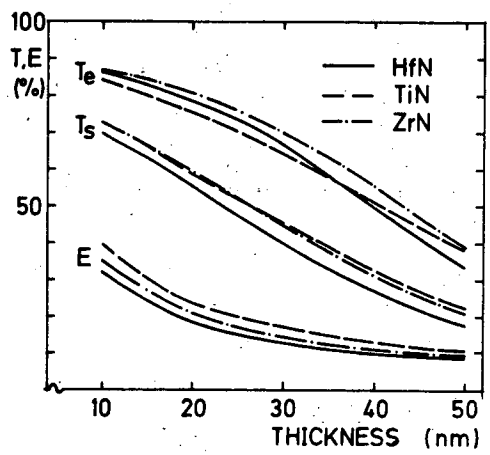

Fig. 9. Solar-transmittance, eye-transmittance and room-temperature emittance of thin films of TiN, ZrN and HfN embedded between two layers of dielectricum (n=2.4) of optimized thickness. The thickness of the dielectrica are typically 300 - 450 Å.

Finally the spectral dependence of the transmittance for selected 3-layer coatings is shown in figure 10. These coatings were designed with the goal to select the thicknesses of the dielectrica to maximize the visible transmittance with nitride-thicknesses of 200 Å. It appears that ZrN and HfN have the highest transmittance in the visible, while TiN has a higher NIR-transmittance due to its lower reflectance in that wavelength range as seen in figure 4. Figure 10 demonstrates a very good potential selective transmittance of those

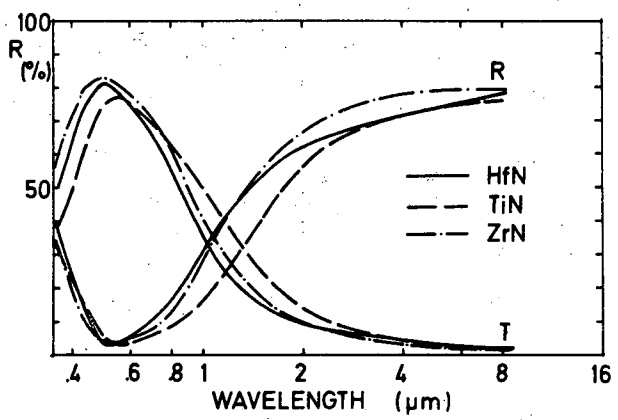

Fig. 10. Spectral reflectance and transmittance of 200 Å thick films of TiN, ZrN and HfN embedded in dielectric (n=2.4). The thicknesses are from the air-side: 400/TiN/450, 350/ZrN/400 and 350/HfN/450.

materials. A visible transmittance around 0.80 combined with an emittance of around 0.20 at a thickness which is probably possible to achieve with retained bulk optical constants. Preliminary measurements have indicated that films with thicknesses of 350 Å have an optical behaviour as predicted from these calculation. Further measurements on thin semi-trans-

parent TiN-films are under way and will be reported shortly[20].

Summary and conclusion

Thin films of the nitrides of Ti, Zr and Hf show, as expected for a free-electron-like metal, high transmittance over the relaxation region. TiN exhibits a transmittance peak at 0.5 μm, while ZrN and HfN have their transmittance-peak around 0.35 μm. It has been demonstrated that the transmittance can be significantly improved by the technique of induced transmittance. The main difference between these compounds and the noble metals is their shorter relaxation-time or equivalently lower mobility which in this case shows up as a relatively low IR-reflectance. This property is, as the resistivity, expected to be very dependent on the quality of the samples. Vacancies are known to be important for these materials.

It is wellknown that island-formation seriously decreases the IR-reflectance of thin films of the noble metals[2]. The difficulties involved in preparing very thin films which retain their bulk optical constants will probably be the limiting factor for the use of these nitrides as selectively transmitting layers.

If it is practically possible to coat large areas of glass with these compounds and with the optical properties described here, we believe that these coatings can be an alternative to the noble metals as selective coatings. This should be especially valuable where a coating of high chemical and mechanical resistance is desired.

Acknowledgements

Mr Anders Lundström is acknowledged for performing computer calculations. The work has been economically supported by the Swedish Natural Science Foundation under contract No. E-EG 4231-102.

References

1. Vossen, J. L., Phys. Thin Films, Vol. 9, 1 (1977).
2. Valkonen, E., Karlsson, B. and Ribbing, C. G., B. Karlsson, Thesis, University of Uppsala 1981, to be published.
3. Karlsson, B., Shimshock, R. P., Haygarth, J. C. and Seraphin, B. O., Nordic Solid Physics Conf., Copenhagen Aug. 1981, to be published, Physica Scripta.
4. Karlsson, B., Sundgren, J. E. and Johansson, B. O., UPTEC 81 98 R. Int. Report, Uppsala University.
5. Karlsson, B., Sundgren, J.-E. and Johansson, B.-O., Thin Solid Films, to be published.
6. Böhm, G. and Coretzki, H., J. Less-Common Met., Vol. 27, 311 (1972).
7. Schlegel, A., Wachter, P., Nikl, J. J. and Lingg, H., J. Phys., C 10, 4889 (1977).
8. Politis, C., Wolf, Th. and Schneider, H., Proc. 7th Int. Conf. on Chemical Vapor Deposition, 1979. The Electrochemical Society, Princeton, New Jersey, Vol. 79-3, 289.
9. Zega, B., Kornmann, M. and Amiguet, J., Thin Solid Films 45, 577 (1977).
10. Chassaing, G., François, J. C., Graner, P., Sigrist, M., Roux, L. and Chevallier, J., Proc. 8th Int. Vac. Congr., Vol. 2, 389 (Cannes 1980).
11. Rivory, J., Behagel, J. M., Berthier, S. and Lafait, J., Thin Solid Films 78, 161 (1981).
12. Knosp, H. and Goretzki, H., Z. Metallkd. 60, 587 (1969).
13. Fluck, F. W., Thesis, University of Karlsruhe (1977).
14. McLeod, H. A., Thin-Film Optical Filter, Adam Hilger LTD, London 1969.
15. Wooten, F., Optical Properties of Solids, Academic Press, New York 1972, ch. 6.
16. Tooth, L. E., Transition Metal Carbides and Nitrides, Refractory Materials 7, Academic Press New York 1971.
17. Bennet, L. H., McAlister, A. J. and Watson, R. E., Physics Today, Sept. 1977, 34 (1977).
18. Karlsson, B. and Valkonen, E., to be published and B. Karlsson thesis, University of Uppsala 1981.
19. Berning, P. H. and Turner, A. F., J. of Opt. Soc. 47, 230 (1957).
20. Karlsson, B., Sundgren, J.-E., Johansson, B.-O. and Ribbing, C.-G., to be published.

Transparent heat reflecting coatings (THRC) based on highly doped tin oxide and indium oxide

G. Frank, E. Kauer, H. Köstlin
Philips GmbH Forschungslaboratorium Aachen
Weisshausstrasse, 5100 Aachen, West Germany

F. J. Schmitte
I. Physikalisches Institut der RWTH Aachen
Sommerfeldstrasse, 5100 Aachen, West Germany

Abstract

A number of highly doped oxides - in particular SnO_2 and In_2O_3 - have been reported to show high infrared reflectivity while being transparent to visible radiation. Their optical behaviour is based on metal-like properties i.e. high concentration and mobility of the conduction electrons and a semiconductor bandgap of about 3 eV or higher. Thin films of these oxides can be adapted for many applications and a few examples will be described. The performance of these filters strongly depends on the doping and preparation conditions. Coatings prepared by spray pyrolysis show excellent electrical and optical properties, the upper limits of which are being discussed on the basis of defect mechanisms in solids.

1. Introduction

Modern energy technology has led to a demand for filters which have a high reflectivity in the infrared part of the spectrum while being transparent for visible radiation. Filters of this type can be realized with thin metal films coated with dielectrics to reduce the visible reflection losses. These filters, however, still show some unavoidable absorption losses which might be prohibitive for some applications. Since the high infrared reflection of metals is a consequence of their high electrical conductivity, i.e. of the presence of free electrons, one can achieve metal-like optical properties in the infrared also with highly doped semiconductors. The basic theoretical description is in both cases the same. There are a number of semiconducting oxides which provide the initial properties for heat-reflecting layers but we shall focus in particular on SnO_2 and In_2O_3 which have proven to be the best candidates as far as high infrared reflectivity and visible transparency are concerned. Although the properties of heat-reflecting films are very sensitive with regard to the preparation methods and conditions which might vary over a wide range, we shall try to answer the question as to the upper limits of electron concentration and mobility from which the basic properties of these filters are determined. Four examples of the application and optimization of such filters for special purposes will be given: (1) high-efficiency low pressure sodium lamps, (2) highly efficient solar collectors, (3) cool light emitting incandescent lamps, and (4) double-glazed windows with improved heat insulation.

2. Principles of heat-reflecting filters

The optical properties of free electrons in metals were explained by Drude[1] as early as 1900 by solving the equation of motion of electrons in an alternating electric field. His findings were slightly modified by modern quantum mechanical treatment but for the sake of clarity we shall use the classical description. In order to calculate the transmission and reflection of thin films the complex refractive index $\tilde{n} = n - ik$ has to be known. For a material containing a free electron gas the following dispersion relations hold for the complex dielectric constant $\tilde{\varepsilon} = \varepsilon' - i\varepsilon'' = \tilde{n}^2$

$$\varepsilon' = n^2 - k^2 = \varepsilon_L - \frac{\omega_N^2}{\omega^2 + \gamma^2} \tag{1}$$

$$\varepsilon'' = 2nk = \frac{\gamma}{\omega}\frac{\omega_N^2}{\omega^2 + \gamma^2} \tag{2}$$

where ε_L represents the dielectric constant of the lattice in the absence of free charge carriers and ε_o the permittivity of free space. The frequency ω_N and the damping constant γ correlate with the density N and mobility μ of the free electrons with $\omega_N^2 = Ne^2/\varepsilon_o m^*$ and $\gamma = e/m^*\mu$, e being the electronic charge and m^* the effective mass of the free electrons in the conduction band. The plasma frequency ω_p and plasma wavelength $\lambda_p = 2\pi c_o/\omega_p$ result from $\varepsilon' = 0$. λ_p is given by

$$\lambda_p = 2\pi c_o (Ne^2/\varepsilon_o \varepsilon_L m^* - \gamma^2)^{-1/2} \qquad (3)$$

It marks a drastic change in the conduction mechanism, namely from a conduction current for $\omega < \omega_p$ to a polarization current for $\omega > \omega_p$. Thin films of highly doped semiconductors show a behaviour which is closely related to this change in the conduction mechanism. We find a region of high transmission at short wavelengths and a region of high reflectivity at long wavelengths provided the dope concentration and film thickness are chosen appropriately.

The slope in the cut-off region of the filter and its maximum infrared reflectivity increase with decreasing γ which therefore should be as small as possible or the mobility μ as high as possible. In the materials under discussion γ can be neglected in equ. (3) allowing the cut-off wavelength λ_p to be adjusted by the electron concentration N or the doping procedure respectively. To obtain a cut-off wavelength within the near infrared region, an electron concentration of the order of 10^{20} to 10^{21} cm^{-3} is required in these materials.

3. Preparation and experimental results

3.1. SnO_2 films

Tin oxide in the form of thin films on glass has long been used as transparent electrodes and transparent electric heater coatings on glass. These early films had however, if at all, a rather low infrared reflectivity. The first large-scale industrial application of SnO_2 heat-reflecting films dates from 1964 when Philips introduced a new type of low pressure sodium lamp.[2] The SnO_2 films which were used in these lamps were prepared by spray pyrolysis, where an aerosol of $SnCl_4$ in an organic solvent is blown together with the dope onto a heated glass substrate. Figure 1 shows the spectral transmission T and the reflection R of three fluorine doped SnO_2 films on glass with different electron densities and Hall mobilities up to 30 cm^2/Vs.[3]

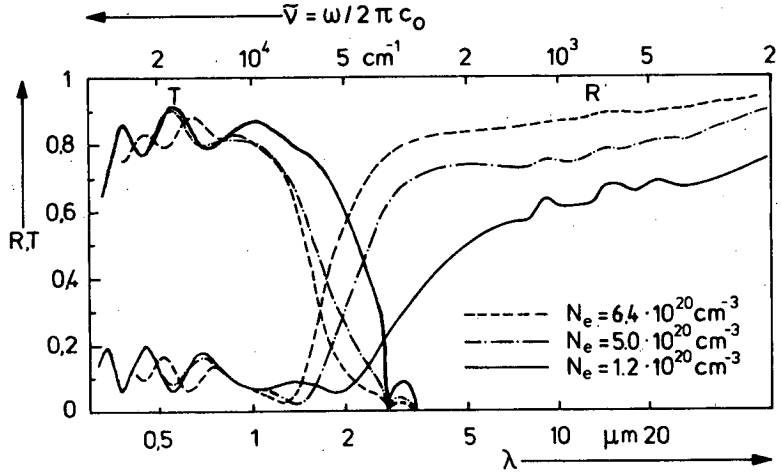

Figure 1. Spectral reflection R and transmission T of three SnO_2:F films, thickness about 0.3 µm.

Many attempts have been made to improve the electrical properties of these films, or at least to understand the limiting physical phenomena. Such attempts are hampered by the variety of preparation methods like evaporation, sputtering, reactive modification of both, chemical vapour deposition and spray pyrolysis. The investigations become even more complicated by the many parameters which might influence the results, i.e.

- kind of dope and doping concentration
- constitution of the reaction atmosphere
- temperature and nature of substrate
- growth rate / preparation time
- film thickness
- annealing in various atmospheres and at various temperatures, etc.

In spite of the complex interaction of these preparational parameters there seems to be a convergence to some upper limits of performance, i.e. electron concentration and mobility. As far as preparation methods are concerned those using high substrate temperatures ($T_S \geq 400^\circ$C) are favourable for achieving a high conductivity. The spray technique which in itself requires high temperatures results in electrical properties which otherwise can hardly be achieved by additional heating or suitable after-treatment of the samples.

The conduction mechanism of SnO_2 is based on a suitable dope, preferably F or Sb, and on oxygen vacancies, all acting as donors. The upper limit of electron density is determined by the solubility of the doping elements. In the case of fluorine the excess is volatile whereas in the case of antimony the excess clusters in the lattice, resulting in a darkening of the films which is not correlated to an increase in free electron density.

Figure 2 shows the resistivity ρ, the electron density N and the mobility μ after a reducing annealing versus the HF dope concentration in the spray solution of films prepared in ambient atmosphere at two temperatures. The resistivity falls with increasing dope concentration and tends to saturate at about 20 mol% HF, where the free electron density reaches a maximum value of about $6 \cdot 10^{20}$ cm^{-3}. The straight line describes the free electron density for the case that every fluorine atom in the spray solution would be incorporated in the film and act as donor. In fact, however, only about one tenth of the expected electron density can be achieved. These observations are in good agreement with the results of Manifacier.[4] At low HF-concentrations the free electron density becomes independent of the doping and is determined by oxygen vacancies. The mobility is nearly independent of the dope but increases with the deposition temperature to values of $\mu > 20$ cm^2/Vs. The temperature influence on the mobility may be due to the observed tendency of the films to form larger crystallites with increasing temperature. A discussion of the free electron scattering mechanism will be given later.

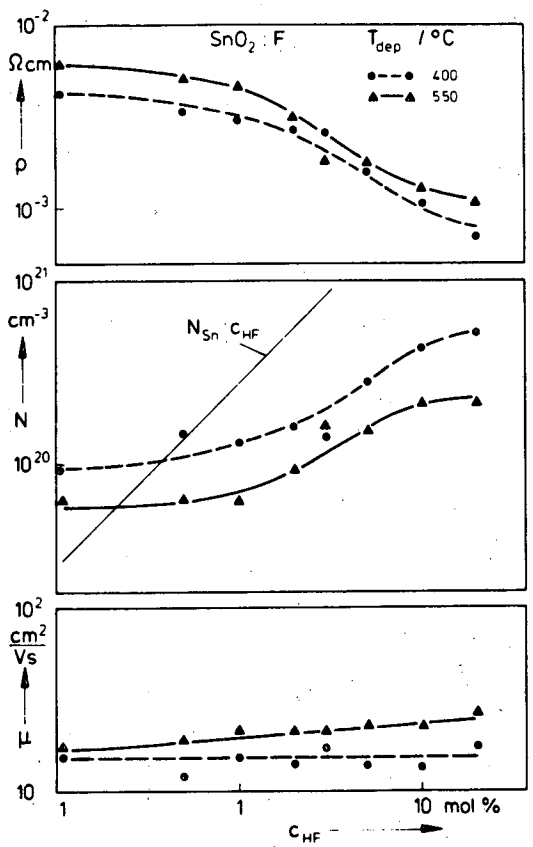

Figure 2. Resistivity ρ, density N and Hall mobility μ of free electrons in SnO_2:F films, spray-deposited at two different substrate temperatures T_{dep}. after reducing heat treatment, versus dope concentration in the spray solution.

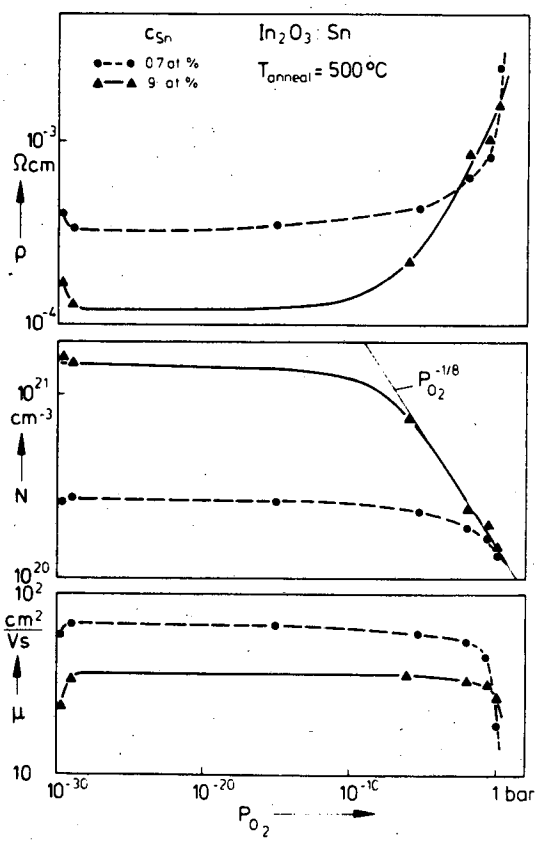

Figure 3. Resistivity ρ, density N and Hall mobility μ of free electrons in In_2O_3:Sn films of two dope concentrations c_{Sn} versus the oxygen partial pressure p_{O_2} of the annealing gas atmosphere.

3.2. In_2O_3 films

Doped indium oxide films on glass have become a favoured material for the preparation of transparent, highly conductive and IR reflecting thin films in the last decade, although indium is a quite costly metal. The In_2O_3 films are superior to SnO_2 films because they can

be prepared with higher conductivity and IR reflectivity and also fine structures for patterned electrode application can be etched more easily in these films. The deposition of the films can be done by the different methods mentioned above. They all lead to more or less the same material properties, provided that the films can grow with good crystallinity which normally requires enhanced substrate temperatures. Various electron donors were investigated, e.g. on anion sites: oxygen vacancies and F, and on cation sites: higher valent metals like Sn, Ti, Zr, Sb, Nb.[5] The influence of the dope is often masked - and this is the most confusing factor in the experimental data given by earlier authors - by additional oxygen. This oxygen acts in two ways which both reduce the conductivity: electrons originally sponsored from the dope are trapped and the mobility of the remaining electrons is decreased. Both effects are independent of the material used as dope. Generally, at low dope concentrations oxygen mainly influences the mobility of the free electrons and at high dope concentrations mainly their density.[6] Figure 3 shows the influence of the oxygen pressure on the electrical properties of tin doped indium oxide films. In the high pressure range the electron density decreases following a $p_{O_2}^{-1/8}$ relation, which can be correlated to the trapping activity of additionally incorporated interstitial oxygen. At the borders of the pressure range shown the mobility falls drastically. Low resistivity can be obtained over a very broad region under mild reducing conditions. A similar but less pronounced behaviour is observed in SnO_2.

To compare the different dopes the oxygen effect should be eliminated. Samples with different dope materials and concentrations were spray-deposited and reduced to their resistivity minimum. Figure 4 shows the electron density obtained versus dope concentration in the films.

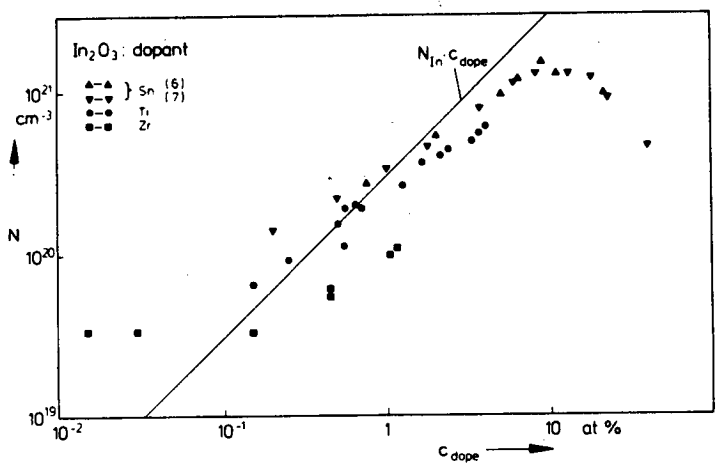

Figure 4. Free electron density N in In_2O_3, doped with Sn, Ti or Zr, versus the concentration of the different dopes c_{dope} in the films.

Within a range of a few at% the experimental results roughly follow the straight line which is to be expected if one dope atom sponsors one free electron. The highest free electron densities obviously result by doping with tin and the absolute maximum of about $1.5 \cdot 10^{21}$ cm^{-3} follows from its solubility limits.[7,8,9] Doping with titanium or zirconium is less effective in the spray-deposited films.

3.3. Comparison of SnO_2 and In_2O_3 films

The special features of both materials regarding their application as transparent heat mirrors may be discussed by comparing the spectral reflectance and transmittance of different films of the same thickness. Such spectra are shown in Figure 5 for two tin doped In_2O_3 films (ITO) and a fluorine doped SnO_2 film.[7,2] The plasma wavelength (arrows) in In_2O_3 can be shifted to shorter wavelengths than in SnO_2, which is a consequence of the higher free electron densities obtainable. In addition, comparing a SnO_2 film with an In_2O_3 film of roughly the same free electron density, a better infrared reflectance and a better visual transmittance is observed in In_2O_3. This is the result of the higher mobility of the free electrons in In_2O_3.[10]

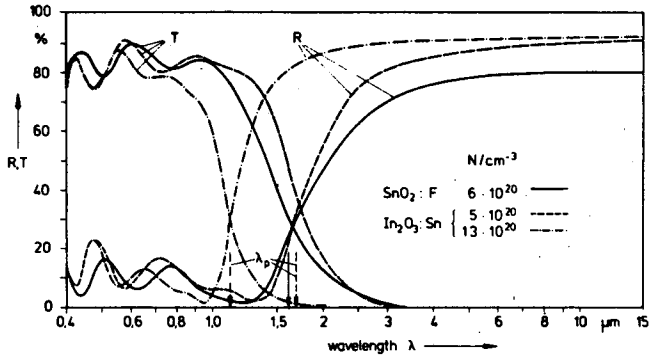

Figure 5. Spectral reflection R and transmission T of two In_2O_3:Sn films compared with a SnO_2:F film, thickness about 0.3 μm. The plasma wavelengths are indicated by arrows.

Furthermore, the analysis of the mobility as a function of the free electron density gives some insight into the limiting mechanisms of the conductivity of the materials. In Figure 6 the mobility is plotted versus the density of the free electrons for SnO_2 doped with F and for In_2O_3 doped with Zr, Ti or Sn. The different dopants in In_2O_3 result in μ-N data which fit quite well with one another on a more or less continuous line. The fully drawn line is calculated for electron scattering by ionized impurities[11], using the parameters $m^* = 0.3\ m_e$ and $\varepsilon_L(\omega=0) = 9.5$. In case of In_2O_3 the mobility roughly follows the fallir μ-N relation of the theory. In contrast, in SnO_2 nearly no influence of the free electron density on the mobility is observed and the values are mostly too low. Anyway, from the magnitude of μ and the μ-N behaviour in In_2O_3 at high free electron densities, ionized impurity scattering seems to be the most probable damping mechanism in both materials.

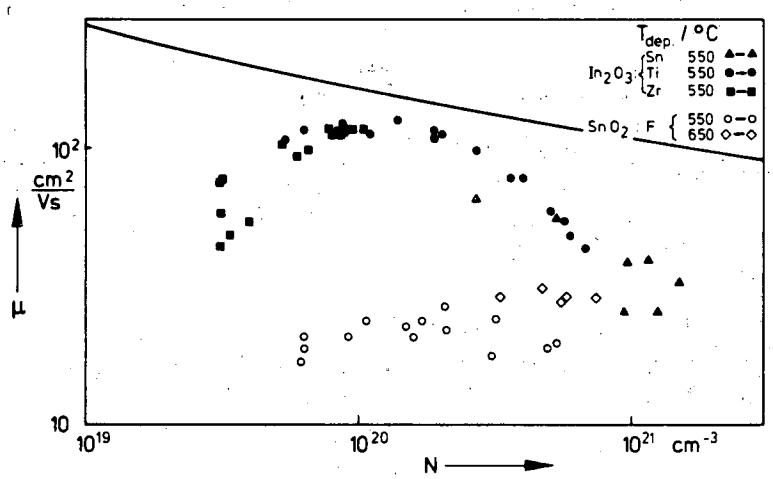

Figure 6. Hall mobility μ versus free electron density N of differently doped In_2O_3 and SnO_2 films. Full line calculated for scattering by ionized impurities.

This can be confirmed additionally by an analysis of the frequency dependent dynamic resistivity $\rho'(\omega)$ which can be derived from the optical data. Theories of different scattering mechanisms lead to characteristic frequency dependences of the form $\rho' \sim \omega^\nu$.[11] In the case of ionized impurity scattering the exponent is $\nu = -3/2$ for high frequencies $\omega > \omega_N$. Figure 7 shows the dynamic resistivity $\rho'(\omega)$ of some SnO_2 and In_2O_3 films. We find constant values at low frequencies, i.e. wavelengths longer than the plasma wavelength which roughly agree with the dc resistivity of the various samples. In the short wavelength region, however, the resistivity ρ' decreases approximately as a function of $\omega^{-3/2}$, which confirms the assumption that ionized impurity scattering is the main damping mechanism of the free electrons in highly doped tin and indium oxide.

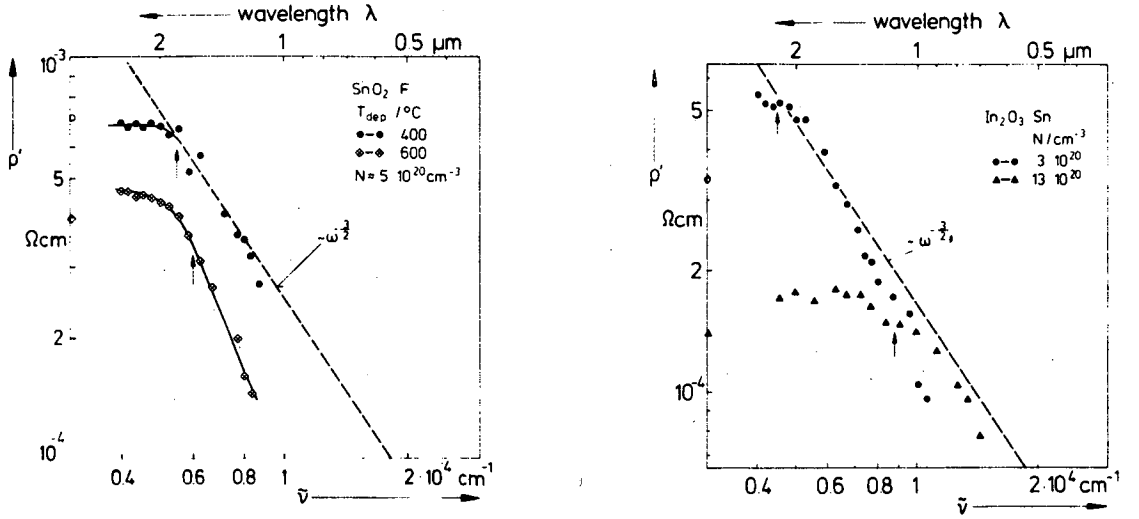

Figure 7. Real part of the dynamic resistivity ρ' of two SnO_2:F and two In_2O_3:Sn films in the spectral range around the plasma wavelength (indicated by arrows). The values of the dc resistivities are plotted on the ordinate axis. The slope of the dashed lines is characteristic for ionized impurity scattering.

The positive consequence of this effect is a visual absorption much lower than that estimated from the dc values of the Drude model.

4. Applications of heat-reflecting filters

4.1. Thermal insulation of sodium lamps

The discharge tube of a low pressure sodium lamp has to be kept at a temperature of about 270°C in order to provide the optimum sodium pressure of some 10^{-6} bar. The convection and conduction losses of the discharge tube are eliminated by evacuating the envelope of the lamp (Figure 8a). The remaining losses mainly consist of the thermal radiation of the discharge tube since glass behaves almost as a black body in the infrared. For an uncoated 140 W lamp about 100 W are lost by thermal radiation. To reduce these losses the interior surface of the outer envelope is coated with a filter as indicated in Figure 8a.

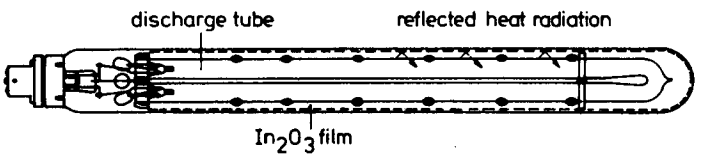

Figure 8a. Schematic diagram of a sodium lamp. The dashed line on the inside of the envelope indicates the heat-reflecting filter.

In a first approach using SnO_2 filters[2] the luminous efficiency could be increased from about 100 lm/W to 150 lm/W. Even better results have been realized with the latest version of the sodium lamp where In_2O_3 filters are used.[12] A typical transmission/reflection curve of an In_2O_3 film used in the sodium lamp is shown in Figure 8b and makes evident that the major fraction of the infrared radiation is reflected onto the discharge tube. Sodium lamps coated with In_2O_3 films achieve a luminous efficiency up to 180 lm/W (laboratory models even 200 lm/W) which is the highest value among present day light sources.

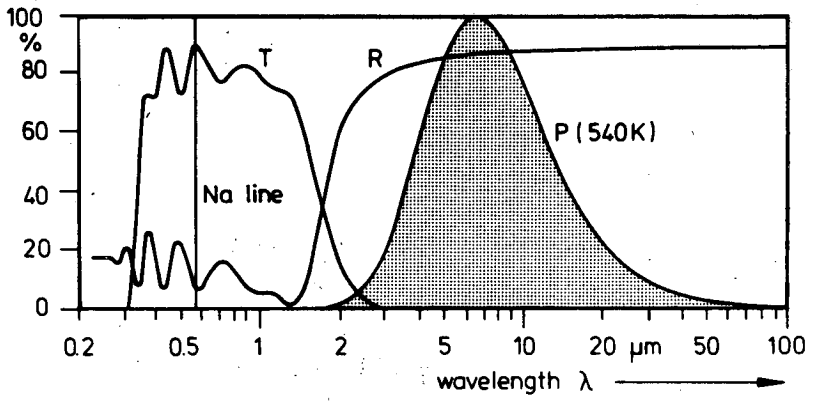

Figure 8b. Spectral transmission T and reflection R of an In_2O_3 film as compared with the energy distribution of a black body at 540 K radiating into surroundings at 300 K, and the position of the sodium lines at 0.59 µm.

4.2. Highly efficient solar collectors

In the most simple case a solar collector for photothermal conversion consists of a black absorber plate through which the exchange fluid circulates. At least one glass cover has to be added to reduce the convection losses of the absorber plate. To reduce the re-radiation losses, which account for about two thirds of the total losses, one has to aim at a low infrared emissivity of the collector plate or at a high infrared reflectivity of the adjacent glass cover. Figure 9b shows the case if a heat-reflecting filter is used. As a consequence of the high reflectivity of the In_2O_3 film in the spectral range of the effective heat radiation the heat losses due to radiation are reduced by almost an order of magnitude. The remaining losses due to conduction and convection can be avoided by evacuating the collector which can be realized by a tubular design. Figure 9a shows the type I collector developed in the Philips Research Lab. Aachen.[13]

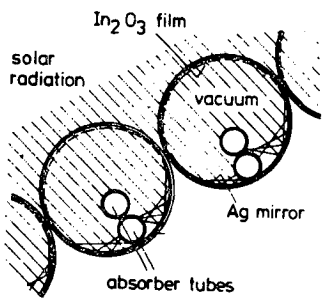

Figure 9a. Cross section of solar collector Philips type I.

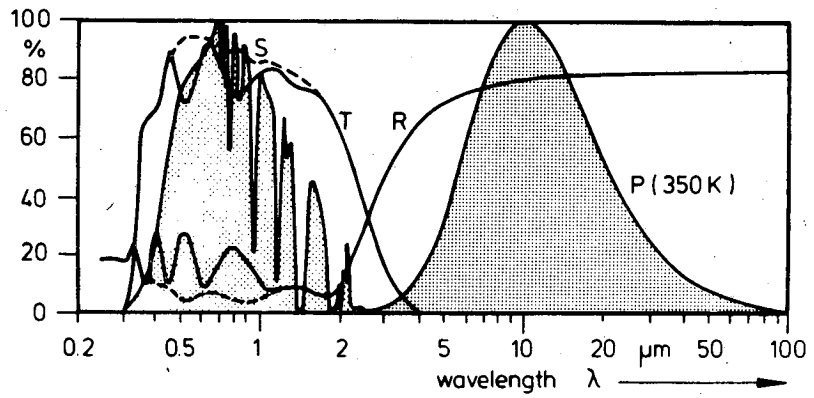

Figure 9b. Relative spectral distribution of solar insolation and heat radiation, transmission and reflection of an In_2O_3 film. Dashed lines: additional anti-reflection coating.

The sunlight passes the outer tube and the In_2O_3 film and is absorbed at the U-shaped absorber tubes either directly or after reflection by the mirrored lower half-cylinder. The incidence characteristic of this collector comes close to that of a flat plate type. The measured performance of a complete collector module consisting of such tubes is $\alpha \cdot \tau = 0.77$ with a loss coefficient between 1.5 and 2.0 W/m^2K which is about half that of conventional flat plate collectors with two glass plates and selective absorber.

4.3. Cool light incandescent lamp

In incandescent lamps only a small amount of their total radiation is emitted as visible light. As shown in Figure 10b, the major part of the radiation is emitted in the infrared with a maximum at about 1 μm. To reduce the heat load of illuminated objects, an In_2O_3 filter might be applied on the inner side of the front plate[14], as indicated in Figure 10a.

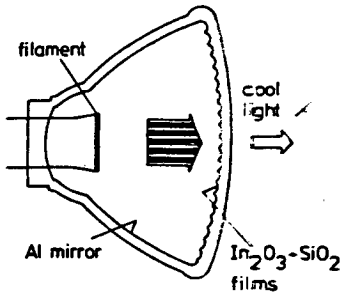

Figure 10a. Incandescent lamp with heat-reflecting filter.

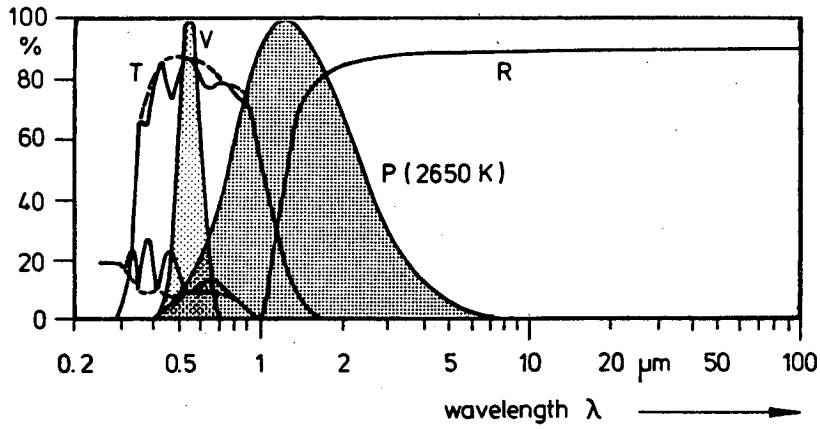

Figure 10b. Spectral distribution of the lamp, sensitivity curve of human eye V(λ), transmission and reflection of the applied filter. Dashed lines: with protective and anti-reflecting SiO_2 coating.

An efficient filter for application in incandescent lamps requires, as Figure 10b demonstrates, a plasma wavelength close to the long wavelength limit of the visual sensitivity coupled with a steep R,T-characteristic. This implies high electron densities and mobilities which, however, can only be realized up to the physical limits already discussed. Nevertheless, the filter shown suppresses two thirds of the heat load.

4.4. Improved heat insulation of double-glazed windows

Heat losses through windows play an important role in the energy balance of buildings. This applies even when double-glazing is used because its overall heat transfer coefficient of k = 3.1 W/m^2K is several times higher than that of well-insulated brickwork which nowadays has k-values lower than 1 W/m^2K. In keeping with the present demand for lower energy consumption there is an urgent need for a form of glazing whose overall heat transfer coefficient is considerably lower than that of contemporary double-glazing. In these windows

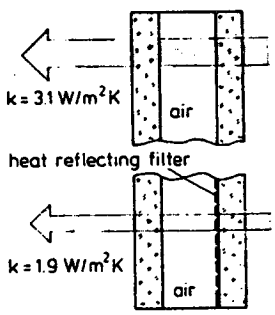

Figure 11a. Cross section of a double-glazed window.

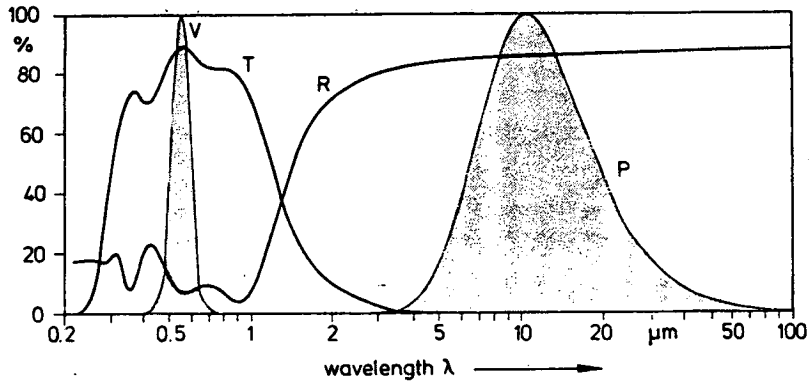

Figure 11b. Spectral distribution of radiation P exchanged between two glass plates at about 273 K. V is the sensitivity curve of the human eye, T and R the spectral transmission and reflection of an In_2O_3 film (thickness ≈ 0.15 μm).

about two thirds of the heat transport take place via thermal radiation between the glass surfaces. This part can be reduced by coating the inner surface(s) of the panes with a heat-reflecting layer of tin or indium oxide[15], as shown in Figure 11a. In Figure 11b curve P represents the spectral distribution of the radiation between black surfaces that differ relatively little in temperature. This curve is obtained as a temperature derivati of the Planck function at 273 K and gives an adequate description of the radiative energy flow between two glass panes.

In the spectral range of P the reflection of the In_2O_3 filter is about 0.85 correspond to a thermal emissivity of about 0.15. This means that the radiation losses are cut down t at least a factor of 6 while the transmission of light is almost unimpaired. A double-gla window supplied with this filter has a heat transfer coefficient of 1.9 W/m^2K. An even lo value might be obtained by filling the space between the panes with a gas of lower thermal conductivity than air.

References

1. Drude, P., Phys. Z. 1, 161 (1900).
2. Groth, R. und E. Kauer, Philips Techn. Rundschau 25, 352 (1963/64).
3. Grosse, P., F.J. Schmitte, G. Frank, H. Köstlin, 5th Int. Conf. on Thin Films, Herzlia, Israel, Sept. 21-25, 1981.
4. Manifacier, J.C., 5th Int. Conf. on Thin Films, Herzlia, Israel, Sept. 21-25, 1981.
5. Groth, R., phys. stat. sol., 14, 69 (1966).
6. Frank, G. and H. Köstlin, submitted to Applied Physics (1981/82).
7. Köstlin, H., R. Jost and W. Lems, phys. stat. sol. (a), 29, 87 (1975).
8. Frank, G., L. Brock and H.D. Bausen, J. of Crystal Growth 36, 179 (1976).
9. Frank, G., H. Köstlin and A. Rabenau, phys. stat. sol. (a), 52, 231 (1979).
10. Frank, G., E. Kauer and H. Köstlin, Thin Solid Films, 77, 107 (1981).
11. Gerlach, E. and P. Grosse, Festkörperprobleme (Advances in Solid State Physics), 17, 157-193, Vieweg, Braunschweig (1977).
12. van Boort, H.J.J. and R. Groth, Philips Techn. Rev. 29, 17 (1968).
13. Hörster, H., R. Kersten and F. Mahdjuri, Klima + Kälte Ingenieur, 13, 113 (1976).
14. Köstlin, H., R. Jost and H. Auding, Deutsche Offenlegungsschrift 26 48 878 (1978).
15. Köstlin, H., Elektrizitätsverwertung, 49, 458 (1974).

This paper is dedicated to Prof. A. Rabenau, Max-Planck-Institut für Festkörperforschung, Federal Republic of Germany, on the occasion of his 60th birthday.

High quality transparent heat reflectors of reactively evaporated indium tin oxide

I. Hamberg, A. Hjortsberg, C. G. Granqvist
Physics Department, Chalmers University of Technology, S-412 96 Gothenburg, Sweden

Abstract

We report on transparent and heat-reflecting Indium-Tin-Oxide (ITO) films prepared by well controlled reactive electron-beam evaporation of In_2O_3 + 9 mol. % SnO_2 onto glass in ~ 5×10^{-4} Torr of O_2. Typical results for 0.3 μm thick films deposited on substrates at 300°C were: visible light absorptance $\lesssim$ 2 %, thermal infrared reflectance $\gtrsim$ 90 %, and dc resistivity $\lesssim 3 \times 10^{-4}$ Ωcm. Similar properties were found for substrate temperatures down to 150°C, whereas a rapid deterioration took place at still lower temperatures. After antireflection coating with ~0.1 μm of evaporated MgF_2, the visible transmittance became ~ 1 % larger than that of the uncoated glass, while the infrared reflectance increased by a few percent only. The ITO + MgF_2 coatings show much weaker iridescence than the bare ITO films.

Introduction

Indium-Tin-Oxide (ITO) is a wide-bandgap n-type semiconductor which can be so heavily doped that the free-electron plasma wavelength falls in the near-infrared range. Properly prepared thin films of this material show a combination of excellent short-wavelength transmittance and long-wavelength reflectance, low resistivity, good substrate adherence, hardness and chemical inertness[1,2]. Such films have interesting applications for example as transparent and infrared-reflecting coatings on windows and on cover glasses of solar collectors.

ITO films can be produced by many different methods[3]. In the present paper we report on films made by slow reactive electron-beam evaporation onto heated glass substrates[4]. This technique, though not useful for large-scale fabrication of coated glass, has the advantage of permitting a very detailed control of the deposition parameters so that an accurate optimization of the film properties can be achieved. As a consequence of this control, the optical and electrical performance of our ITO coatings matches - or is superior to - the best data obtained for this kind of films prepared by any technique. In particular, the absorptance of our optimized ITO films is so weak that an antireflection coating of evaporated MgF_2 yields a visual transmittance which is larger than for the uncoated glass while the infrared reflectance remains $\gtrsim$ 90 %. Furthermore, the MgF_2 film efficiently wipes out the interference colours (iridescence) resulting from small unintensional variations in the ITO thickness.

Preparation of ITO films

The films were made by e-beam evaporation of ITO in the unit shown in Fig. 1. It comprises a stainless steel vacuum chamber with LN_2-trapped diffusion pump, e-gun, vibrating quartz microbalance, shutter, and substrates clamped to an electrically heated holder. The distance between e-gun and substrates is ~ 50 cm. The system was first pumped to

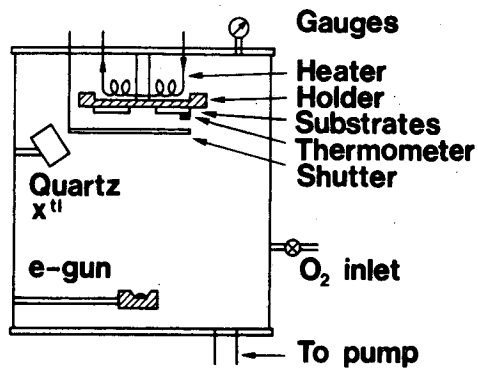

Figure 1. Schematic diagram of the evaporation system.

~ 10^{-6} Torr and a constant O_2 pressure was then maintained by continuous inlet through a precision leak-valve at full pump capacity. Uniform films were produced by evaporating In_2O_3 + 9 mol. % SnO_2 (hot-pressed pellets from Kyodo International, Japan; 4N purity) from the 8 kW e-gun by automatically sweeping the e-beam over the hearth. The evaporation rate was monitored on a vibrating quartz microbalance, whose output was used to feed-back control the e-gun power. In this way we maintained constant rates (generally 0.2 nm/s) up to ultimate thicknesses of 0.3 to 0.4 μm. Accurate film thicknesses were determined after deposition by use of a mechanical stylus instrument and several optical techniques. To provide the needed temperatures of the substrates (Corning 7059 glass or standard microscope slides), these were clamped to a copper plate held at a constant temperature in the 25 - 400 - ^{o}C range. Small resistance thermometers were used to measure the surface temperature of the substrates during deposition.

Transmittance and reflectance of ITO films

Figure 2 shows near-normal transmittance (T) and reflectance (R) for a 0.42 μm thick ITO film evaporated in an atmosphere of 10^{-3} Torr of O_2 onto Corning 7059 glass at ~ 310^{o}C. The dashed line indicates the transmittance of the uncoated glass. These data were recorded on double-beam spectrophotometers with specular reflectance attachments; a Beckman ACTA MVII instrument was used in the 0.3 - 2.5-μm range and a Perkin-Elmer 580B instrument in the 2.5 - 50-μm range. The mean transmittance in the visible range is found from Fig. 2 to lie ~ 8 % below that of the uncoated glass, and the reflectance for room-temperature thermal radiation is ~ 92 %. The transition between short-wavelength transmittance and long-wavelength reflectance is very abrupt. The overall shape of our curves is in good agreement with transmittance and reflectance data for the best films prepared by alternative techniques such as sputtering[5-7] and chemical vapour deposition[8,9]. From Fig. 2 we note that the absorptance (given by 1 - T - R) is only a few per cent over the entire visible spectral range.

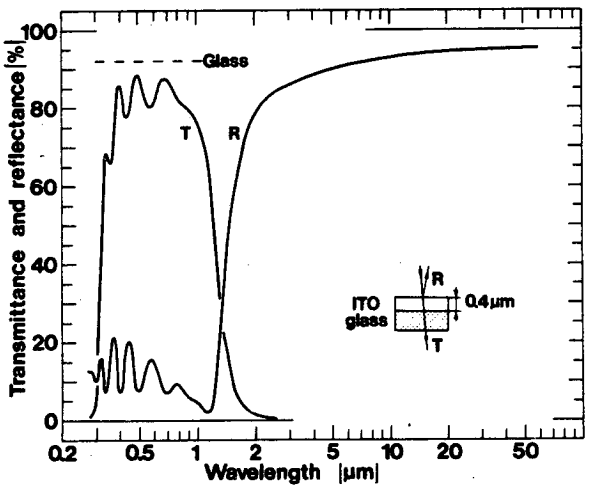

Figure 2. Measured near-normal transmittance and reflectance for an ITO film. The measurement configuration is shown in the inset.

The optical properties of our optimized ITO films could be accurately reproduced over the whole wavelength range by using the Drude free-electron model to account for the free carriers in the films[4]. Typically, we found a plasma energy of 0.9 eV, a relaxation energy of 0.1 eV and a high frequency (visible) dielectric constant of 3.5. These data compare well with published results for sputtered ITO films[5-7].

Film quality versus deposition parameters

The optical and electrical quality of the e-beam evaporated ITO films is dependent on the deposition parameters - such as substrate temperature, oxygen pressure and deposition rate - in an intricate manner. Films prepared by vacuum evaporation were opaque. Mass spectrometry clearly showed a release of free oxygen during the deposition, so these films were metal-rich. With low O_2 pressure in the evaporation chamber ($\lesssim 10^{-4}$ Torr) the visible transmittance increased continuously with increasing substrate temperature, T_s, up to ~350^{o}C. However, at sufficiently high O_2 pressure ($\gtrsim 5 \times 10^{-4}$ Torr in our experimental configuration) high-quality films with properties like those in Fig. 2 were obtained provided that T_s was sufficiently high. This temperature dependence is elaborated below.

The main part of Fig. 3 shows mean visible absorptance (averaged linearly over the 0.5 - 0.6-μm range) versus T_s for approximately 0.3 μm thick films produced by evaporation in ~5×10^{-4} Torr of O_2 at a rate of 0.2 nm/s. The scatter among the individual data points is partly due to somewhat varying thicknesses. The curve is drawn only as a guide to the eye. The absorptance is seen to be low for $T_s \gtrsim 150^{\circ}C$ and to increase rapidly at lower temperatures. At $T_s = 320^{\circ}C$ the absorptance is as low as ~2 %; this value contains a substrate absorptance of roughly 1 %, so the actual film absorptance is in the one-percent-range. The inset in Fig. 3 depicts spectral absorptance for four ITO films. An absorptance minimum is found to lie in the mid-visible range in the films prepared at $T_s \gtrsim 150^{\circ}C$.

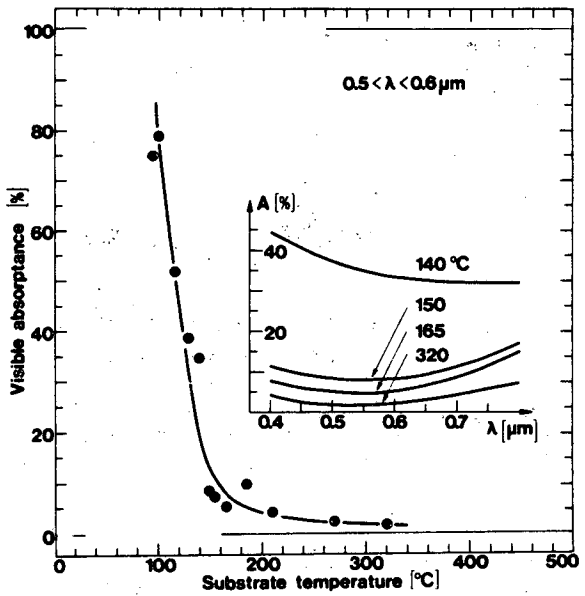

Figure 3. Visible absorptance versus substrate temperature for e-beam evaporated ITO films.

Figure 4 shows near-normal reflectance at 10 μm wavelength for the same ITO films as reported in Fig. 3. A reflectance of ~90 % is found at $T_s \gtrsim 150^{\circ}C$, whereas a rapid deterioration takes place at lower substrate temperatures, similar to the case of the visible transmittance.

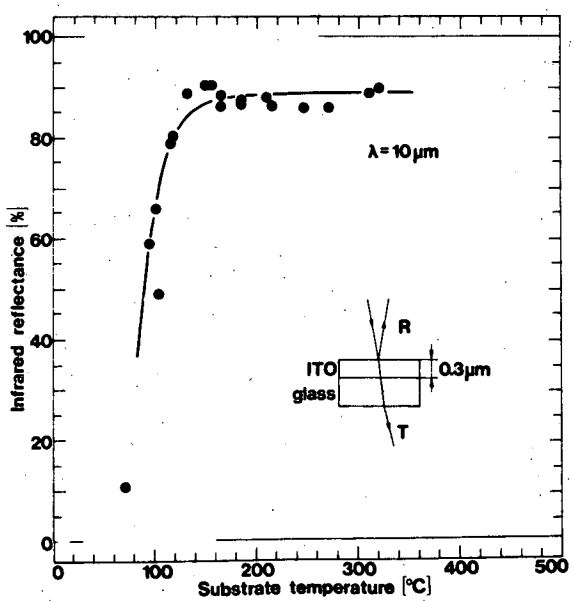

Figure 4. Infrared reflectance versus substrate temperature for e-beam evaporated ITO films.

The dc resistivity is closely correlated with the infrared reflectance. Figure 5, which pertains to the same films as in Figs. 3 and 4, shows the expected behaviour, viz. the resistivity rapidly increases at $T_s \leq 150^{\circ}C$. At $T_s \geq 300^{\circ}C$ the resistivity can be as low as $\sim 2 \times 10^{-4}$ Ωcm. This is in agreement with some earlier results.[10]

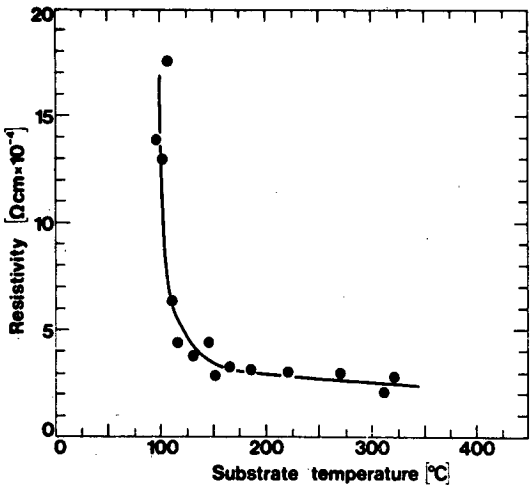

Figure 5. Dc resistivity versus substrate temperature for e-beam evaporated ITO films.

Antireflection coated ITO films

The refractive index of ITO films is rather high in the visible wavelength range (~ 1.9 for our films) and their inherent absorptance can be very weak. Hence a suitable antireflection coating can provide a substantial enhancement of the transmittance by bringing down the front surface loss. We used MgF_2, which has a refractive index of 1.38. These films were deposited onto the ITO coated glass at room temperature by resistive evaporation from a molybdenum boat in a small standard bell-jar system. The reflectance from the tandem coating was monitored continuously during the MgF_2 evaporation by use of a monochromatized Hg lamp (wavelength 436 nm) and a photo-diode, and the deposition was stopped when the signal was close to a minimum. The MgF_2 thickness was then ~0.1 μm.

Figure 6 shows spectral transmittance for a bare glass substrate, after ITO deposition, and after overcoating with MgF_2. The film thicknesses are shown in the inset. The final transmittance is higher than for the uncoated glass over the whole visible spectrum, as indicated by the shaded area in the figure. It is also found that the interference fringes, which are pronounced in the ITO + glass structure, become much less apparent after the MgF_2 coating.

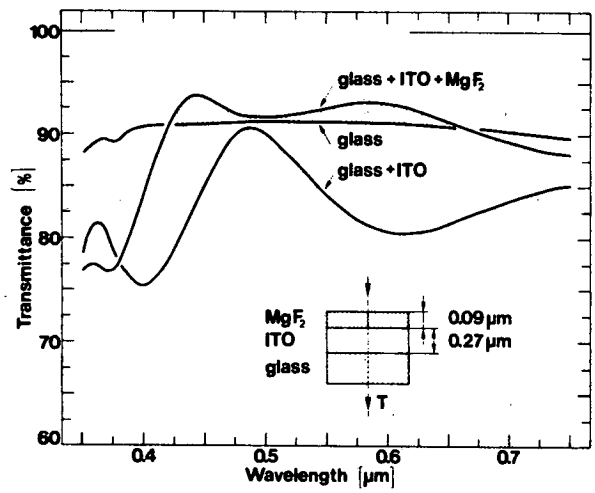

Figure 6. Spectral visible transmittance for an antireflection coated ITO film on glass.

If the ITO + MgF_2 coating is to be used on a low-emittance window, it is essential that the antireflection film does not significantly impair the infrared reflectance. This was verified by spectrophotometry for wavelengths longer than 3 μm. The measured near-normal reflectance of the ITO + MgF_2 films could not be distinguished from the corresponding data for ITO only. At off-normal angles the MgF_2 played some role though. Figure 7 gives recordings for 45° incidence onto the same structure as reported on in Fig. 6. The p-polarised light exhibits a clear minimum at ~17 μm wavelength as a consequence of the MgF_2 film, whereas the s-polarised light is unaffected. These results are consistent with the published[11] dielectric function of crystalline MgF_2. The increase of the integrated thermal emittance provided by the 0.1 μm thick MgF_2 film is only a few per cent.

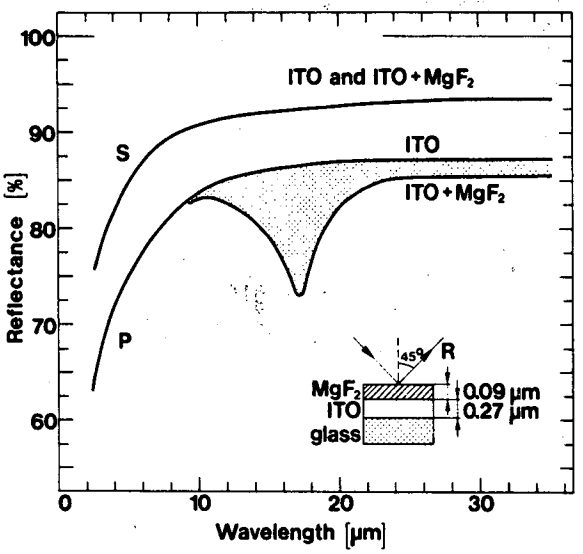

Figure 7. Spectral infrared reflectance for an antireflection coated ITO film.

Conclusion

Indium-Tin-Oxide films were prepared by reactive e-beam evaporation onto heated substrates. Optical measurements showed that the coatings were excellent transparent heat-mirrors. When deposited onto glass with a temperature $\gtrsim 200^{\circ}C$, the visible absorptance is so low that an antireflection film produces a transmittance in excess of that for uncoated glass, and, more important, the iridescence of the ITO film is strongly reduced. Our experimental results were obtained with MgF_2 coatings, which are commonplace for antireflecting optical components, but similar results could have been achieved with other materials. It was also found that neither the ITO thickness nor the MgF_2 thickness is very critical for giving low iridescence. Thus it requires less elaborate thickness control to make acceptable ITO + MgF_2 films than to make single-layer ITO films of comparable quality.

"Good" ITO films were obtained at substrate temperatures as low as $150^{\circ}C$, and hence it is possible to employ plastic substrates. Preliminary experiments using polyester sheets (9 μm thick Melinex, Type 442; manufactured by ICI Ltd., England) showed promising results though not yet as good as for deposition on glass.

This work was economically supported by grants from the Swedish Natural Science Research Council and the National Swedish Board for Technical Development.

References

1. Vossen, J. L., "Transparent Conducting Films", Phys. Thin Films, Vol. 9, pp. 1-71, 1971.
2. Haacke, G., "Transparent Conducting Coatings", Ann. Rev. Mater. Sci., Vol. 7, pp. 73-93, 1977.
3. Granqvist, C. G., "Radiative Heating and Cooling with Spectrally Selective Surfaces", Appl. Opt., Vol. 20, pp. 2606-2615, 1981.
4. Hamberg, I., Hjortsberg, A., and Granqvist, C. G., "High Quality Transparent Heat-Reflectors of Reactively Evaporated Indium-Tin-Oxide", to be published.
5. Fan, J. C. C., and Bachner, F. J., "Properties of Sn-Doped In_2O_3 Films Prepared by RF Sputtering", J. Electrochem. Soc., Vol. 112, pp. 1719-1725, 1975.

6. Fan, J. C. C., and Bachner, F. J., "Transparent Heat Mirrors for Solar-Energy Applications", Appl. Opt., Vol. 15, pp. 1012-1017, 1976.
7. Yoshida, S., "Efficiency of Drude Mirror-Type Selective Transparent Filters for Solar Thermal Conversion", Appl. Opt., Vol. 17, pp. 145-150, 1978.
8. Köstlin, H., Jost, R., and Lems, W., "Optical and Electrical Properties of Doped In_2O_3 Films", Phys. Stat. Sol. (a), Vol. 29, pp. 87-93, 1975.
9. Frank, G., Kauer, E., and Köstlin, H., "Transparent Heat-Reflecting Coatings Based on Highly Doped Semiconductors", Thin Solid Films, Vol. 77, pp. 107-117, 1981.
10. Nath, P., Bunshah, R. F., Basol, B.M., and Staffsud, O. M., "Electrical and Optical Properties of In_2O_3:Sn Films Prepared by Activated Reactive Evaporation", Thin Solid Films, Vol. 72, pp. 463-468, 1980.
11. Hunt, G.R., Perry, C. H., and Ferguson, J., "Far-Infrared Reflectance and Transmittance of Potassium Magnesium Fluoride and Magnesium Fluoride", Phys. Rev., Vol. 134, pp. A688-A691, 1964.

Heat mirrors on plastic sheet using transparent oxide conducting coatings

Ronald P. Howson, Martin I. Ridge
Department of Physics, University of Technology, Loughborough LE11 3TU, United Kingdom

Abstract

A technique of reactive d.c. magnetron sputtering with r.f. substrate bias has been evolved to give metal oxide films which exhibit heat reflecting properties while remaining highly transparent. Films of indium-tin, indium and cadmium-tin oxide have been deposited onto plastic sheet at room temperature at rates of greater than 0.5 μm min.$^{-1}$

Preliminary assessments of durability with accelerated weathering with exposure to high U.V. levels and high humidities have given very encouraging results. The properties achieved with a single coating of about 300 nm of oxide to a 50 μm thick P.E.T. sheet are visible transmittances of over 70% with heat emissivities lower than 0.3. These properties are commensurate with them providing an energy and cost effective addition to new and existing windows.

Introduction

The techniques and design for optical coatings for application in the utilisation of solar energy, and in increasing insulation, have to meet new standards. They will be judged by their optical performance, like any coating, but also they need to meet the difficult criteria of being able to be made in very large areas and at a cost which will justify their application with the energy that is saved. The coatings, therefore, have to be relatively simple and be able to be manufactured at a high rate, the determining factor in their cost.

One particularly important application of a selective optical filter is within the domestic window. Two thirds of the heat transferred by a double pane window is by radiation between the two panes. Suppression of this can lead to much greater gains in performance than can be expected by going to vacuum or special gas filling, or even by adding to the number of panes. A filter is, therefore, required which has a low heat emissivity, and hence a high I.R. reflectance, and a good visible transmittance to maintain good visual contact with the environment for the occupant and to allow solar gain to be effectively utilised. It should be durable to allow the energy and financial return to be obtained during its serviceable life.

There are two general types of film available for this application: a very thin metal film sandwiched between two dielectric layers or a semiconducting oxide with a high doping level[1]. The active material in each case uses the properties given to it by the mobile charge carriers it contains. The metal has a very high density of these, and also exhibits absorption due to inter-state electronic transitions, but if it is used as a very thin layer and careful interference matching is achieved with the dielectric layers, than a very good performance may be achieved. The best metal is silver, but copper or gold may also be used with some loss in performance.[2] They do not provide a transition from being visibly transmitting to infra-red reflecting in the optimum place for maintaining solar gain whilst limiting radiative heat transfer, which is around three micrometres, but change around one micrometre. The principal problem with their use is that the thickness required is close to that where the thin film structure becomes that of a series of isolated islands, rather than a continuous sheet, and the optical properties become useless. This thickness of around 10 nm also allows little protection against atmospheric chemical attack, mechanical abrasion or heat resistance, where coalescence and island formation occur with a continuous film. They do give very low emissivities and will find application where they can be well protected.

Semi-conducting oxide films have previously required high substrate temperatures to achieve the desired optical properties.[3] They have to be thicker films which can also show interference colours and in general cannot achieve such low emissivities as exhibited by metals. They do, however, have the potential of being very durable and forming a very simple optical system.

It was our opinion that the properties of an oxide film were those required for a universal coating technique for windows and that this should be also onto a flexible plastic sheet. It is only this technique which will allow the production of an element at sufficient rate and cost and in sufficient volume to cause any significant effect in the use of energy for home heating. The escalation in energy costs is such that a technique

for improving the performance of existing windows in a cost and energy effective way is urgently required.

Techniques

Our original hypothesis was that the addition of energy to a growing film by exposure to bombardment by neutral heavy ions should lead to properties being attained which were normally seen only at higher temperatures. This was tested with evaporation and sputtering methods[4]. Only reactive methods using pure metal sources were considered in order to achieve the simplest realisable system which could achieve high rates. This gave good results with both systems but has proved to be symptomatic of a more important factor, which is the careful control of the oxygen to metal ratio. With the high rate used it was apparent that it was oxygen gas admission rate versus deposition rate that determined the properties obtained.[5] The precision control of rate combined with a high rate capability, and operation at a relatively high gas pressure to provide the reactive gas has led us to the system of d.c. planar magnetron sputtering of the metal or alloy in an atmosphere of argon and oxygen. The ion bombardment of the substrate provided by a r.f. discharge activates the oxygen reacting on the substrate surface to give higher rates of deposition. In order to achieve optimum properties in the films we have found it necessary to control the power to the sputtering source and the oxygen gas admission rate to within 0.1%. The conditions were adjusted in accordance with the properties of the film continuously monitored in a roll coating apparatus. This apparatus is described in a further paper in these proceedings.[6]

Figure 1

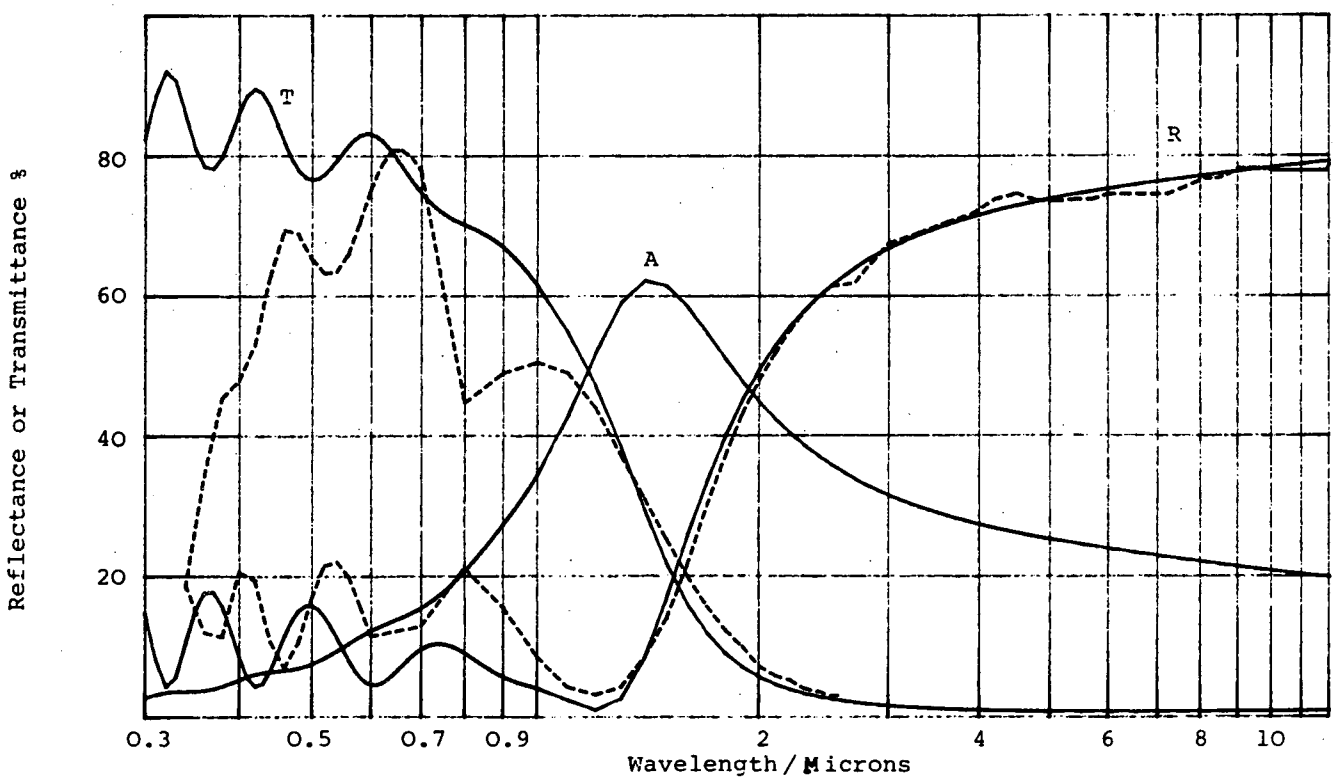

Reflectance (R), Transmittance (T) and Absorptance (A) calculated from the parameters provided by the electrical and optical measurements on a film of Indium Tin Oxide (I.T.O.) on glass compared with the actual detailed measurements of R and T shown in a dotted line.

Results

The optical properties of films of indium 10% tin oxide, indium oxide and cadmium 2:1 tin oxide are shown in Figures 1 through 3. Indicated on these graphs are the theoretically expected properties using simple dielectric and Drude theory derived from the electrical properties and the film thickness which are listed in Table 1.[7] Samples of indium oxide and indium 10% tin oxide films on plastic were subject to weathering tests including temperatures cycling in a high humidity with a high U.V. exposure and showed good durability. Some film damage was apparent in the most severe case which was found on inspection to be due to differential expansion, but in these cases in many films bubbling of the surface had occurred without breaking. Attention is obviously needed to create the correct stress level in the films that are produced.

Figure 2

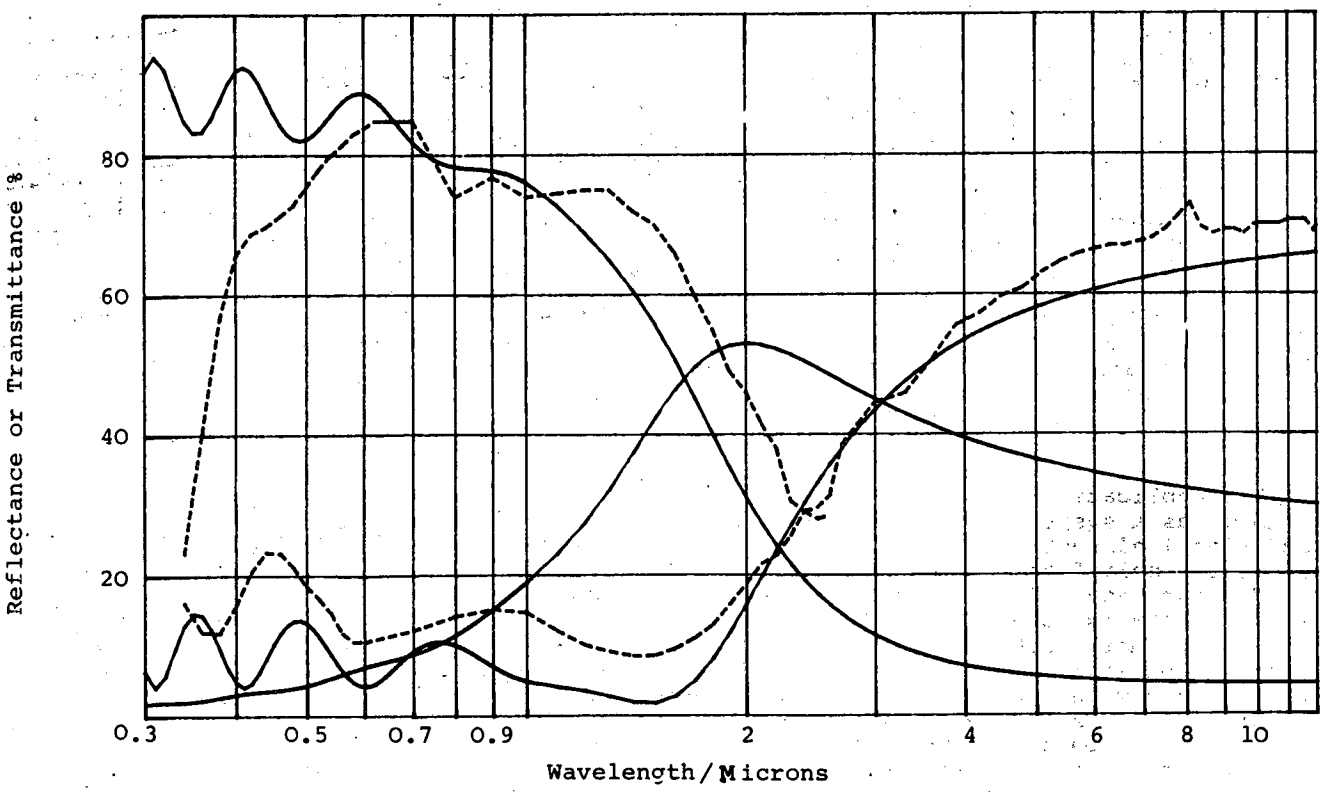

Reflectance (R), Transmittance (T) and Absorptance (A) calculated from the parameters provided by the electrical and optical measurements on a film of Indium Oxide (I.O.) on glass compared with the actual detailed measurements of R and T shown in a dotted line.

Detailed parameters are given in Table 1.

Figure 3

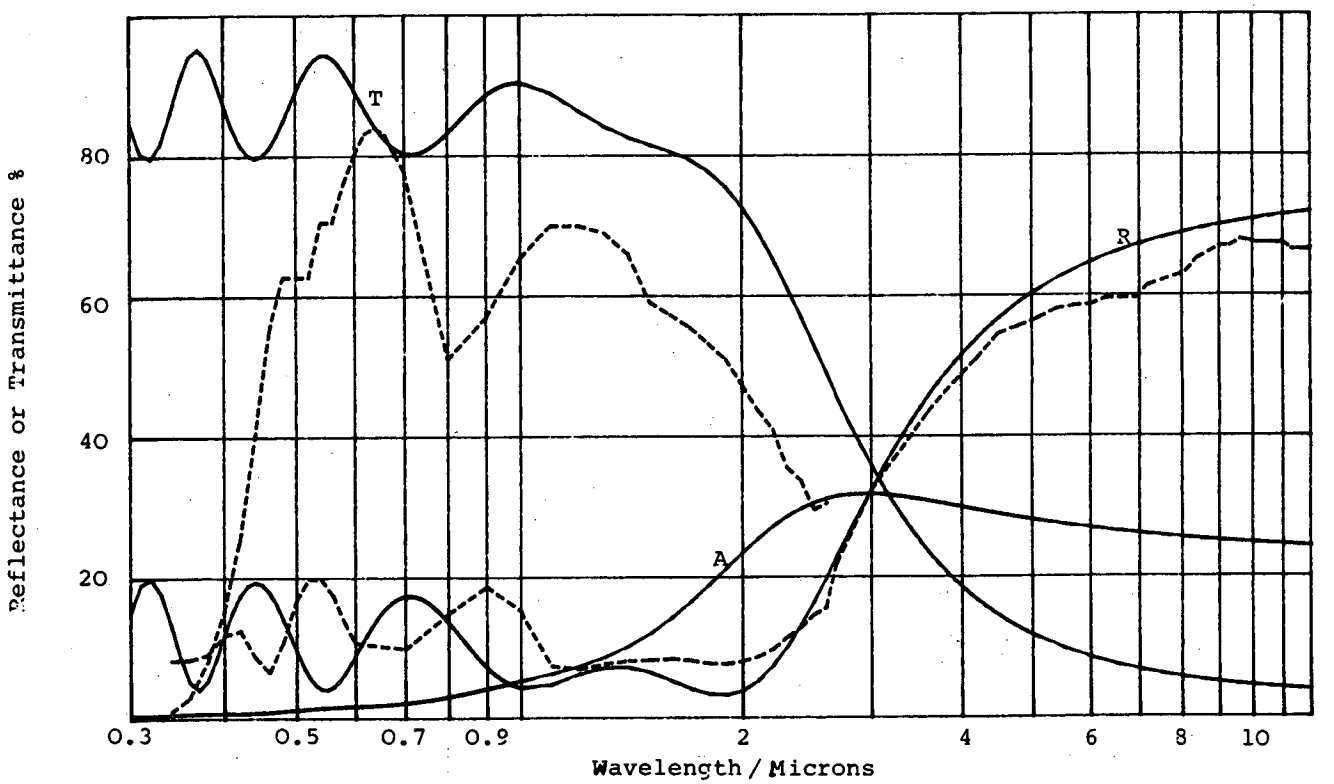

Reflectance (R), Transmittance (T) and Absorptance (A) calculated from the parameters provided by the electrical and optical measurements on a film of Cadmium Tin Oxide (C.T.O.) on glass compared with the actual detailed measurements of R and T shown in a dotted line.

Application

The application of such a coated plastic film as a 'stuck-on' element in a single pane window, as a suspended element in the centre of a double pane window and as suspended additional element to an existing single pane is considered in the Figures 4, 5 and 6. It is our belief that the addition of a lightweight element to the interior of an existing window can result in a genuine cost-effective improvement to the insulation of a building which maintains solar gain. The simple 'stuck-on' film does not offer a real solution as it is even more liable to cause condensation on the surface, which destroys the effect of the low emissivity coating. A sheet stretched in a frame offers a much higher gain in performance with the advantages of easy replacement of the sheet if it is damaged. The light weight also allows application in many situations where the weight of a glass element would be an embarrassment. A plastic sheet coated both sides with an optical filter stretched in an aluminium frame and attached in a simple way to an existing single pane window could lead to a performance considerably better than existing triple glazing.

Figure 4

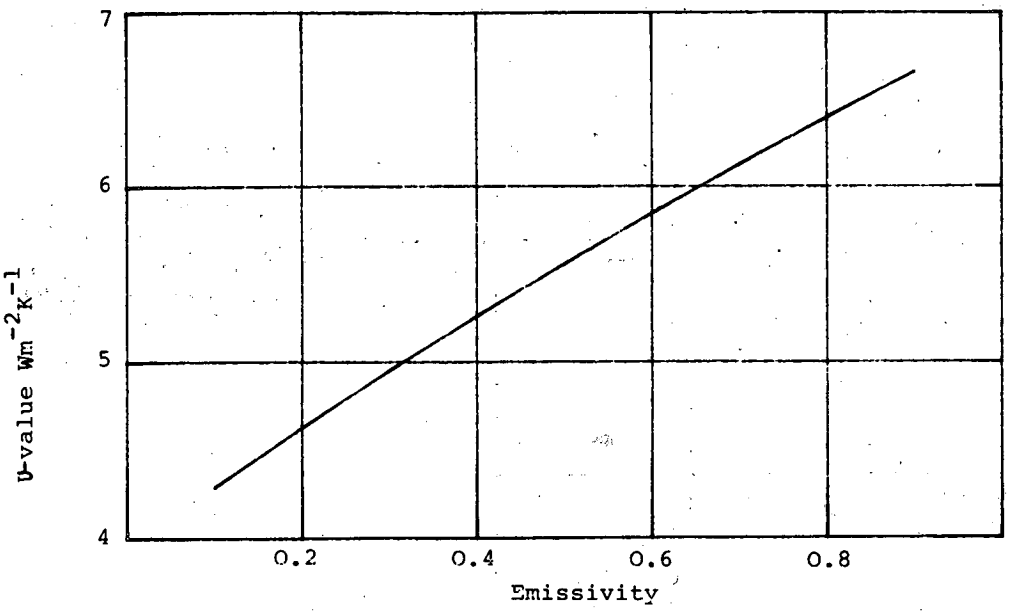

The U-value for a single pane window shown as a function of the emissivity of the inside surface. The calculations are adopted from Mahdjuri with a glazing element being assigned a value of 0.9.

Figure 5

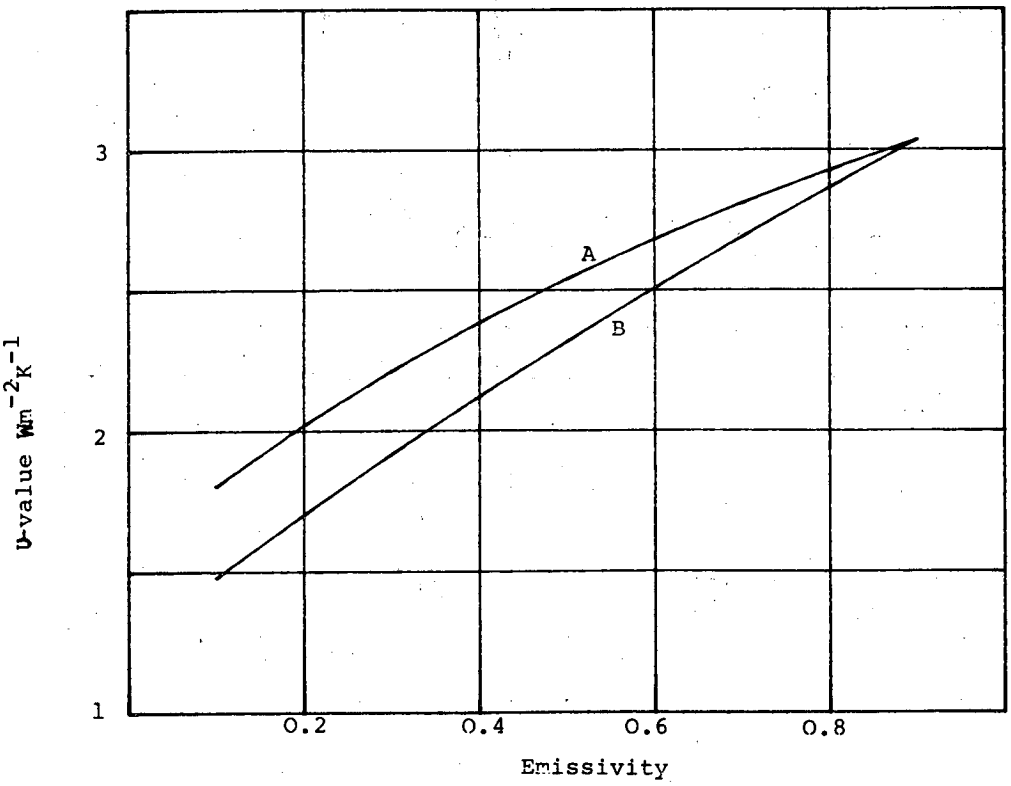

The U-value for a double pane window with the inside pane having a coating (A) on the side facing the other pane only and (B) on both sides.

Figure 6

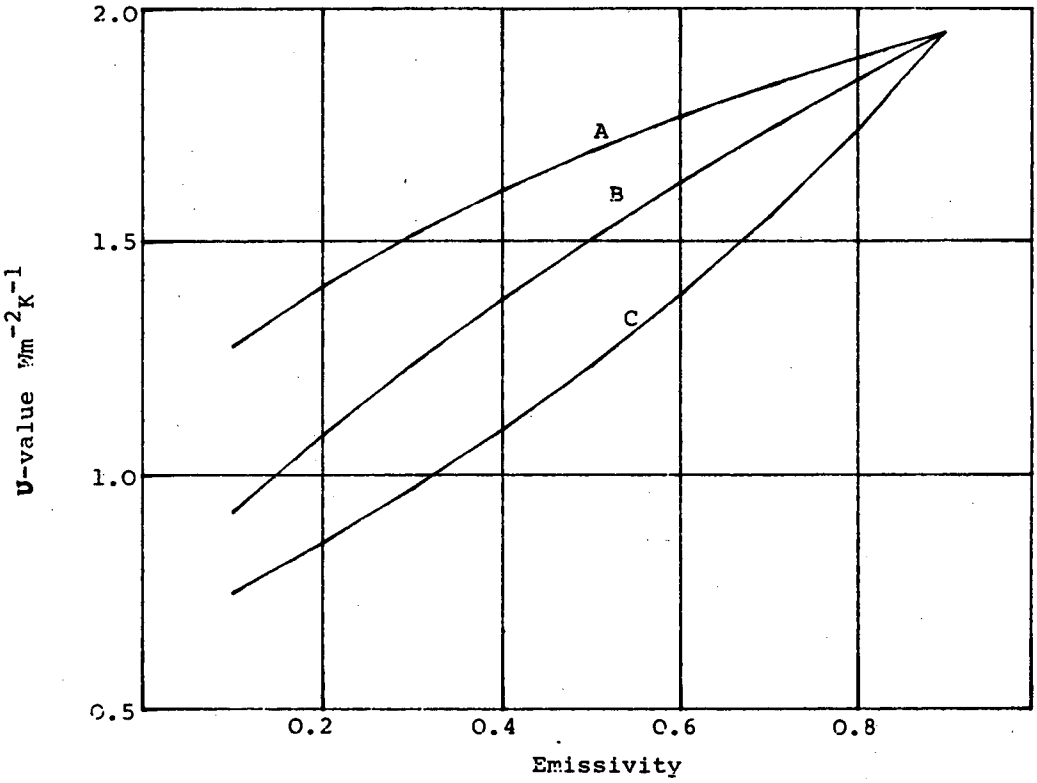

U-value for triple glazing formed with a centre element coated one side (A) on both sides (B) and with the inside pane coated on both sides as well (C)

Data for Indium Tin Oxide, Cadmium Tin Oxide and Indium Oxide.

Parameter	I.T.O.	C.T.O.	I.O.
Relative electric permittivity	4	4	3.5
Wavelength for reflectance minimum (x 10^{-6}m)	1.2	1.9	1.45
Plasma wavelength (x 10^{-6}m)	1.3	2.5	2.0
Plasma frequency (x 10^{30})	1.45	0.75	0.94
Sheet resistance (/)	17	24	30
Film thickness (x 10^{-9}m)	330	280	336
Carrier density (x $10^{26}m^{-3}$)	6.1	3.4	2.1
Electrical mobility (x $10^{-4}m^2V^{-1}s^{-1}$)	17	30	29
Carrier relaxation time (x 10^{-15}s)	2.8	5.8	2.6
Effective mass	0.29	0.34	0.16

Table 1

The presence of a low emissivity surface on the inside of the window has a large effect upon the radiative environment experienced within the room. For a temperature difference between the room and the outside of 22°C the equivalent black body temperature seen by an occupant goes from 14°C below ambient to 5°C for a coating with an emissivity of 0.3 and 1.7°C for one with a value of 0.1. A double glazed structure has the effect of reducing this to 7°C which falls to 0.7°C if a coating, facing the exterior pane, is used with an emissivity of 0.1. If an additional coating is applied facing the room, or the pane is transparent to heat radiation, then this falls to 0.5°C. These figures become 2.2°C and 1.7°C respectively for a coating with an emissivity of 0.3. If two additional panes coated both sides with a surface having an emissivity of 0.1 are added to a single pane, then the equivalent black body temperature falls to 0.4°C. This is lower if only the centre element is coated. A value of 1°C is obtained if an emissivity of 0.3 is used. 'Normal' triple glazing gives a value of 4.5°C.

Conclusion

The properties of metal and alloy oxide films produced at high rates onto plastic sheet has been described. They reflect more than 70% of the heat spectrum whilst being transparent to more than 70% of the visible spectrum. Such a process offers the possibility of an element being provided for both new and existing windows which will allow an improvement in the insulating performance for little penalty of weight or cost. The process is adapted to the production of very large areas of sheet which could make a significant impact on national energy consumption. The availability of such a large area filter allows the concept of a window insulation performance similar to that of a well insulated wall but having the advantage of admitting solar radiation to heat the house whilst maintaining visual contact for the occupant, making the domestic window a very effective utiliser of solar radiation.

References

1. Fan, J.C.C. and Bachner F.J.
   Transparent heat mirrors for solar-energy applications
   Applied Optics Vol. 15, pp 1012 - 1017 (1976)

2. Glazer, H.J.
   Highly transparent low emissive coatings on the basis of ZnO/Ag/Zno, ZnO/Au/ZnO, BiO_3,Au/Bi_2O_3, ZnO/Cu/Zno and Bi_2O_3/Cu/Bi_2O_3.
   Proceeds of the 8th International Vacuum Congress, Cannes 1980 (Suppl. "Le Vide les Couches Minces No. 201). Vol. 1 pp 723-726.

3. Frank, G, Kaner E and Kostlin.
   Transparent heat-reflecting coatings based on highly doped semi-conductors.
   Thin Solid Films Vol 77 pp 107-117 (1981).

4. Howson, R.P., Avaritsiotis, J.N., Ridge, M.I. and Bishop, C.A.
   Properties of conducting transparent oxide films produced by ion plating onto room temperature substrates.
   Applied Phys. Letters Vol 35 pp 161-162 (1979)

5. Howson, R.P. and Ridge, M.I.
   Deposition of Transparent heat-reflecting coatings of metal oxides using reactive planar magnetron sputtering of a metal and/or alloy.
   Thin Solid Films Vol 77 pp 119-125 (1981).

6. Ridge, M.I., Howson, R.P. and Bishop, C.A.
   New Techniques for the roll coating of optical thin films.
   These proceedings.

7. Howson, R.P., Ridge, M.I. and Bishop, C.A.
   Production of transparent electrically conducting films by ion plating.
   Thin Solid Films Vol 80 pp 137-142 (1981).

8. Mahdjuri, F.
   Highly insulated window glazing.
   Energy Research Vol 1 pp 135-142 (1977).

Transparent heat insulating coatings on a polyester film

Kiyoshi Chiba, Shigenobu Sobajima, Utami Yonemura, Nobuo Suzuki
Central Research Laboratories, Teijin Ltd., Hino, Tokyo, Japan

Abstract

Multi-layer coatings of metal-dielectric type were prepared on a poly(ethylene terephthalate) (PET) film using chemical and physical preparation techniques. Hydrolysis of tetrabutyl titanate (TBT) followed by condensation gave rise to well-controlled transparent dielectric layers with relatively high refractive index and a silver layer was prepared by vacuum evaporation. Changes of chemical coating condition gave various types of optical characteristics. This film reduces energy dissipation from a single windowpane by around 35%.

Introduction

Transparent heat insulating coatings are well known to be effective to control radiative heat losses and to reduce energy consumption in various applications in the field like industrial and architectural sectors.[1] Many types of these coatings on plastics films have been proposed and studied by several researchers.[2] They are classified into three groups. The first is the type of thin metal layers such as Au and Al. Aluminum on poly(ethylene terephthalate) (PET) film is used for sun-shading applications; but it has large amount of absorption losses at visible wavelength region.[3] Gold coating on a PET film has been used for heat insulation, although the material is too expensive to be used widely. Second group is transparent semiconducting materials such as SnO_2, and In_2O_3-SnO_2 (ITO). This type of coatings should be formed as relatively thick layers because of much lower electroconductivity compared with metal coatings. For example, ITO coatings should be thicker than around 4000 Å if it is required to reflect more than 80% of infrared ray of the wavelength of 10 μm. There are several reports[2] to prepare ITO-coating on a PET film for this purpose by means of reactive evaporation or reactive sputtering. However preparation rate is actually limited by low deposition rate of metal oxide coatings. Third type is the metal-dielectric multi-coatings, where visible reflection is extremely reduced on account of interference effect while high infrared reflectance is preserved.[4] This type of coatings has a great potential from the view point of good performance and productivity. Fig. 1 shows the basic structure of this type of coatings. Typically a thin metal layer like Au or Ag is sandwiched by two transparent dielectric layers with large index of refraction such as TiO_2, TiO_x, ZnO, ZnS, Bi_2O_3, SiO, etc. As far as the metal oxide layer is prepared by means of reactive evaporation or reactive sputtering, it is not easy to prepare this film stably at high rate, with good uniformity in large area, and with reasonable economics.

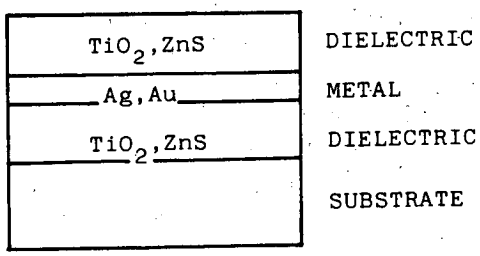

Fig. 1. Concept of metal-dielectric transparent heat insulating coatings

In this report, the third group of multi-coatings was prepared by entirely different approach; the dielectric layers were formed by means of hydrolysis of metal alkoxide such as tetra-alkyl titanate, and zirconate, while the metal layer was formed by vacuum evaporation. Metal alkoxides are known to be hydrolyzed to form a network structure consisting of metal oxide such as titanium oxide, and zirconium oxide. Since the refractive index of the prepared layer is higher for tatanium oxide than for zirconium oxide, tetra-alkyl titanates were chosen for chemical coating materials.[5]

Experimental procedure

PET films of thickness of 25 or 75 μm were used as substrate. Chemical coating was applied by using a spinner apparatus equipped with optical monitoring system shown schematically in Fig. 2. A simple type of spinner was constructed inside a chamber made of acrylic plates. The spinning speed was set at either 1000 or 1400 rpm. A 1 *ml* pipette was positioned at the top plate of the chamber located away from the center of the spinning plate by 5 mm. With a rubber bulb 0.3 *ml* coating solution was poured for about 2 sec on the surface of PET film attached to the aluminum plate rotating at proper speed. A 1 mw He-Ne laser beam was introduced on the film surface at normal incidence, adjusted by a mirror after attenuated by a factor of one-fiftieth. A small hole of 1 mm diameter was drilled in

alminum spinner plate located 20 mm off the center of the plate. At the bottom of the drilled position a rectangular prism (5×5 mm) was bonded to deflect the beam direction. By adjusting the optical path properly, the monitor laser beam which was synchronously transmitted was detected by a photo detector and displayed on an oscilloscope. The chamber was usually kept at 20°C and 60% RH. When more humid condition was needed, ultrasonic humidifier was used.

Tetrabutyl titanate (TBT) was used for coating materials because it shows controllable stability in the coating process. For metal layer, silver was chosen due to its good optical property.

Vacuum evaporation was carried out at a pressure of 2.7×10^{-3} Pa and the evaporation rate was 30 Å/sec.

Surface analysis of the film was performed by x-ray photoemission spectroscopy (Hewlett-Packard) and ion microprobe mass analyser (Hitachi IMA-type 2).

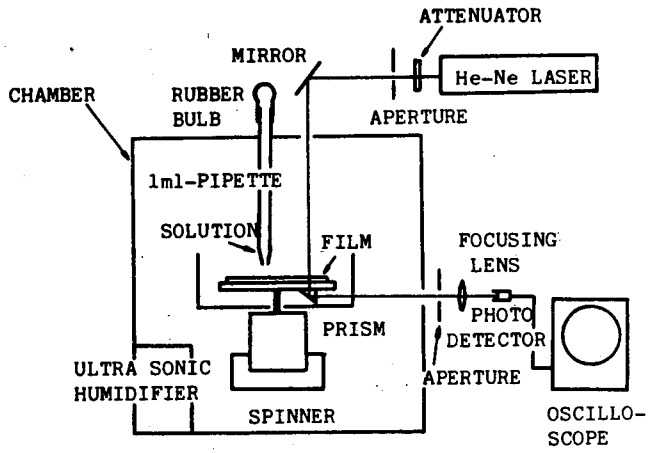

Fig. 2. Experimental setup of the spinner apparatus equipped with the optical monitoring system

Measurement of heat insulating property was carried out by using a heat flux meter (Showa Denko HFM-MU).

Preparation of trilayer coatings on a PET film

Many factors have been investigated to prepare trilayer transparent heat insulating coatings on a PET film. Chemically prepared layers have to be formed smooth and kept uniform in thickness and optical properties not to damage interference effects. In the trilayer structure, the dielectric layers whose thickness is 200–500 Å is desired to have thickness uniformity within ± 10%. This requirement was fulfiled by utilizing TBT solution which has good coating capability on PET and silver surfaces.

0.3 *ml* of 5 wt% TBT-n-hexane solution was poured on a 75 μm-PET film surface attached to spinner plate spinning at 1000 rpm and the film was dried for 2 min at 120°C. Then 140 Å silver layer was vacuum deposited on it at the rate of 30 Å/sec. and 2.7×10^{-3} Pa. In Fig. 3 the dashed line shows the spectrum of the film formed to this extent, where fairly good transmission at the wavelength around 500 nm is observed. Finally the top layer was coated at the same conditions as the first coated layer. The solid line shows observed spectrum of the trilayer coatings on PET film prepared in this manner. This spectrum shows good optically selective properties; almost 80% is transmitted at 500 nm wavelength, while more than 97% of infrared is reflected at the wavelength larger than 2.5 μm.

Changes of concentration of the solution lead to different spectrum selectivities as shown in Fig. 4. Careful choice of concentration makes it possible to obtain desired spectrum. Fig. 5 also shows computed curves of spectrum where the refractive index of the dielectric layer is assumed to be 2.0. Comparing these two figures, it is indicated that

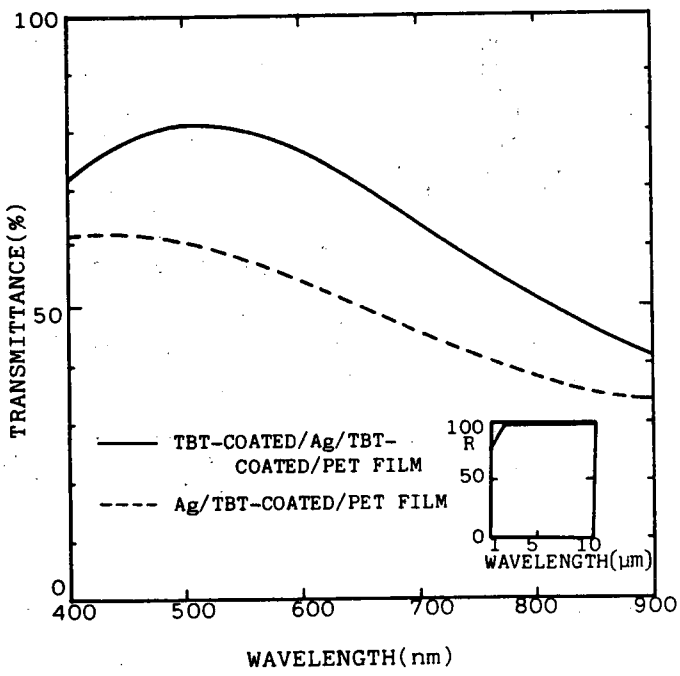

Fig. 3. Measured selective transparency and infrared reflectance of prepared film

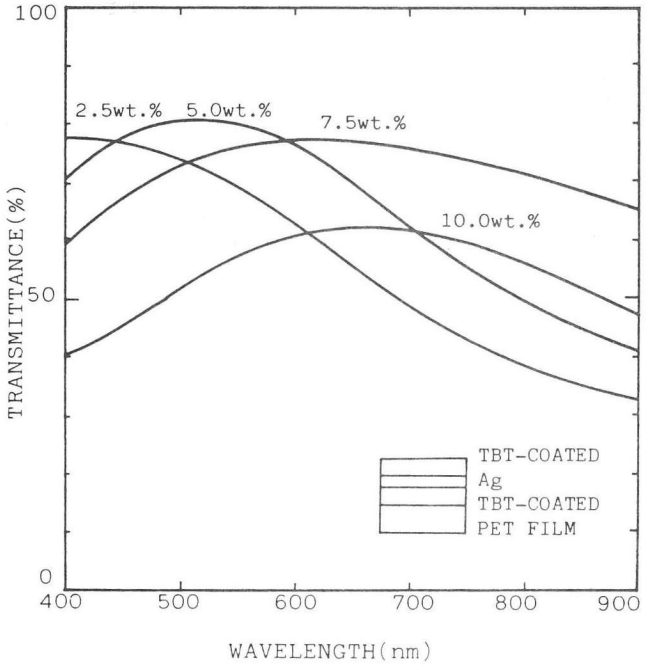

Fig. 4. Concentration dependence of selective transparency of trilayer coatings.

Thickness of the silver layer: 140 Å
The figures represent concentration of TBT/n-hexane mixture

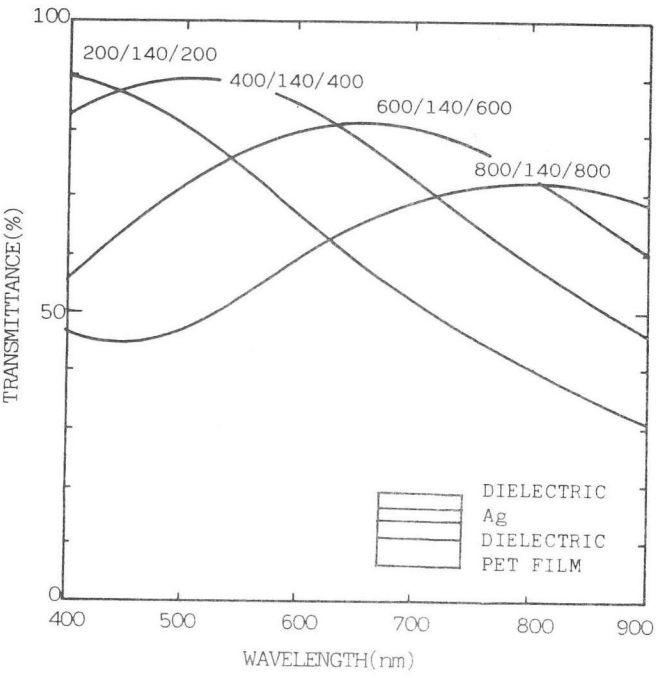

Fig. 5. Calculated selective transparency

The figures represent thickness of the constituent layer in Å

the optical properties of the film are able to be controlled even in the thickness range less than 500 Å. These results were also confirmed when conventional coating method was used.

Effect of the solvent

Initial stage of coating process was observed using monitoring system described in the previous section. Advantages of this system are as follows. (1) Laser beam monitors

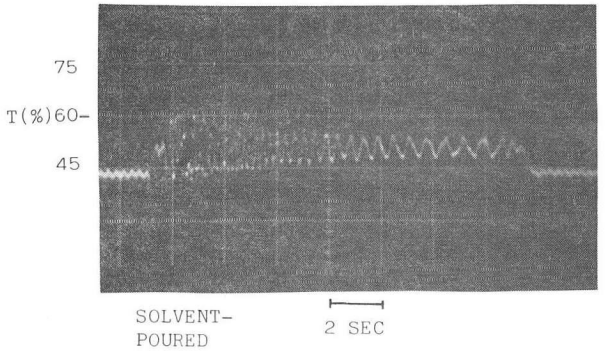

(a) n BuOH

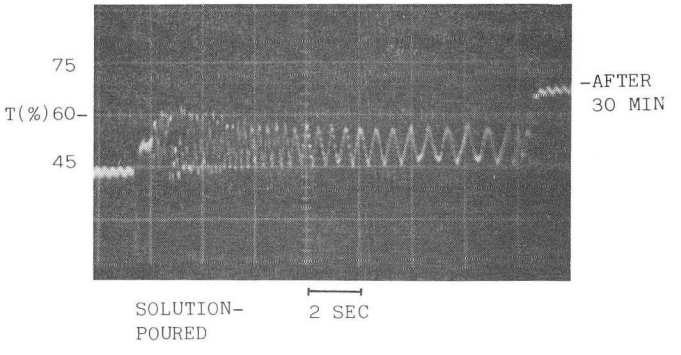

(b) 5 wt% TBT/n-BuOH

Fig. 6. Example of coating dynamics displayed on an oscilloscope.

Coating condition: 20°C, 60% RH
Substrate: Ag (140 Å)/TBT-coated (300 Å)/PET film

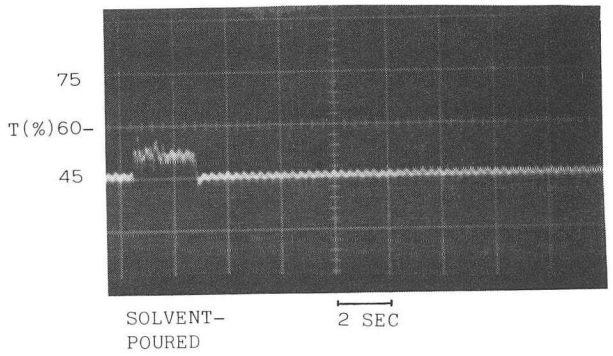

(c) n-heptane

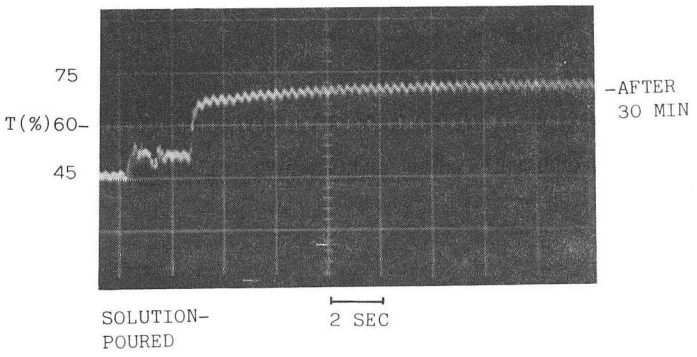

(d) 5 wt% TBT/n-heptane

limited small portion synchronously. Therefore the variation in the film surfaces does not affect detected signals. (2) When coating process of an upper dielectric layer is monitored, changes of detected signal are enlarged by interference effect associated with metal/dielectric/PET film base.

Many kinds of solvent have been investigated. Fig. 6 (a)–(d) show typical examples observed in the series of runs. In Fig. 6(b) the solution is composed of n-BuOH and TBT (5 wt%) and in Fig. 6(d) n-heptane and TBT (5 wt%). For comparison, Fig. 6(a) shows the case of pure solvent of n-BuOH and Fig. 6(c) n-heptane respectively.

These figures represent time-resolved process where as -coated liquid layer changes to transform into thin solid film. Fig. 6(b) shows this process clearly. From the interference pattern the thickness of as-coated layer is estimated as around 5–7 μm. It decreases at the rate of more than 1 μm/sec at the thickness in excess of 5 μm and 0.4 μm/sec at less than 2 μm respectively. In the highly diluted solution, difference between solution and pure solvent is not observed during this stage. Then at the right end of the figure, there is an abrupt rise of the curve corresponding to the formation of the solid film. This is also indicated from the

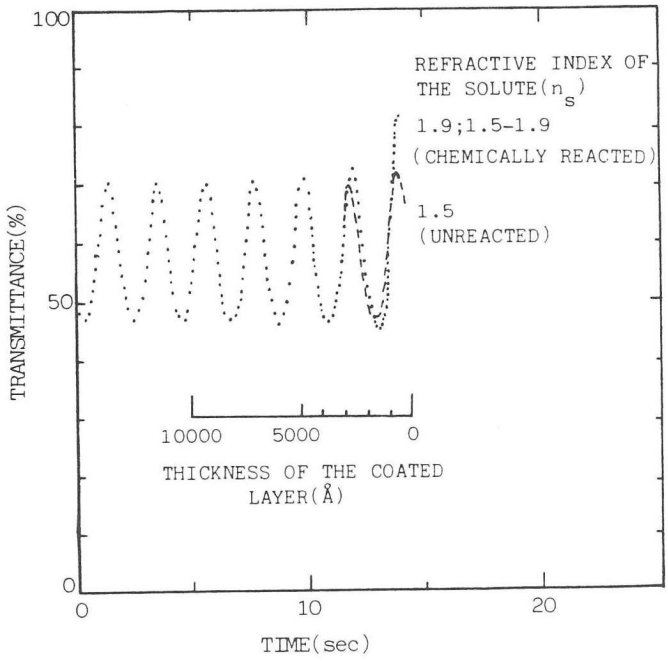

Fig. 7. Simulation pattern of coating dynamics.

Substrate: Ag (140 Å)/dielectric [n=2: 300 Å)/PET film
Coated layer: initial thickness 1.55 μm
final thickness 450 Å
Evaporation time: 14 sec

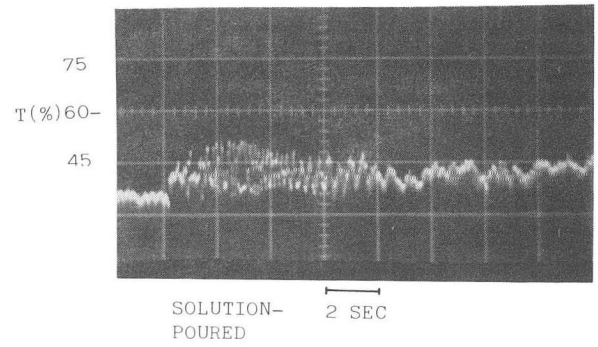

Fig. 8. Effect of humidity on the coating dynamics

Solution: 5 wt% TBT/n-BuOH
Condition: 22°C, 85% RH

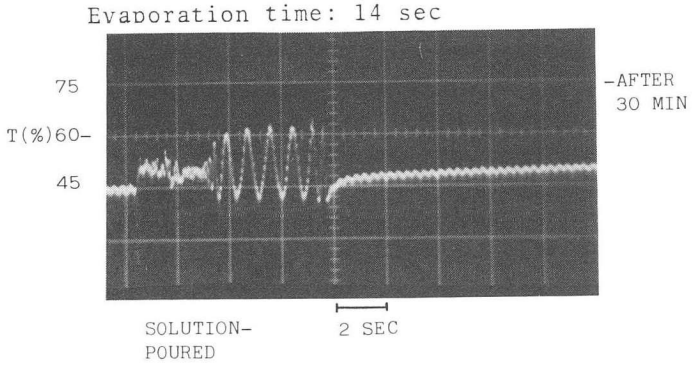

Fig. 9. Effect of the solvent showing different as-coated pattern

calculated curves in Fig. 7. Namely, under the constant speed of evaporation, the transmittance of the trilayer film changes as the thickness decreases. For the solvent of refractive index 1.4 and the solute of 1.5 (TBT), the transmittance of the trilayer film is represented as broken line; and, for the same solvent and the solute of 1.9, the interference is calculated as dotted line. The latter curve also corresponds to the case, in which the TBT, whose refractive index is 1.5, undergoes any chemical reactions during or at the end of the evaporation and changes its index up to 1.9. Thus, the experimental curve and the calculated pattern both indicate that a certain chemical reaction occurs either during or at the end of the evaporation process. In TBT-n-heptane mixture, this whole process occured much faster than in the case of TBT-n-BuOH mixture. From many trials it was concluded that this deposition process is reproducible and controllabe.

Fig. 8 shows another observation at highly humid condition where 5 wt% TBT-n-BuOH mixture was coated at 85% RH and 22°C. In this case clearness of interference pattern diminishes significantly. It must be due to precipitation of scattering nuclei in the film, which are composed of particles of titanium oxide and hydroxide. When the mixed solvent is used, both deposition rate and environmental stability can be controlled simultaneously.

Proper chcice of the solvent could produce the different state of as-coated layer. Fig. 9 shows an example of quite different pattern from Fig. 6(b). Between these two patterns, coating conditions are exactly same except for the solvent. The kinds of the solvent do not only give rise to difference at this state but also influences the final optical properties of the trilayer coatings

Effect of drying

As-coated dielectric layer contains some amount of organic contents consisting of unevaporated solvent and unreacted elements. Although the organic contents decrease as aging proceeds, drying accelates this step. Fig. 10 shows typical spectrum changes of trilayer coatings before and after drying for 2 min at 125°C. The dashed line shows as-coated spectrum while solid line shows the one after dried. Chemical analysis also indicates the carbon content of the layer decreases to about 2–4 wt% after this processing. The content decreases further to the level less than 1 wt% when aging proceeds. But no significant change in the spectrum is observed after drying. The drying process is also controllable and reproducible.

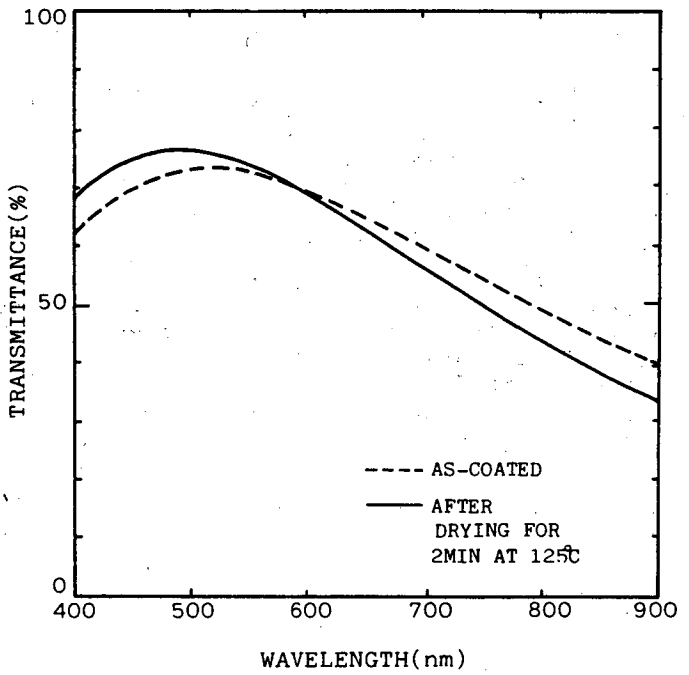

Fig. 10. Spectral changes of the trilayer coating before and after drying

Stability of the silver layer deposited on chemically formed dielectric layer

In this experiment, silver was deposited by vacuum evaporation. Two types of deposited state have been reported to exist in evaporated silver coatings when applied on glass surfaces.[6] One is quite similar to massive silver of good electrical and optical properties; another is of poor electrical conductivity and of large amount of optical scattering.

Similar phenomenon was observed when silver is deposited on TBT-coated film surface. Depending on the thickness of the silver layer, the transmittance of the composed film variou as shown in Fig. 11. There are also shown the theoretical curves which were computed based on the optical constants as the bulk material. For the thickness more than around 100 Å, the observed transmittance of the prepared coating agrees well with the computed curves: while for the thickness less than around 100 Å, discrepancy exist between them. In the latter region, the electrical and mechanical properties of the silver layer are much poorer. Also, the stability of the silver layer is inferior for the thickness around 100 Å. According to this instability, as-deposited silver coatings frequently turn poor state, when the thickness is close to around 100 Å. This instability can be improved by changing of the properties of the metal layer by, for instance, alloying with gold.

Properties of transparent heat insulating coatings

Optical properties

A chemically prepared titanium oxide coating is formed in completely different mechanism from physically prepared one such as by vacuum evaporation and sputtering process. In the chemical reaction the thin solid coating is formed from relatively thick coated layer. Therefore it lead to small amount of inhomogeneity and irregularity in the coating when film formation rate is relatively high.

Surface analyses were carried out to investigate prepared films using the x-ray photoelectron spectroscopy (XPS) and the ion microprobe mass analyzer (IMMA). Fig. 12 shows XPS spectrum of the surface of the trilayer coatings on a PET film. Fig. 13 also shows in-depth profile of silver of the coatings by IMMA analysis. From these characterization techniques, some indications are given as follows: the titanium oxide layer is clearly formed; the trilayer coatings are formed well; but, some amount of uncovered silver surface is still observed. This inhomogeneity can be improved by proper choice of the coating conditions.

The index of refraction depends on final residual organic content and state of network structure. Typical value of prepared titanium oxide from TBT solution is around 1.9–2.0 at the wavelength of 500 nm. Fig. 14 shows refractive indices prepared by various techniques for comparison.

In Fig. 15 a typical spectrum of prepared transparent heat insulating coatings on a PET film is shown at the wavelength from ultra-violet to infrared region. The structure is TBT-coated layer (270 Å)/Ag layer (150 Å)/TBT-coated layer (270 Å)/ PET film (25 μm) which shows good optical selectivity.

Heat insulation characteristics

Since infrared reflectance of the trilayer coatings is very high, the prepared coatings show good heat insulation. Its effect is well represented by K-value which is defined by the following equation.

$$Q = K \times \Delta T$$

Where Q is the heat flux (Kcal/m^{2}h), K the heat transfer coefficient (Kcal/m^{2}deg h), and ΔT the temperature difference (deg), respectively. K-values of the film were measured at various application forms where temperature is 20°C in inner area, and 0°C in outer area and wind of 3 m/sec blows at outer area. For single window pane K-value is 5.3. When the film is attached as its coatings faces inner area it shows 3.5. For double glazing spaced by 10 mm-air it is 2.8. When the film is attached to the inner pane whose coatings face outer space it shows 1.8. These results suggest a single window pane attached by the film reduces energy dissipation by around 35%, and a double glazing attached by the film

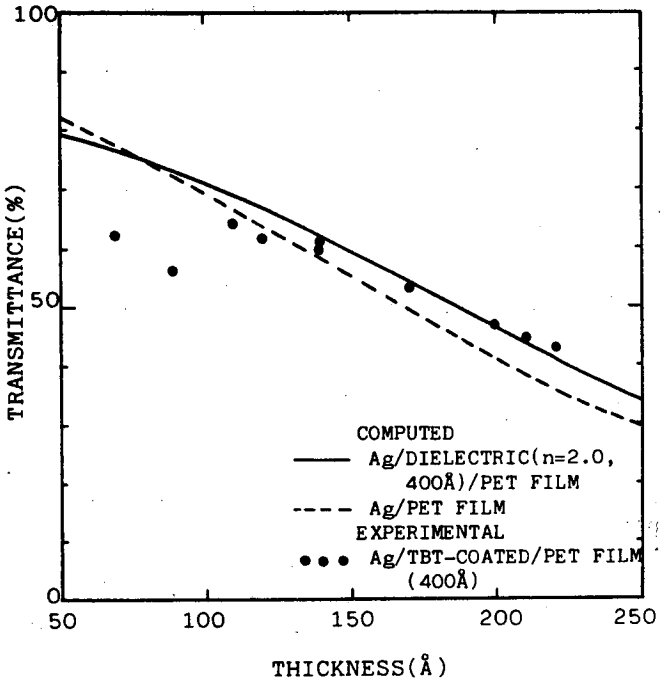

Fig. 11. Transmittance of the silver coating as a function of thickness at a wavelength of 500 nm

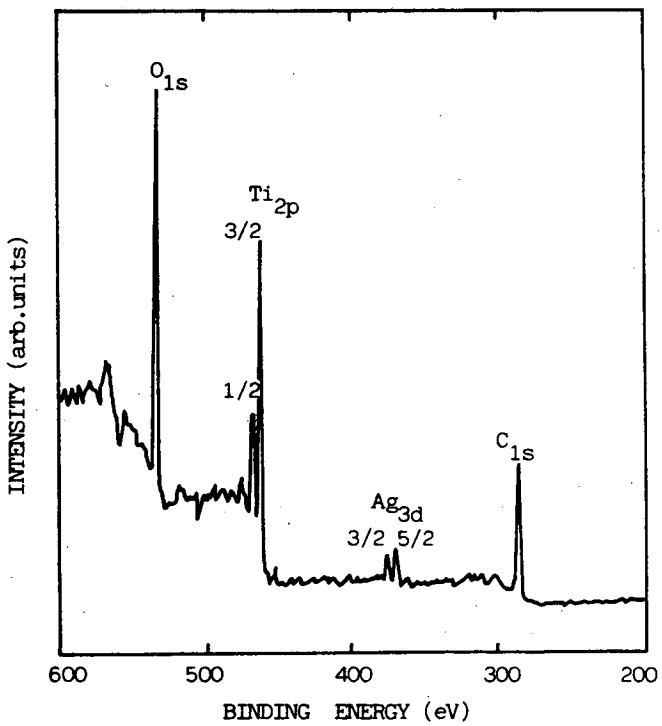

Fig. 12. XPS spectrum

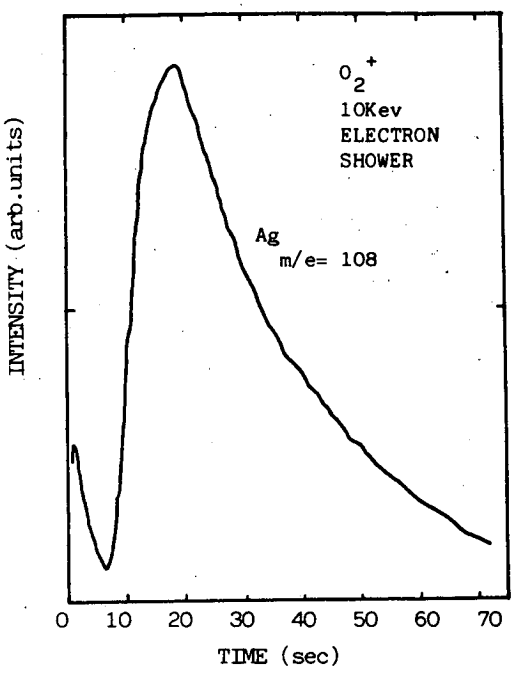

Fig. 13. IMMA depth profile of silver of the trilayer coatings

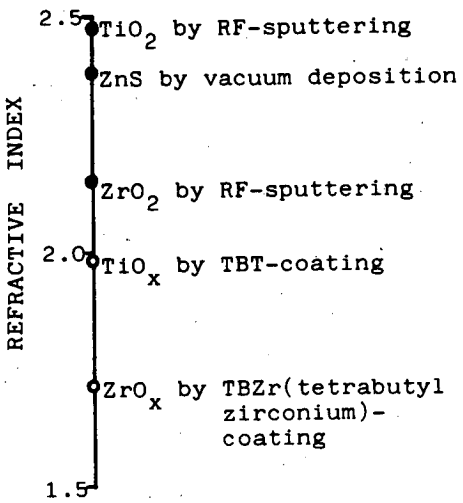

Fig. 14. Refractive indices of the prepared dielectric layer (measured at 500 nm)

has same degree of insulation effect as a triple glazing. These heat insulation characteristics are very promissing for practical applications in the industrial and architectual sectors.

Conclusions

Transparent heat insulating coatings of metal-dielectric type were prepared on a poly(ethylene terephthalate) film using chemical and physical coating techniques. Even in the thickness from 100 to 500 Å chemically prepared titanium oxide layer has shown controllable properties. Therefore optical selectivity can be controlled using proper coating conditions. The present preparation method can be applied to the conventional coating apparatus like roll-up machine for large scale production.

As a heat insulator the prepared films have shown good characteristics capable of large amount of energy saving in various fields.

Acknowledgement

The authors would like to thank Dr. T. Shima for his continuous guidance and I. Ouchi

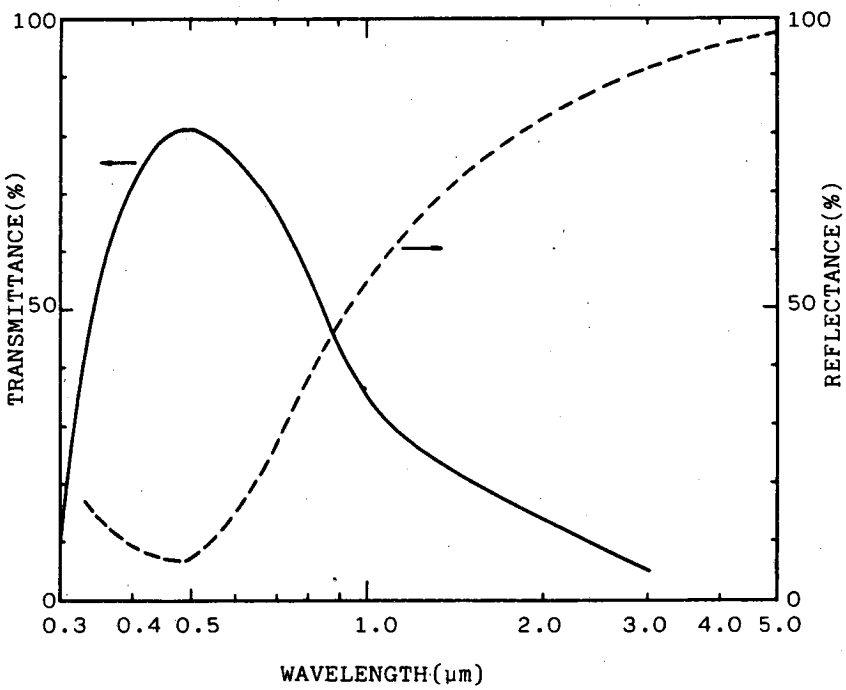

Fig. 15. Typical spectrum of the transparent heat insulating coatings on a PET film

for his discussion. Earlier work on chemical coating by K. Itoh and advice on IMMA analysis by Dr. A. Nishijima of National Chemical Laboratories are very much acknowledged. The authors are also thankful to T. Nishihara, Dr. I. Sugiyama, T. Yatabe and other colleagues at Central Research Labs. for their help in many respects.

References

1. Granquist, C. G., "Radiative Heating and Cooling with Spectrally Selective Surfaces," Appl. Opt., Vol. 20, pp. 2606–2615. 1981.

2. Howson, R. P., M. I. Ridge, and C. A. Bishop, "Production of Transparent Electrically Conducting Films by Ion Plating," Thin Solid Films, Vol. 80, pp. 137–142. 1981

3. Pracchia, J. A., and J. M. Simon, "Transparent Heat Mirrors: Influence of the Materials on the Optical Characteristics," Appl. Opt., Vol. 20, pp. 251–258. 1981

4. Fan, J. C. C., and F. J. Backner, "Transparent Heat Mirrors for Solar-energy Applications," Appl. Opt., Vol. 15, pp. 1012–1017. 1976

5. Boyd, T., "Preparation and Properties of Esters of Polyorthotitanic Acid," J. Poly. Sci., Vol. 7, pp. 591–602. 1952

6. Holland, L., Vacuum Deposition of Thin Films, Chapman and Hall, London. 1970

Performance and sputtering criteria of modern architectural glass coatings

Wolf-Dieter Münz, Stefan R. Reineck
Department Research and Development for Coating, Leybold-Heraeus GmbH
Wilhelm-Rohn-Str. 25, D-6450 Hanau, Federal Republic of Germany

Abstract

Architectural glass coating has gained relevance in the entire energy consumption discussion worldwide. This affects solar control films for the reduction of climatisation costs in hot climate regions and heat mirrot coatings to reduce energy costs for room heating in regions of moderate climate conditions. Both types of coatings are deposited in a high rate sputtering process. The specific requirements to the magnetron cathode to reach special film properties are described. For the solar control films a low magnetic field strength version of the magnetron cathode is used to improve film hardness. For the heat mirror coatings a high magnetic field strength version of the magnetron cathode is described, especially to prevent the oxidation of IR-reflecting intermediate metal film. Optical values of solar control films on the base of stainless steel and titanium are given. Special colour effects, especially in reflection are described. Heat mirrors are exhibited as three films systems with silver or copper as the intermediate metal films. Transmission and reflectivity values are reported.

Introduction

Energy costs have been increased immensely through the last few years and architectural glass coating has gained a growing importance for heat insulation of building windows.[1] Two types of coating are applied depending on the geographic and typical wheather situation. Solar control films exhibit a low transmission over the visible (typically 8-20 % at 550 nm wavelength) and reduce energy transfer from the solar radiation into the buildings interior.[2] Heat mirror coatings are nearly transparent in the visible and have a high reflectivity in the far infrared. This wavelength selective filter keeps heat radiation inside the buildings. Monolayer coatings as well as multi-film systems are used.[3]

Both types of glass coatings can be deposited economically in an in-line production plant using the high rate sputtering process.[4] High rate sputtering additionally offers the advantage to obtain special film properties as adhesion, hardness or high purity by choice of the special types of cathodes as will be shown.

A 1 µm thick indium-tin-oxide coating for heat mirrors exhibits a transmission of about 80 % at 550 nm wavelength and 90 % in IR-reflectivity.[5] Moreover, the layers give a variety of colour adjustable in reflection of the coated panes depending on the particular thickness, whereas colour in transmission is nearly neutral. Because of the high material costs these indium-tin-oxide-layers are not used commercially up to now. The most common multifilm coating for heat mirrors is the gold-bismuth oxide film system.[6] As gold prices were raised immensely, gold had to be replaced by cheaper metals, as copper or silver.[7,8]

So three film systems oxide / metal / oxide have been investigated intensively and these film systems have been transfered to the recent production of architectural glass coatings with copper or silver as the intermediate metal layer.

The IR-reflectivity of these coatings has to be fixed via the conductivity of the metal films which has to be optimized for a high transparency in the visible. Especially in in-line production machines, when oxide and metal are sputtered simultaneously, one has to take care that the silver or copper film oxidation is kept at a minimum tolerable level. The transparency has to be optimized by adjusting the oxide layer thickness. Desired effects concerning the colour of the coated panes (in reflection) can be gained by choosing a non-symmetric set-up of the film system with different film thickness of the both oxide layers.

Because of the special situation solar control films are reasonably used on one pane windows. For this reason this kind of coating additionally has to be resistant to scratch and cleaning treatment. This demands hard and well adherent coatings.

The heat mirror coatings are usually used in two or three pane windows, where the coating is placed on one of the inner glass surfaces. So there are no major requirements for the mechanical properties of this kind of coating.

Experimental

The experiments reported have been carried out on a load-lock two-chamber plant type A 900 H2 (Leybold-Heraeus GmbH). The coating chamber is pumped down by a turbomolecular pump TMP 1500 [9] with a pumping efficiency of 1500 l/s. The residual gas pressure of the coating chamber is typically 5 x 10^{-5}mbar. Two high rate sputtering cathodes PK 750 with alternatively directly or indirectly watercooled rectangular targets of 750 x 230 mm² in size are installed. Multi-layer coatings are deposited in multipass mode.

The cathodes with 230 mm in width are standardized Leybold-Heraeus-cathode types and the length of the cathode can be chosen for the special application. From the experiences up to now experimental results can be transferred without major problems from the 750 mm-cathode to larger ones up to 3.50 m in length.

The cathode profile is given in Figure 1. The typical magnet arrangement in the magnetron cathode is shown. By means of the magnetic field the plasma expansion is restricted to a definite distance in front of the target and the particle density is maximum. By means of this effect the sputtering rate is optimized.[10] Thus the plasma can be confined not to touch the substrate for a given geometry. On the other hand if a self biasing effect of a floating substrate is desired the magnetic field strength of the magnet array has to be adjusted so that the substrate itself gets in contact with the plasma. Figure 2 shows schematically the situation for two different magnetic field strengths. Keeping the target-substrate-distance constant in the second case the magnetic field strength is weakened and the plasma expansion is enlarged. A considerable surface potential will arise.

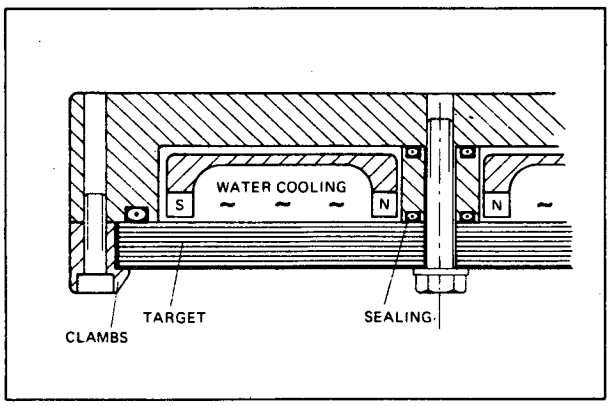

Figure 1. Cross-section of the magnetron cathode PK 750 (Leybold-Heraeus GmbH)

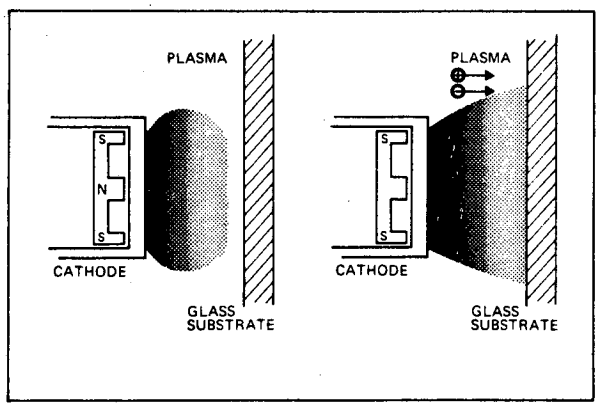

Figure 2. Schematically sketched expansion of the plasma cloud for a high and low magnetic field strength version of the magnetron cathode

For the experiments described the target-substrate distance is 100 mm. The maximum substrate dimensions in the sputtering plant used are 40 cm to 40 cm. The substrates are moved linearly in front of the cathodes. The speed of substrate motion is adjustable.

The power supply of the high rate sputtering cathodes is current controlled with a maximum current of 60 Amps.

Three gas lines are installed, flow controlled separately. Gases are mixed before entering the gas inlet system, which is mounted in front of the target.

Solar control films

Various materials have been investigated for use as solar control films. Stainless steel, for example, is attractive from the point of view of target material costs. However, properties of sputter deposited films are different from those of the bulk materials. Sputtering stainless steel results in coatings which actually are quickly corroded by the ambient atmosphere. So a protective overlayer is necessary.

Chromium is one of the most favourbale candidates for solar control films. The experiments show that Cr should be sputtered in a semi-reactive process in an oxygen/argon mixture. The pure Cr films would not achieve the hardness which withstands a typical scratch test.

Metal compound films as TiC are also suitable for solar control films. They are hard so that they are also used for tool coating.[11] The transparency of these films can be influenced by varying the carbon content during the reactive sputter process.

The colour in reflection of the coated panes can be varied, if a film system of metal oxide plus TiC, for example, is used.

Requirements to the sputtering process

Because of the special applications coatings for solar control films have to be optimized in hardness and adhesion. For coatings on metals or other conductive substrate materials bias sputtering would be applied to improve hardness as well as adhesion.

With glass as an electrically insulating substrate a bias voltage cannot be used if one consideres an in-line production plant with panes of up to 3 m by 6 m size. A movable surface contact to the conducting layers would not deliver satisfying results because of the high series resistances and the correlated voltage drop over the large substrate area.

Coating the glass panes at elevated temperatures does not work as the panes could break. But basically there is a possibility to influence the mechanical properties of deposited layers even on glass substrates in a 'quasi-bias' sputtering process. If an insulator is immersed in a plasma an electrical surface potential on the insulator surface will arise. This is due to the high electron mobility. In the plasma electrons immediately will be weakly bound to the glass surface to produce a negative surface potential. As a consequence ions will be attracted impinging the glass surface. For this reason the plasma confinement of the magnetron cathode must be adjusted exactly to the given geometry. Then the substrate gets directly in contact with the plasma (Figure 2), and the surface potential will be raised to approximately 60 V - 70 V. The current density to the glass surface will be increased. In this way the hardness and the adhesion of the deposited films can be improved significantly.

For the deposition of TiC, for example, a reactive high rate sputtering process is applied. The total gas pressure is kept relatively low at 2×10^{-3}mbar to prevent backsputtering. The reactive gas is C_2H_2 with a partial pressure of $3{,}5 \times 10^{-4}$mbar. The resulting deposition rate is 5 nm/s with a power load of 11 Watts/cm². The deposition rate and the hardness of the TiC-films are found to be very sensitive against only small - variations of the C_2H_2-partial pressure.

Results

Transmission and reflectivity curves of sputter deposited stainless steel films are plotted in Figure 3 and Figure 4. Reflectivity is shown to be about 20 % to 35 % over the visible, depending on the correlated transmission values (8 %, 14 % and 20 % respectively). Obviously these films show essential absorption. Reflection curves are rather flat, so that the colour in reflection viewed from the glass side appears greyish neutral.

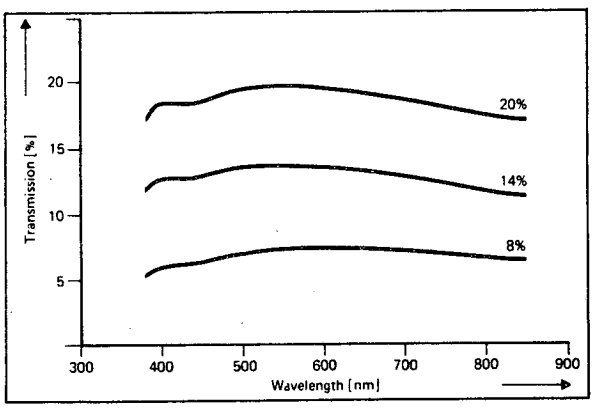

Figure 3. Transmission curves over the visible for stainless steel coated single panes

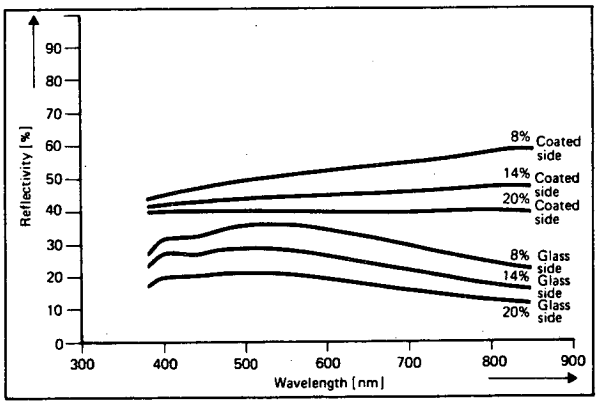

Figure 4. Reflectance curve over the visible for stainless steel coated single panes, related to transmission values in Figure 3

In Figure 5 and 6 the transmission and reflection curves of a TiC-coated glass pane are shown. The colour in transmission and in reflection again is greyish.

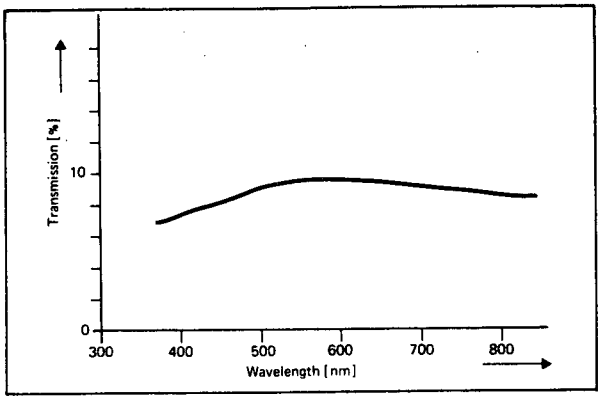

Figure 5. Transmission curve over the visible of a TiC-coated single pane

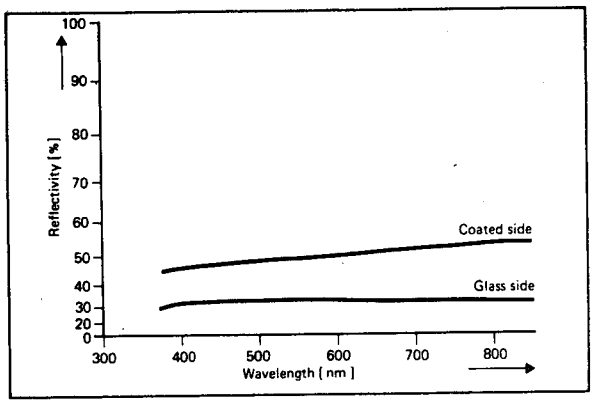

Figure 6. Reflectance curve over the visible of a TiC-coated single pane, related to the transmission curve of Figure 5

Now investigations have been done to influence the colour, especially in reflection, viewed through the glass panes (from the outside of the building). For this purpose a SnO_2-underlayer has been deposited on the glass substrate. The TiC-film is coated on this oxide. By means of interference effects of the tin-oxide films, now the colour in reflection can be varied. In Figure 7 three curves are shown for the reflectivity over the visible, measured through the glass pane. The transmission curve is not affected considerably by the tin oxide layer. Varying the tin oxide layer thickness the reflection maximum can be shifted from brown, green, blue to violet or even red.

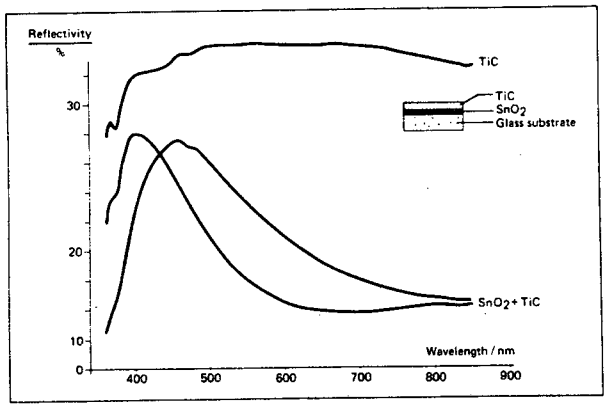

Figure 7. Reflectance curves over the visible of a TiC and two TiC + SnO_2-coated single panes. The SnO_2-film thickness is 800 Å and 1100 Å

Colour variations can be measured in reflection. In Table 1 colour measurements for these TiC and TiC + SnO_2-coated panes are given using a MACBETH-colourimeter. [12]

The L*-values indicate the integral reflection intensity over the visible, the A*-values indicate a green colour if the sign is negative and a red colour if the sign is positive. B*-values are standing for blue if negative and yellow if positive.

The pure TiC-coated pane measured through the glass is nearly neutral in colour (A*=-0.97, B*=1.02), whereas the both SnO_2-TiC coated panes show colour variations. The first one is significantly blue (A*=-0.17, B*= -15,92). The second one with A*=+10.57 (red) and B*= -22.05 (blue) appears violet.

Table 1. Colour measurement of coated panes (measured in reflection through glass, coating in position 2)

film system	L*	A*	B*
TiC (7 % transmission)	63,9	- 0.97	1.02
SnO_2 (800 Å) + TiC	46.9	- 0.17	-15.9
SnO_2 (1100 Å) + TiC	45.0	10.5	-22.0

A*: + red, - green B*: + yellow, - blue

Comparing the hardness and adhesion of the various films one has to state that the mechanical properties of stainless steel and TiC are quite similar. Especially TiC-films can be optimized for hardness as the properties are significantly influenced by the carbon content in the film (C_2H_2-partial pressure during deposition).

On the other hand a AES-depth profile of a TiC-film shows an oxidation of the TiC-surface. Therefore the film hardness seems to be improved by the hard TiO_2-surface, generated by oxidation from the atmosphere under room temperature. Annealing TiC-films in air results in a proceeding TiO_2-depth as can be seen from Figure 8 and Figure 9, which show AES-depth profiles of TiC-films after 1 hour annealing at 100°C and 300°C, respectively.

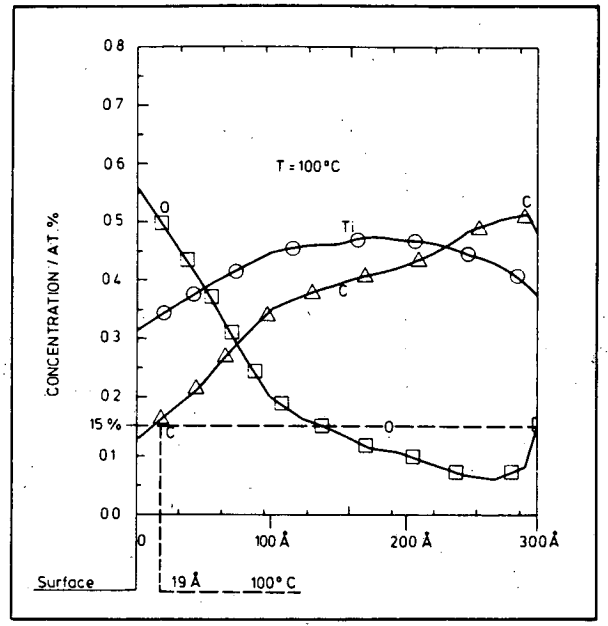

Figure 8. AES-depth profile of a 1 h/ 100°C annealed TiC-film on glass

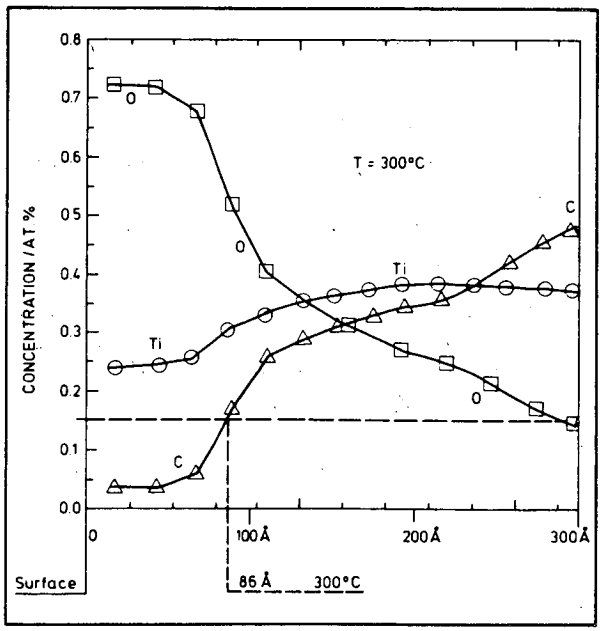

Figure 9. AES-depth profile of a 1 h/300°C annealed TiC-film on glass

The surface region is defined arbitrarily as the depth, at which the carbon concentration reaches 15 atom %. It is shown that the carbon concentration drops as the oxygen concentration is raised. The surface region grows with higher temperatures from approximately 20 Å at 100°C to approx. 90 Å at 300°C.

The film uniformity available is less than 2 percent variations in transmission over large scale substrated up to 3 m by 6 m.

Heat mirror coatings

Copper and silver are used replacing gold for an IR-reflecting film. These heat mirror coatings are deposited as a film system of oxide/metal/oxide. A typical metal film thickness is 80 Å to 100 Å for silver and 100 Å to 150 Å for copper.

The electrical conductivity defines the IR-reflectivity. So a correlation between square resistance and IR-reflectivity can be given.

The metal fim deposition process itself must provide the deposition of a pure metal film with highest conductivity or lowest specific resistance. Residual impurities would also influence the specific resistance resulting in absorption and lowered transmission over the visible.

The oxide layers (Indium-tin-oxide, titanium oxide for instance) are used for improved adhesion, as a protective layer and for optimization of the transmission. Moreover, colour effects as desired can be influenced, especially if a non-symmetric set-up of different film thicknesses is applied. Typical oxide film thicknesses are in the range of 400 Å to 600 Å.

Requirements to the sputtering process

For the deposition of a high purity metal film the ratio of sputtered particle density to residual gas particle density has to be maximized. That means for a given residual gas pressure, that the deposition rate must be as high as possible.

And a high sputtering rate supports nucleation in the films deposited so that the stability of the films against long-term effects will be improved.

From both points of view best results have to be expected if the low rate areas of the stationary sputtering distribution are shielded so that only high rate areas contribute to the film deposition. [13]

Therefore a special shielding is used for a metal film deposition as can be seen from Figure 11. The oxygen concentration in the reactive oxide sputtering process has to be minimized carefully just for the deposition of fully oxidized oxide films but preventing the incorporation of exceeding oxygen particles. This would cause long-term oxidation by diffusing oxygen particles. The oxide sputtering process is described in detail in ref. [13] .

Furthermore, for this application the target should be directly water cooled for a maximum applicable power input for high rates. The magnetic strength should be high (more than 280 Oe), so that the plasma confinement is determining a relative small sputtering area of high local sputtering rates.

The IR-reflectivity is decreased as the metal film is oxidized. This oxidation can occur during the deposition process, especially if the oxide and the pure metal film is sputtered simultaneously. The experiments show that the sheet resitance of the metal film is not affected by the first oxide film. More critical is the deposition of the second oxide film deposited on this metal film. If the metal film enters the reactive gas atmosphere with an essential oxygen gas partial pressure the sheet resistance of this film is slightly increased by about 10 %, equivalent to a change in the IR-reflectivity of only 1-2 percent.

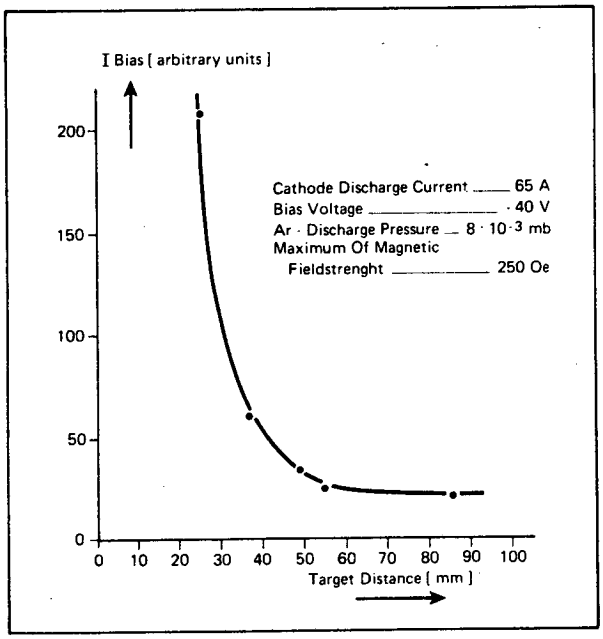

Figure 10. Ion current density versus probe-target distance for a high magnetic field strength version of the magnetron cathode PK 750

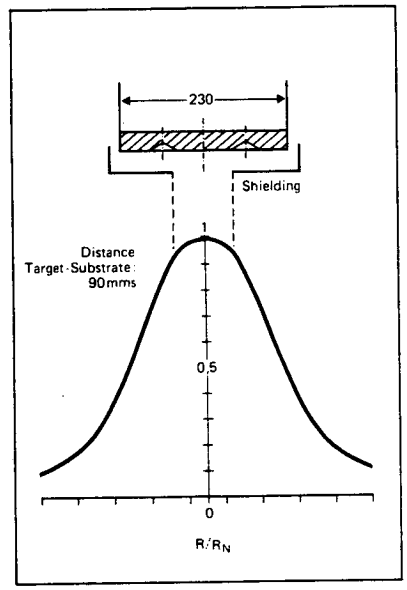

Figure 11. Normalized stationary deposition rate distribution for a target-substrate distance of 90 mms. A special shielding is used for the only utilization of the high deposition rate plateau.

However, if this metal film now gets in contact with the plasma and the oxygen gas, a drastical increase of the sheet resistance from 10 Ohms to 60 Ohms, for example is observed. This is caused by a high degree of oxidation, induced by the charged particles energy and thermal energy. For this reason, the magnetic field strength of the magnetron cathode must be adjusted so that the palsma is confined to a narrow area in front of the target, not to touch the substrate directly (see Figure 2). In this case also the heat load of the substrate is minimized.

Using such a high magnetic field strength version of the magnetron cathode the charged particle density is minimized at the substrate position as can be seen from Figure 10.There the ion current density is plotted versus the target-probe distance. The high ion current density directly in front of the target indicates the strong plasma confinement.

With this version of the magnetron cathode, the square resistance of the metal film is only increased by 10 to 15 percent during the second oxide film deposition. This is tolerable.

Results

The IR-reflectivity can be measured very quickly measuring the square resistance. In Figure 12 the IR-reflectivity is plotted against the square resistance. These measurements are carried out for copper and silver as intermediate metal layer between various metal oxide films. There are some considerable deviations between the various materials.

Figure 13 gives the transmission curves of $TiO_2/Ag/TiO_2$ and $TiO_2/Cu/TiO_2$ over the visible. The corresponding IR-reflectivity at 8 µm wavelength is 89 % to 90 % for $TiO_2/Ag/TiO_2$ and 85 % for $TiO_2/Cu/TiO_2$.

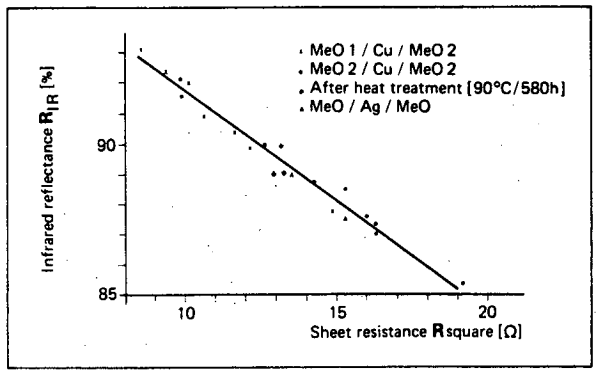

Figure 12. IR-reflectivity (measured at 8 µm wavelength)vs. the sheet resistance

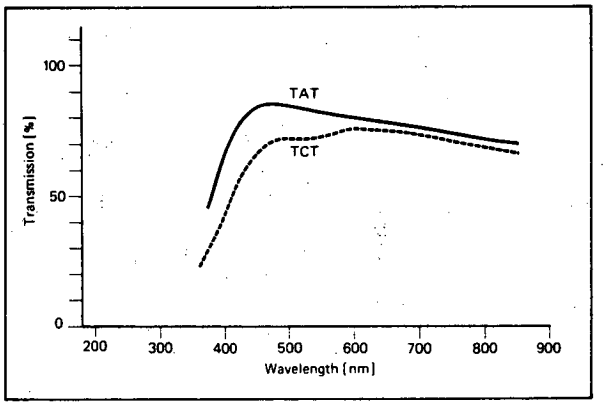

Figure 13. Transmission curves over the visible for $TiO_2/Ag/TiO_2$ and $TiO_2/Cu/TiO_2$

The oxide film thickness is 450 Å. The transmission at 550 nm for the silver system is about 80 %, for the copper system about 70 %. In Figure 14 the reflectance values over the far infrared (between 2 and 9 µm wavelength) are shown. If the intermediate metal layer is slightly oxidized, the transmission values and the IR-reflectivity are lowered.

The resulting effect is illustrated for silver in Fig. 15 and Fig. 16. AES-depth profiles of an almost ideal $In_2O_3:SnO_2/Ag/In_2O_3:SnO_2$ and of the same system with a partially oxidized silver film are shown.

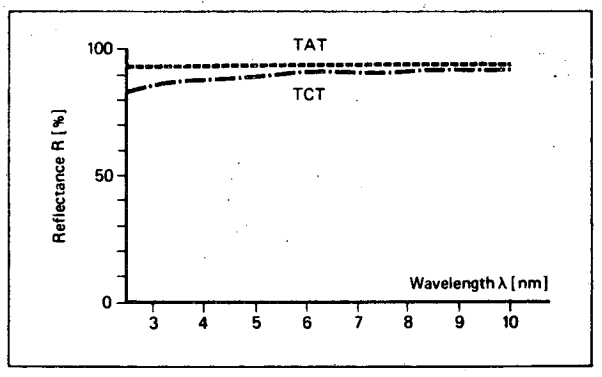

Figure 14. IR-reflectance curves for $TiO_2/Ag/TiO_2$ and $TiO_2/Cu/TiO_2$

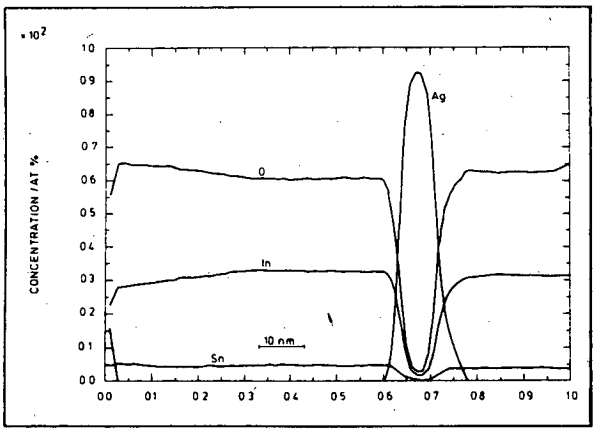

Figure 15. AES depth profile of an alomost ideal non-symmetric ITO/Ag/ITO - three film system

In the first case one observes a significant decrease in the oxygen signal to less than 5 %, when the silver peak goes up to 95 %.

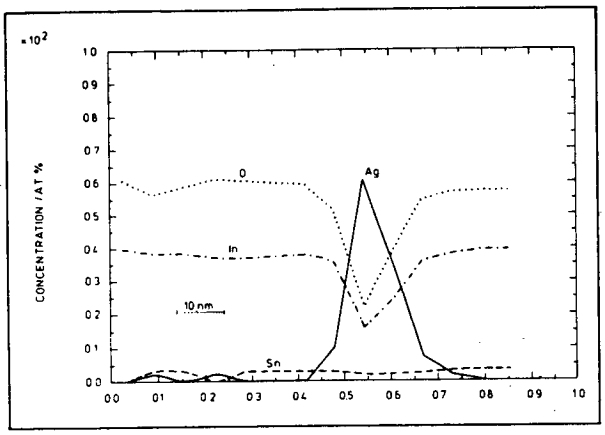

Figure 16. AES-depth profile of a ITO/Ag/ITO-system with a broadened Ag-region

In the second case (Figure 16) the silver region is broadened. The maximum value is only about 60 % and the oxygen signal does not drop to less than 20 %. This second coating appears blueish in transmission. The transmission maximum does not exceed 65 %.

Colour measurements in reflection of $TiO_2/Ag/TiO_2$ and $TiO_2/Cu/TiO_2$-coated panes are given in Table 2. The silver system appears blue in reflection whereas the copper system is green in reflection, corresponding to the slightly red colour in transmission.

Table 2. Colour measurement of coated panes (measured in reflection through glass, coating in position 2)

film system	L*	A*	B*
$TiO_2/Ag/TiO_2$	41.4	1.4	-10.6
$TiO_2/Cu/TiO_2$	53.0	-7.4	1.5

Variations of the absolute transmission value again can be kept at a level of less than 2 percent over large scale substrates. But, moreover, the colour variations which are more sensitive to the human eye can be kept to not observable deviations.

Conclusions

High rate sputtering processes have gained a high sophisticated state of the art. Process controll as well as process performances are of high reliability and successfully used in recent production lines. Especially the adjustment of a special version of the magnetron cathode to a special application offers the full utilization of all advantages of the high rate sputtering process. Solar control films are sputter deposited in a low magnetic field strength version for the improvement of the film hardness as required. Heat mirror coatings use a high magnetic field strength version to prevent a close plasma contact to the substrates, as the metal film oxidation has to be avoided.

Solar control films are deposited with optical and mechanical properties to meet the recent market requirements. Moreover in wide ranges a desired colour variation can be reached using an additional metal oxide layer.

Three films heat mirror coatings with silver or copper as the infrared reflecting intermediate layer exhibit transmission values of approx. 80 % in the visible for silver and 70% for copper while IR-reflectivity is in the range of 85 % to 90 % at 8 µm wavelength.

Both types of coatings are successfully used in recent production lines.

Acknowledgement

The authors wih to thank Dr. Klaus Hartig, Leybold-Heraeus GmbH for measuring the AES-depth profiles and helpful discussions for interpretations.

The works reported have been supported by the Bundesministerium für Forschung und Technologie of the F.R.G.

References

1. Libbey-Owens-Ford-Company brochure, Glass Glazing, Jan., 1978
2. Dittmer, G., Flêcher, P.:Thermische Eigenschaften von Glasfenstern, Berechnungsgrundlagen und theoretische Zusammenhänge. Publication prepared. Leybold-Heraeus Data Sheet, 14-102-1, 1980.
3. Lampert, L.M., Heat Mirror Coatings for Energy-Conserving Windows; Materials and Molecular Research Division and Energy and Environmental Division, Lawrence Berkeley Laboratory, California, August 1980.
4. Münz, W.D. Metallbeschichtung von Substraten durch Magnetron-Sputtern, Elektronik, Produktion und Prüftechnik, Dez. 1980, p. 591-593.
5. Köstlin, H., Doppelglasfenster mit erhöhter Wärmeisolation, techn. Rdsch. 34 (1974/75) 240-241.
6. Gläser, H.J., Highly transparent Low Emissivie Coating on the Basis of ZnO/Ag/ZnO, ZnO/Au/ZnO, Bi_2O_3/Au/Bi_2O_3, ZnO/Cu/ZnO, and Bi_2O_3/Cu/Bi_2O_3, Proceedings of the 8th International Vacuum Congress, Cannes, 1981.
7. Kienel, G., Meyer, B., Münz, W.D. Moderne Beschichtungstechnologie von Architekturglas, Vakuumtechnik, 30. Jhrg., Heft 8, 1981, p. 236-246
8. Fan, J.C.V. and Backner, F.J. Transparent mirrors for solar energy applications, Appl. Opt., 15 (1976), 1012-1017.
9. Leybold-Heraeus Datenblätter TMP
10. Waits, R.K. Planar Magnetron Sputtering, Academic Press, N.Y., 1978
11. J.-E. Sundgren, B.-O. Johansson and S.E. Karlsson, Influence of Substrate Bias on Composition and Structure of Reactively R.F.-Sputtered TiC-Films, Thin Solid Films, Vol. 80 No. 1/2/3, 1981.
12. Macbeth, A Division of Kollmorgen Corp., Operator's Manual,Newburgh, New York 12550, Manual No. 1500-2, Dec. 1980.
13. Deppisch, G. Schichtdickengleichmäßigkeit von aufgestäubten Schichten, Vakuumtechnik, 4/1981, p. 106-114.
14. Münz, W.D., Heimbach, J. and Reineck, S.R. Reactive High Rate Sputtering of Oxides, Thin Solid Films, 86, 1982

Production techniques for high volume sputtered films

Albany D. Grubb, Thomas S. Mosakowski, Walter G. Overacker
Airco Temescal, Solar Products, 2850 Seventh Street, Berkeley, California 94710

Abstract

Production techniques have been developed and proven in a production facility owned and operated by Airco Temescal in Carleton, Michigan. This plant deposits single- and multilayer films by sputtering on glass for architectural applications. Other plants have been built for handling glass substrates up to 100 inches wide to 144 inches long with average line speeds up to 12 feet per minute. This proven technology is applicable to the manufacture of other products, such as mirrors and glass with conductive coatings in large quantitites.

Introduction

Since the 1950s Airco Temescal has had a reputation for building large, thin-film vacuum coaters employing evaporation and utilizing electron-beam guns as the heat source. By the 1970s, the problems of achieving coating uniformity and of working with multiple sources, high vacuum, and the high voltage of electron-beam guns had made clear the need for some alternate method of deposition. Fortunately, we had already started developing a new type of sputtering source, with the objective of dramatically speeding up the traditional dc sputtering process. Our work produced a magnetically enhanced cathode of linear construction. We could see quite early in the game that our new sputtering source was ideally suited to coating large, flat surfaces, so we immediately began to consider glass-coating applications.

Developing a sputtering technology for glass

To be compatible with glass-industry requirements, we thought in terms of a truly in-line system in which raw glass would go in one end and the coated product would come out the other. We decided to handle the glass horizontally and sputter downward. To combat the prevailing skepticism concerning the feasibility of sputtering downward, we built and installed a pilot unit in our Berkeley, California, facility. The pilot unit had one lock for both entry and exit and a single sputtering zone capable of accepting two cathodes, each 54 inches long. Research efforts in that system aided us in the design of vacuum components and sputtering sources that clearly demonstrated downward sputtering as the best approach. The technology was not perfected easily, but suffice to say an excellent product is now being produced by this method every day with materials-handling that is infinitely simpler than it would be if we were loading work carriers for either vertical or upward coating.

Once in command of the technology, our next objective was to introduce it into the marketplace. To do this, we built a plant in Carleton, Michigan, whose output was dedicated to the needs of the adjacent Guardian Industries Corporation. The glass is trucked to the Airco Temescal plant, coated, and returned to Guardian Industries. The Airco Temescal plant, which went on stream October 1, 1977, coats lites of glass up to 78 inches wide by 135 inches long. The coater is equipped with six cathodes in two individual process chambers to produce the wide variety of coated architectural films marketed by Guardian Industries. The Airco Temescal plant normally operates two shifts, although on occasion it has operated a full three shifts, six days a week. With target changing and equipment cleanup occurring during scheduled downtime, our experience indicates equipment availability, including unscheduled maintenance, to be over 90 percent of scheduled uptime. Load-to-load time varies with the product, in a range between 1 and 2 minutes, with an average of approximately 1.5 minutes.

Facilities for research and development

Glass coating is in its early stages, and the need for more efficient films will continue, particularly with the escalating cost of energy. With this in mind, we set up a research and development laboratory in Concord, California, in 1981. A pilot line-coater designed to handle glass lites 1 meter wide by 2 meters long is scheduled to begin operation at the new facility early in 1982. In that pilot system, we have designed a vacuum coater with more flexibility than any other yet built for production. That system has four successive coating chambers, each of which can be equipped with two cathodes. Each chamber can be effectively isolated from adjacent chambers so that dissimilar coatings can be put down in succession--a metallic oxide in the first chamber, for example, followed by a metal and then by another oxide. We have developed techniques for this whereby a metal very sensitive to oxygen can be deposited in a chamber adjacent to a chamber in which an oxide is being laid down.

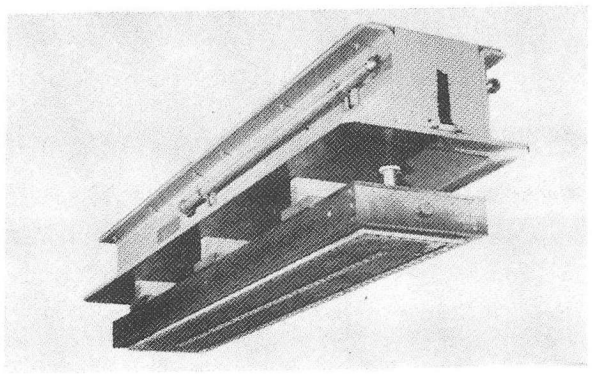

Figure 1

This machine offers unequaled development capabilities, for which we have lined up a number of projects that we are confident will lead to exciting new products. We are supporting the pilot system with state-of-the-art equipment, from the latest in film-measuring instruments to a variety of environmental testing units to be used in evaluating the durability of our coatings. In addition, our research and development facilities include a small in-line laboratory coater and a batch-type box coater for film development. The small in-line system is used to coat samples up to 6 inches by 12 inches in order to establish material properties and process parameters for scale-up to the 1-meter by 2-meter pilot system. Fundamental to all this activity are the facilities of the Airco, Inc., Central Research Laboratories in Murray Hill, New Jersey, which is dedicated to basic research.

Equipment

Our equipment is varied and flexible. Figure 1 shows the patented Airco Temescal planar magnetron cathode that represents the heart of the in-line system. The cathode is suspended from a cover plate that forms part of the top of the process chamber. Because all utilities pass through the plate, the complete cathode assembly can be removed quickly. Most targets are 13 inches wide, and of a length compatible with the width of the glass being coated. The large-inventory targets are bolted onto the cathode structure from the front. The erosion path on the target forms the racetrack pattern characteristic of magnetically-enhanced sputtering. Approximately one-third of the target material is sputtered onto the glass. Since the Airco Temescal architectural films employ inexpensive materials, the remaining two-thirds of the target material is commonly scrapped. Of course, in dealing with expensive materials, the unused part of the target would be recovered. Incidentally, Airco Temescal has been awarded a patent on the cathode described, in the United States, Canada, and the United Kingdom.

The in-line system at the Carleton, Michigan, plant is shown from the inlet end in figure 2. At right is the conveyor on which a full load of glass is held until the processor starts it through the washer. The washer is followed in line by a hooded station where the glass is held before it enters the load lock. Holding the freshly washed glass in a hooded station with filtered air at a slight positive pressure keeps the washed glass free of dust particles.

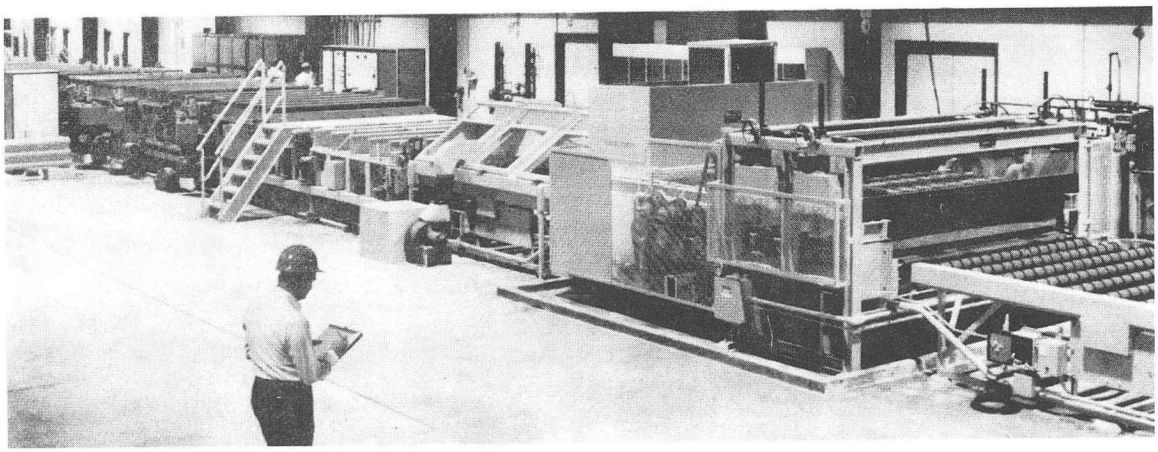

Figure 2

Valve Key

V-1—*Entry load lock*
V-2—*Entry hold chamber*
V-3—*Entry process chamber (buffer zone)*
V-4—*Exit process chamber (buffer zone)*
V-5—*Exit hold chamber*
V-6—*Exit load lock*

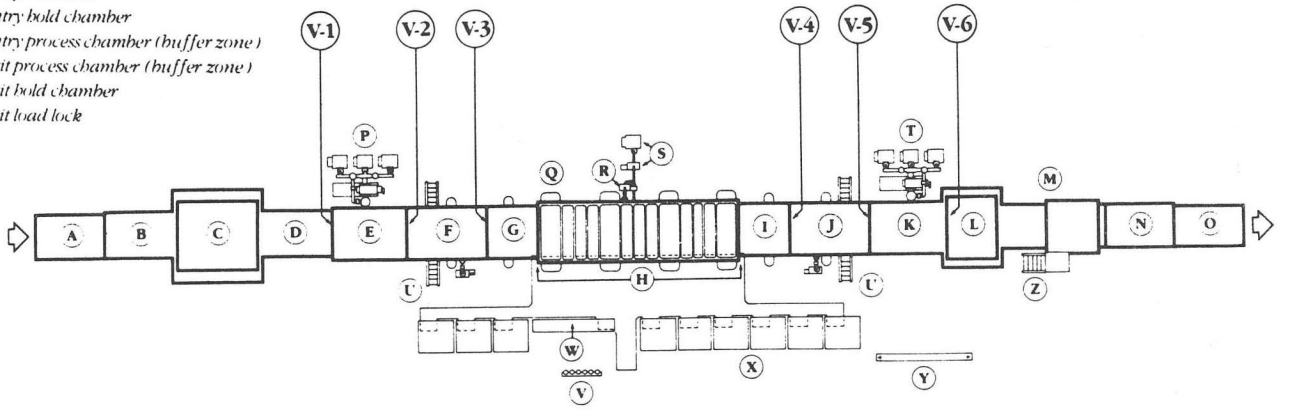

Figure 3

A. Loading conveyor
B. Holding conveyor
C. Inlet washer
D. Entry hold station
E. Entry load lock
F. Entry hold chamber
G. Entry buffer zone
H. Coating zones
I. Exit buffer zone
J. Exit hold chamber
K. Exit load lock
L. Exit washer
M. Exit inspection
N. Exit hold station
O. Unloading conveyor
P. Inlet lock pumping system
Q. Dual pumping plenums
R. Diffusion-pump backing boosters
S. Backing booster pumping system
T. Exit-lock pumping system
U. Stairs
V. Process gas supply
W. Control console
X. Sputtering power supplies
Y. Motor-control center
Z. Stairs to inspection booth

The entire in-line system is represented schematically in figure 3. Holding conveyor B, shown in figure 2, is followed by inlet glass washer C, in which a lite of glass is cleaned with detergent and scrub brushes and then rinsed and rotary brushed. The deionized rinse water is blown off using air knives, top and bottom. The lite of glass then moves into hold station D, where it is held until load lock E has been cleared, valve V-2 is closed, and valve V-1 is opened. The glass moves quickly into the load lock, and valve V-1 is closed. The high-capacity pumping system utilizes a large Roots-type pump backed by multiple mechanical pumps to pull the load-lock pressure down to the low-micron range in about half a minute. The glass then moves into entry hold chamber F, which is diffusion-pumped to a pressure less than 1 micron. When valve V-3 is opened, the glass moves into the main processing chamber. In section G, the buffer zone, the glass is accelerated to catch up with the glass ahead of it so that, as the pieces of glass move under the cathodes, they present a virtually continuous surface with only small spaces between pieces. Figure 3 represents a system having three coating chambers (H), each containing three cathodes. This arrangement permits the manufacture of a full range of products, from conventional architectural films to oxide-metal-oxide low-emissivity (low-E) films. The exit equipment (I-N) is similar to the entrance equipment. Note, however, second washer L, which washes the glass a second time to expose any imperfections in the coating. (This is a better time to find imperfections than months later, when the lites are glazed into a building.) The finished product goes through an inspection station, brightly lighted from below. After that, the glass is unloaded from the exit conveyor for shipment. Typically, control console W is located on one side of the system and the power supplies and pumping equipment on the other. The final layout, of course, depends on the space available and on user preferences, but we recommend that pumps and power supplies be as close to the line equipment as possible.

The upper portion of the typical control panel pictured in figure 4 displays a schematic arrangement with lamps to indicate the condition of every pump and valve in the vacuum part of the system. Below the vacuum-system schematic is a map of the complete line, on which lamps also indicate the condition of system components.

In normal operation, the entire coating process is controlled by a solid-state processor. Processes for individual products are controlled by front-panel settings. Operating troubles are quickly diagnosed using a cathode-ray-tube (CRT) display. With such control, a single experienced operator can operate the complete system--supported, of course, by materials-handling people on both ends of the line.

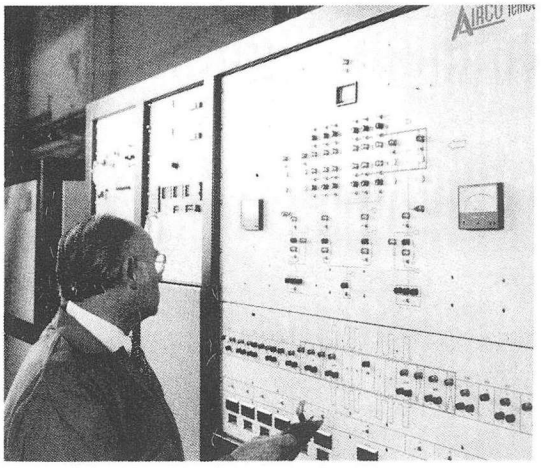

Figure 4

Although we have standardized on systems of the sizes considered in table 1, we have made systems of other dimensions, as well. Standard systems handle glass from 48 inches to 100 inches wide, up to 144 inches long. The equipment is generally capable of a 1-minute load-to-load cycle, although the cycle for any given product depends upon the particular process applied. High humidity can affect cycle time adversely unless special provisions are made, such as venting the load lock and unload lock with dry air. On-stream time for these systems, as mentioned earlier, is approximately 90 percent of scheduled uptime. Shrinkage is typically 4 percent. The loading factor varies greatly from one installation to another, depending on the product; where stock sizes of glass are handled, the loading conveyor can be almost full, whereas in other situations, where small pieces or varying sizes of glass are handled, the loading factor declines. The 70-percent loading factor from which the annual capacities displayed in table 1 were calculated is conservative.

All in-line systems manufactured in the Airco Temescal plant in Berkeley, California, are set up and operated there for customer acceptance. Figure 5 shows an architectural glass line in Berkeley being prepared for testing. The test layout in the plant is the same as the customer will use in his plant, so all of the manifolding and wiring is cut to length, which facilitates final installation.

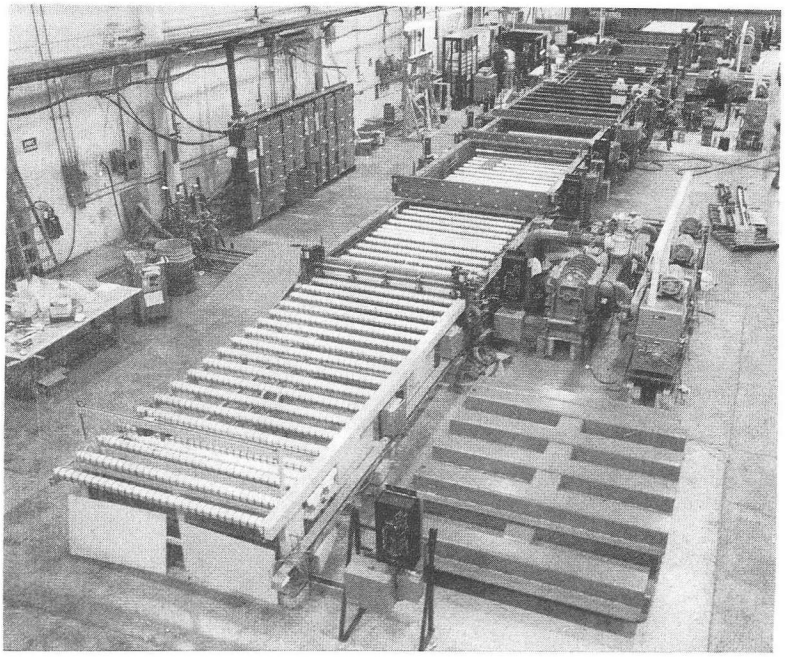

Figure 5

Productivity

Glass size			
Width (max.) -inches	48	84	100
Length (max.) -inches	96	144	144
Thickness - inches	--	0.1 to 0.5	--
Cycle time and output			
Cycle/hour	60*	60*	60*
Area/cycle-sq. ft.	32	84	100
Area/hour-sq. ft.	1920	5040	6000
Hours/day	24	24	24
Days/week	5	5	5
Weeks/year	50	50	50
Area/year-sq. ft.	11,520,000	30,240,000	36,000,000
On-stream time as percentage of scheduled time - %	90**	90**	90**
Product loss due to coating approximate - %	4	4	4
Loading Factor (varies, depending on the product) - %	70	70	70
Capacity/year based on above sq. ft.	7,000,000	18,000,000	21,500,000

*The equipment is capable of 1.0-minute cycle time, although some films require a longer cycle of up to 1.5 minutes. High humidities require longer pumpdown times, which, without special consideration, will also elongate the cycle.

**Experience at our Carleton plant indicates on-stream time of 90% is possible with preventive and scheduled maintenance. Preventive and scheduled maintenance should be performed on weekends if the production schedule is 5 days per week, 3 shifts per day.

The system shown in figure 6 was built for making first- and second-surface mirrors. This system coats glass lites up to 100 inches wide by 144 inches long in a 1-minute cycle. Since it deposits a single metal film, the system includes only one process chamber, rather than three. If the value of silver rises--as seems inevitable--we foresee a demand for many such systems to replace the expensive silver mirror coatings with less expensive coatings of aluminum and other metals.

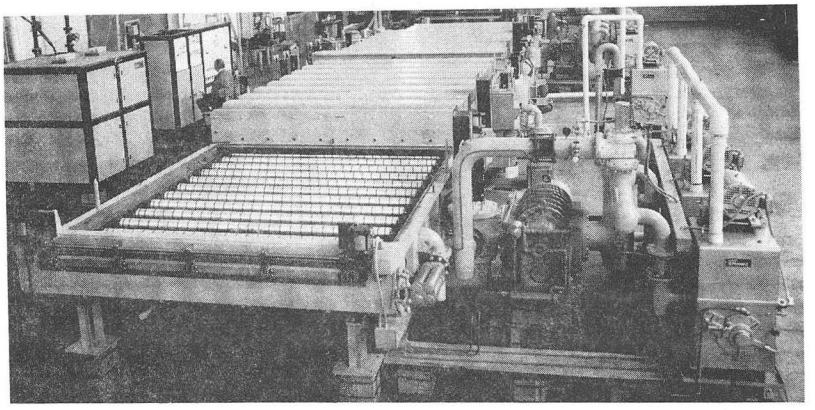

Figure 6

The cathode service fixture shown in figure 7 is used for changing targets and cathode servicing. When a cathode is lifted out of the system, it is facing downward. The fixture holds the cathode (which can be 3 meters long) and turns it over for easy access.

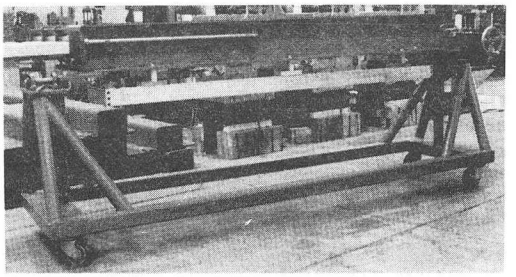

Figure 7

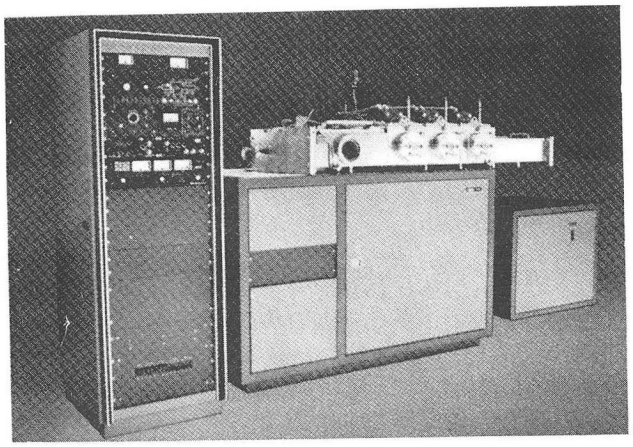

Figure 8

The LS-1600 system in figure 8 resembles the small laboratory unit used for film development at Airco Temescal in Concord. The system pictured accommodates three cathodes and coats glass 12 inches by 12 inches.

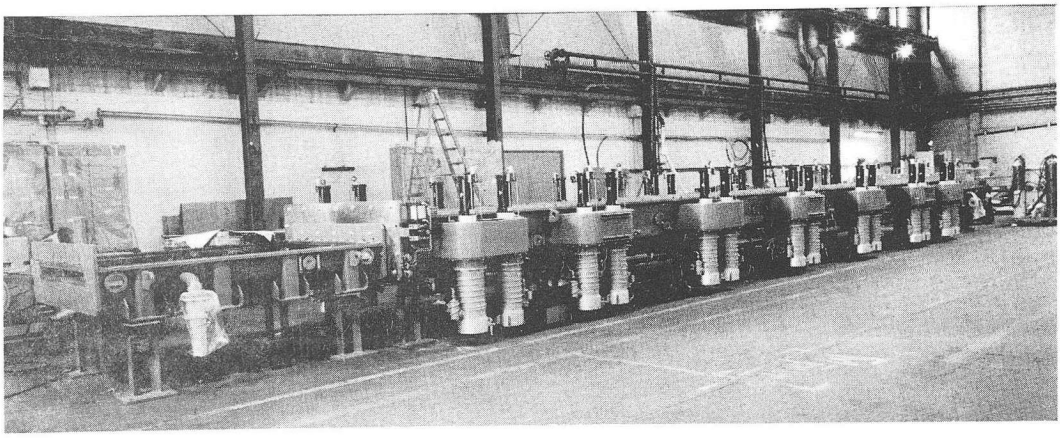

Figure 9

The 1-meter by 2-meter pilot unit installed in Concord appears in figure 9 as it was during assembly in Berkeley.

Materials

The dc planar magnetron sputters virtually any metal or metal alloy. As mentioned earlier, Airco Temescal architectural films do not use expensive materials. They generally employ stainless steel, titanium, copper, aluminum, chromium, and alloys of those materials. The coating systems deposit transparent protective topcoats as well, particularly for monolithic glass; they commonly deposit titanium dioxide or titanium nitride using reactive dc sputtering. (Incidentally, Airco Temescal systems do not use radio-frequency (RF) sputtering, as it is entirely too slow and its requirements far exceed the state of the art for power supplies and RF shielding.) The systems described here can also deposit metallic oxides such as indium tin oxide for either their electrical or ther optical properties. Because the system does not employ substrate heating, it can deposit an indium tin oxide film at essentially room temperature, to give a resistivity as low as from 10 to 20 ohms per square. Indium tin oxide can also be used in low-E films having high solar transparency. Dielectric multilayer films of other metals offer an alternate potential for low-E work. In addition to the mirrors mentioned earlier, Airco Temescal systems also produce first-surface mirrors using materials like corrosion-resistant chromium and stainless steel, which are extensively used without protective topcoats.

Applications

The major uses for architectural films today, of course, are in commercial building. A great amount of research is under way around the world to evaluate and expand the present applications. A good example is the Crystal Pavilion built in Cambridge, Massachusetts, on the campus of Massachusetts Institute of Technology by a group headed by Professor Tim Johnson (figure 10).

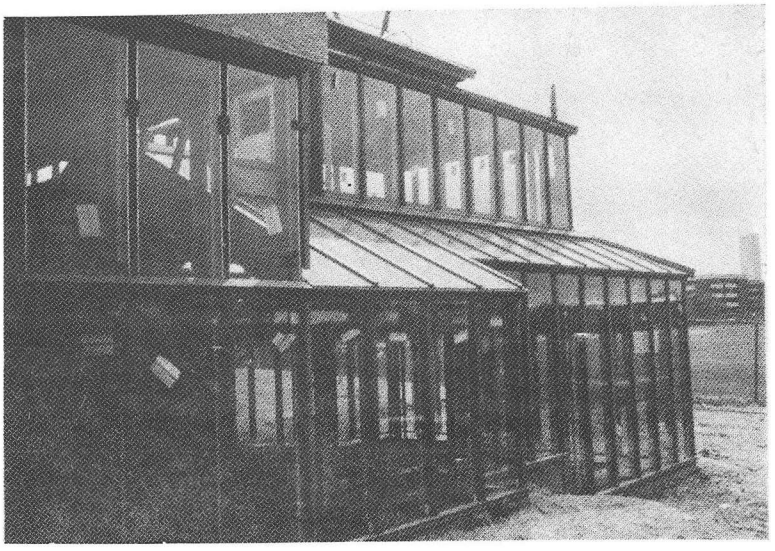

Figure 10

The objective of the building is to demonstrate that 100 percent solar heating can be accomplished in the northern United States even on cloudy days, as long as the outside temperature is greater than 40 degrees F. This structure is glazed with Airco Temescal low-E coated glass. In a different application, the reflective coating on an automobile "moon roof," shown in figure 11, adds comfort to driving by preventing heat buildup inside the car.

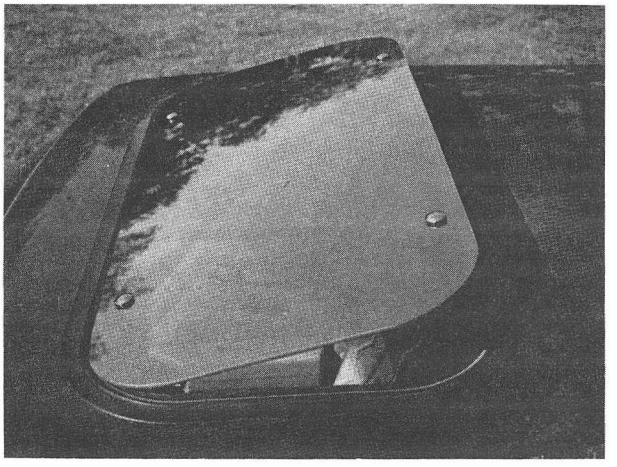

Figure 11

We foresee many further applications in displays, solar collectors (both reflecting and absorbing), special films for different building exposures, and the like. In fact, new applications for this exciting technology are the main thrust of our Concord research and development facility--which, incidentally, is available for you to see.

Conclusion

The technology has been proved in more than four years of production experience in Carleton. Costs are known, in-plant training is available, and the technology is supported by an aggressive research and development program for new products.

In-line systems have recently gone on stream in Sweden and in Italy. The mirror coater shown in figure 6 went into production at the end of 1981, and an architectural-glass plant is just starting up in Canada. A unit is under contract in the United States and another in Mexico and we are looking forward to more. We would be glad to hear from you.

Optical coatings by conveyorized atmospheric chemical vapor deposition (CVD)

Nicholas M. Gralenski
Watkins-Johnson Co., 440 Mt. Herman Rd., Scotts Valley, California 95066

Thin films. We're considering their importance and use in great quantity. But how do you get thin films?- especially in great quantity, big sizes, high quality and still cheap?

"Thin" , where coatings are concerned is often defined as less than one mil or so. "Thick" films are more than a mil or so. For optical coatings we're often in the tenth micron (1000 A, 0.004 mil) range or less.

We usually think of vacuum for controlled thin film deposition (evaporation, sputtering, low pressure CVD etc.). But vacuum has its limitations; especially high equipment costs, high process cost, slow coating rate, molecular dissociation etc. As the production requirement gets bigger, vacuum processes get more prohibitive.

Another method which has been in use for many years is liquid spray. Tin oxide coating on glass is commonly done this way. In this method a solution is prepared for spraying against a hot glass surface. It is a variety of CVD in that the sprayed droplets are supposed to evaporate on their way towards the hot surface and then react as a gas to produce a coating. A review of Fig 1 however, shows this can be a very tall order for reliable quality results. It is a deceptively simple arrangement; like paint spraying but the coating is never in the liquid state. Droplets of various size and velocity leave the nozzle. Some may actually splatter as liquid on the hot glass. Others vaporize very early but then the dissolved salts are left as dust and smoke. Some material reacts too early forming particles which end up as inclusions in the coating. Precipitates which accumulate at the spray nozzle blow off to form defects. The glass is warped by the cool spray. Sometimes an alcohol laden spray bursts into flame or explodes when conditions aren't quite right. A very small proportion of spray ends up as coating. The rest must be drawn off in a veritable tornado of noxious fumes. In spite of the problems, respectable results can often be achieved and it is a tempting method for big sheets and big production. The usual limitations are micro roughness, inconsistency, warpage and lots of pollution control.

Dip coating is another method which is used. Carefully cleaned glass in a carefully controlled atmosphere is dipped into a carefully prepared solution. The glass is carefully withdrawn, leaving a thin chemical layer (on both sides) which is dried and fired. Although exceptional uniformity on big sheets can be achieved, the process and firing can be tricky. The coatings can be porous and contaminated with solution residues.

About ten years ago, work began at Watkins-Johnson to develop a coating method which could rival vacuum in control, yet rival liquid spray, dip coating and others in productivity and cost effectiveness. The work grew out of conveyor furnace technology. Figure 2 shows such a machine; horizontal, atmospheric pressure, fully conveyorized. In operation, work is simply loaded on the moving belt. Heat up rate, time at temperature, atmosphere control and cool down temperature are all controlled automatically. This particular machine has a 14 inch wide belt, is 40 feet long and was made for electronic thick film firing.

Figure 3 shows the interior design principles. An endless wire mesh belt moves through a metal muffle which provides atmosphere and dust control. Heating is electric. Gas purging and vent control are provided. Work is simply loaded on the belt, goes through automatically, comes out done. The forte' of such an arrangement is that it is very production oriented and very cost effective. It has been the object of the CVD development work to produce thin as well as thick films that way.

Figure 4 shows such a furnace concept adapted to produce thin films by CVD (Chemical Vapor Deposition). The furnace is required because chemical vapors are reacted by heat to produce a coating. However, only a small section, the coating chamber, contains chemicals. Otherwise the chemical reaction would be uncontrolled and the muffle would soon be filled with dust and debris. The actual furnace, smallest size, has a 4 inch wide belt, is 15 feet long overall and has a coating chamber 5 inches long. Gaseous chemicals flow towards the coating chamber and into the dispenser or injector. Reactive chemicals are kept separated until they enter the furnace. The gases flow towards the substrates, which are moving continuously through the coating chamber. The reaction produces a coating and the by products are vented out. It's important that the chemicals be carefully metered for good coating control. It's equally important that the venting be carefully metered. A controlled chemical atmosphere is being maintained in the coating chamber while work and belt move through continuously. If the vent rate is too slow, chemicals drift into the furnace muffle. If the vent rate is too fast, chemicals have insufficient time to react.

Since the coating chamber takes up such a small part of the furnace length it's quite feasible to have more than one.

Figure 5 shows a multi stage concept. Multi stages pile up a heavier coating at a higher belt speed or as the figure shows, produce several coatings in one transit. This is a hypothetical combination where a silica coating is applied in the first chamber, tin oxide in the second, pure silicon in the third, more silicon in the fourth and pure nickel in the fifth.

Figure 6 shows a closer look at one of the coating chambers. Chemical vapors flow through the injector, produce a coating and are vented out. Curtains or flapper doors help to isolate from the rest of the muffle.

Figure 7 shows more detail. The actual coating zone is inside the vent assembly which is separate from the chamber and muffle. For periodic maintenance the entire vent assembly which includes the injector (about the size of a lunch box) is lifted out. The furnace itself does not have to be shutdown or cleaned. A spare vent assembly is dropped in and the furnace is back in production in minutes.

One of the important components in the machine is the injector. Considering that the coatings are often a millionth of an inch or so and the coating tolerance much smaller than that, one might expect that the injector would have to be impossibly precise and a nightmare to maintain. Although precision is important, it's not that extreme. The design details also have an important bearing on whether the structure can be achieved in a practical way.

Figure 8 shows the design principle which has given us the best results. Three tubes are positioned triaxially. The tubes are small (the largest about 5 millimeter diameter) because the usual gas flows are small. The object is to keep the reagents completely separate to avoid prereaction and fouling. At the same time they must mix together efficiently in the furnace to produce the coating reaction. At the exit there is a short laminar flow region consisting of the two reactive gases separated by a thin inert gas curtain. The gases begin to heat up, mix together and prereact before coating the substrate which is about an inch away. Very complicated processes are obviously going on in this one inch space.

The triaxial tubes would only be suitable for a tiny coating area.

Figure 9 shows this structure stretched out across the width of the belt.

It is one thing to make a diagram, but another thing to make the hardware.

Figure 10 shows more closely how the structure is actually produced. Two metering slots are used to supply each gas flow. This enhances uniformity and makes a symmetrical structure.

Figure 11 shows a production model tin oxide coating furnace. It has an 8 inch wide belt and is about 30 feet long. The cabinet in the center is where initial chemical dispensing takes place. In this case there are four chemicals, all liquids, kept at constant temperature and evaporated in a carrier gas before going to the injector.

Figure 12 shows tin oxide coated glass exiting the furnace.

Figure 13 shows silicon wafers exiting a smaller furnace. The coating is phosphorous doped silicon dioxide. In principle, any coating can be produced this way but the chemistry and numerous other parameters have to be worked out for each one. Belt speeds are typically one foot per minute but range from about 6 inches to 24 inches per minute. The effective coating rate is about one micron per minute.

Figure 14 shows titanium dioxide coated solar cells exiting a 12 inch furnace. The coating is 700 angstroms thick, the belt speed 15 inches per minute.

Figure 15 shows a 3 stage machine recently completed for the semiconductor industry. Semiconductor coatings are extremely critical. Extensive studies have been made which show that coatings made this way are indeed suitable for critical requirements.

CVD often has a witchcraftish character to it because of the many subtle parameters at work. Consider two part coatings such as antimony doped tin oxide or phosphorous doped silica. The two reactions are almost certain to proceed at different rates. That would mean the chemical proportions in the gas would be different than the proportions in the film.

Figure 16 shows that historically this is so. Data which falls on the dotted line in the chart means the chemical proportions in the gas phase exactly match the proportions in the coating. Typically reported data falls substantially to the right where as the Watkins-Johnson coatings are right on target. This strongly implies that the Watkins-Johnson process is controlled by chemical delivery rather than reaction rates. It means the equipment, rather than the chemistry, has the control.

Figure 17 shows the coating rates are much higher than for earlier methods. It also shows the working areas, the plateaus, are much broader and there fore much easier to control

Chemical reaction rates approximately double for every 10 percent change in temperature. This would imply that CVD process temperatures would have to be tightly (and expensively) controlled.

Figure 18 shows however that the tin oxide on glass process is substantially independent of temperature in the vicinity of 500°C. The reason for this is that the chemical efficiency is very high. The reaction rate is limited by the chemistry at low temperature but by delivery rate at high temperature. If the chemicals are all used up, it just doesn't make much difference if the temperature goes higher.

Conveyorized CVD furnaces are now being used to produce coatings for digital displays, touch switches, flash tubes, smoke alarms, semiconductors and solar cells. Years of production history have been accumulated and millions of parts made. Tin oxide, silicon dioxide, silicon nitride, poly silicon, amorphous silicon and titanium dioxide coatings have been made this way. The coatings can be doped. Multilayers can be applied. New coatings are being developed. Bigger furnaces are being built (we can do 14 inch widths now). As the technology advances, the product list will include electronic components, solar heating, infra-red reflecting glass and architectural applications.

References

1. L.W. Winkle, C.W. Nelson SOLID STATE TECHNOLOGY OCT. 1981 Pgs. 123-128

2. W. Kern, G.L. Schnable, and A.W. Fisher, RCA Rev. 37, 3, (1976)

3. M. Shibata and K. Sugawara, J. Electrochem. Soc. 122, 155 (1975)

4. N.M. Gralenski, paper presented at the 32nd Annual Meeting of the American Ceramics Society, Chicago, Ill., April 29, 1980.

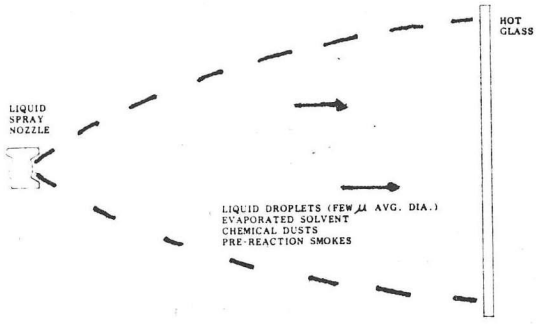

Fig. 1 CVD by Liquid Spray

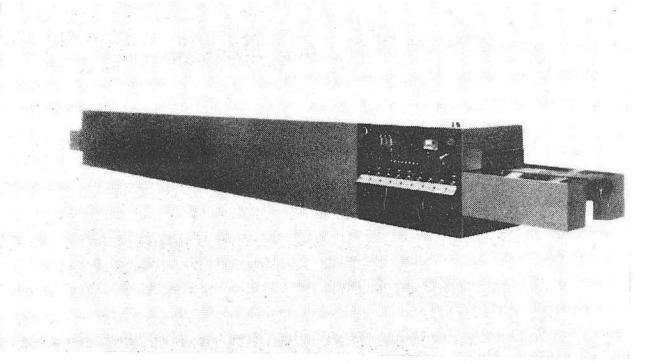

Fig. 2 Production Model Thick Film Conveyor Furnace (9588-1)

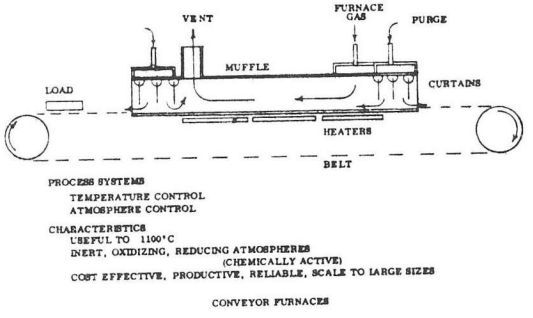

Fig. 3 Conveyor Furnace Design Diagram

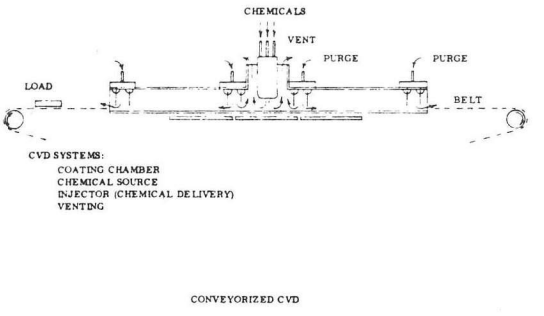

Fig. 4 Conveyorized Atmospheric Pressure CVD (APCVD) Design Diagram

CONVEYOR FURNACE DESIGN

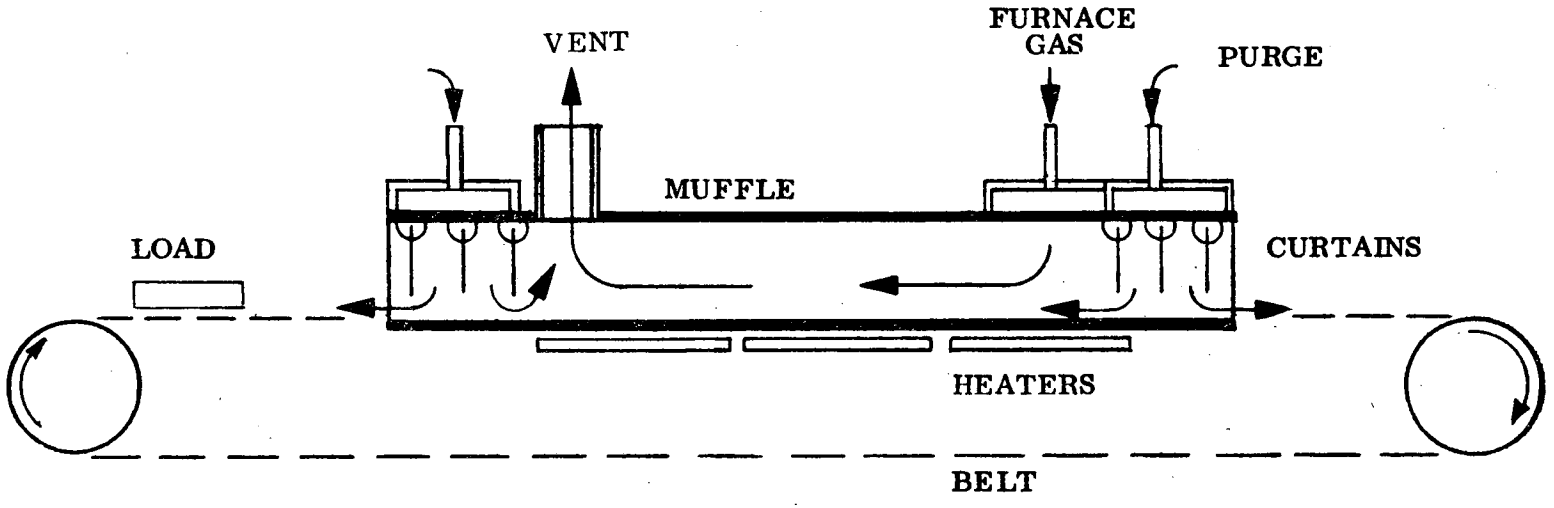

PROCESS SYSTEMS

- TEMPERATURE CONTROL
- ATMOSPHERE CONTROL

CHARACTERISTICS

- USEFUL TO 1100°C
- INERT, OXIDIZING, REDUCING ATMOSPHERES (CHEMICALLY ACTIVE)
- COST EFFECTIVE, PRODUCTIVE, RELIABLE, SCALE TO LARGE SIZES

1330

CONVEYORIZED ATMOSPHERIC PRESSURE CVD (APCVD) DESIGN

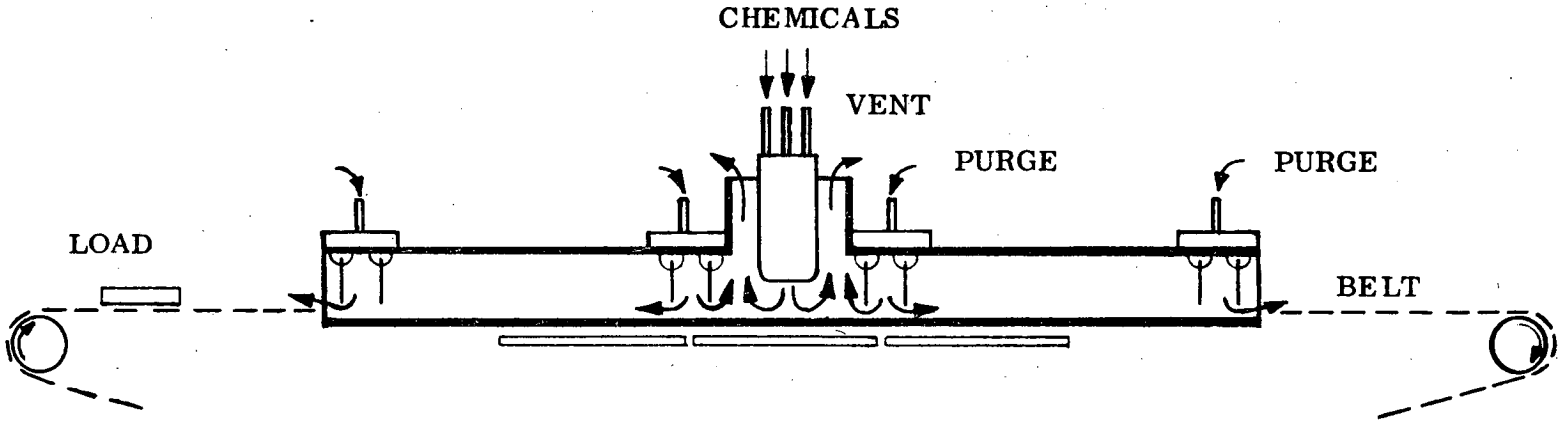

CVD SYSTEMS:

- COATING CHAMBER
- CHEMICAL SOURCE
- INJECTOR (CHEMICAL DELIVERY)
- VENTING

1329

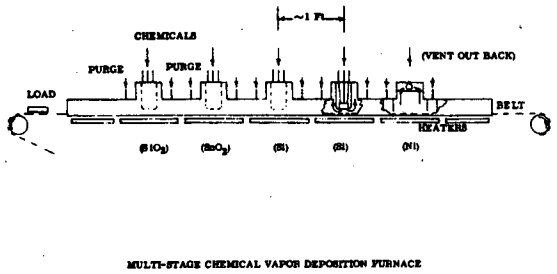

Fig. 5 Multistage Conveyorized APCVD

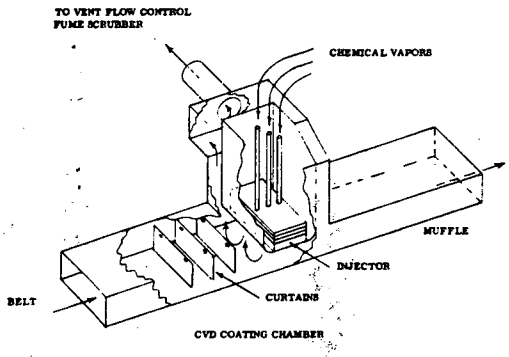

Fig. 6 CVD Chamber

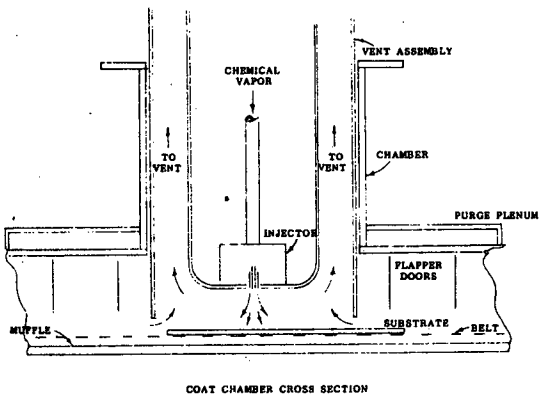

Fig. 7 CVD Chamber Detail

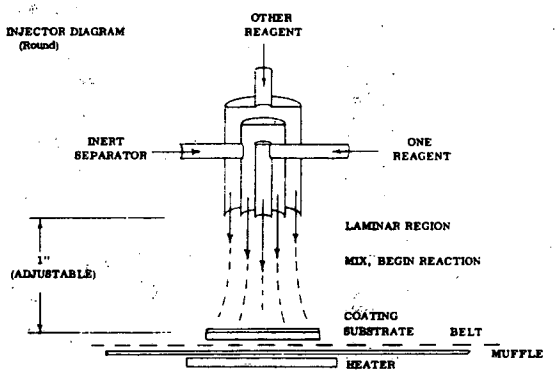

Fig. 8 Injector Design Principle (Tube)

MULTI-STAGE CONVEYORIZED APCVD

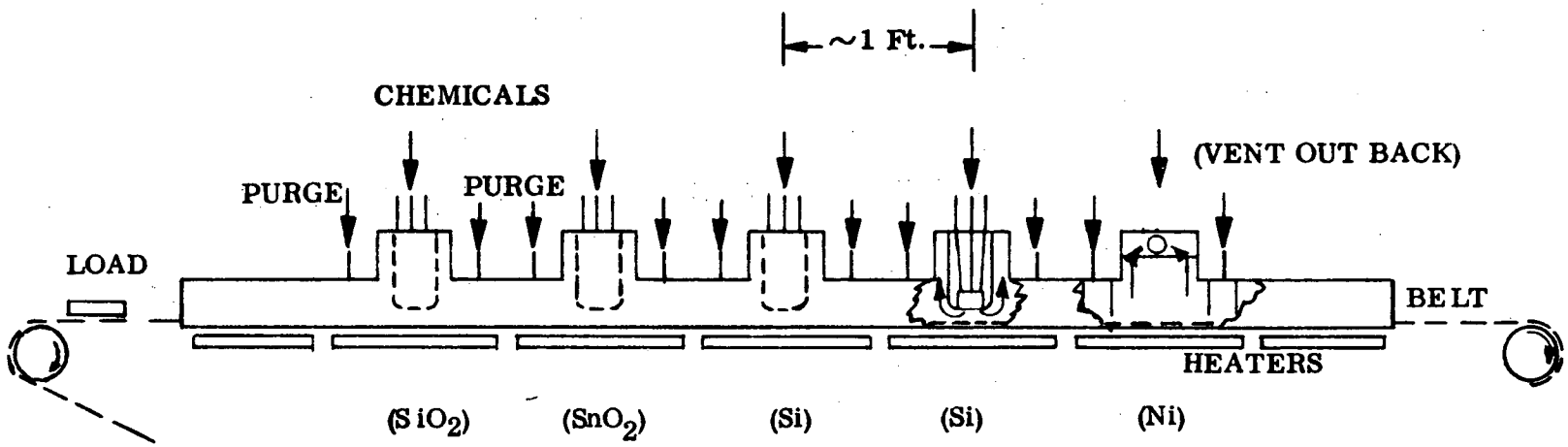

1331

CVD CHAMBER

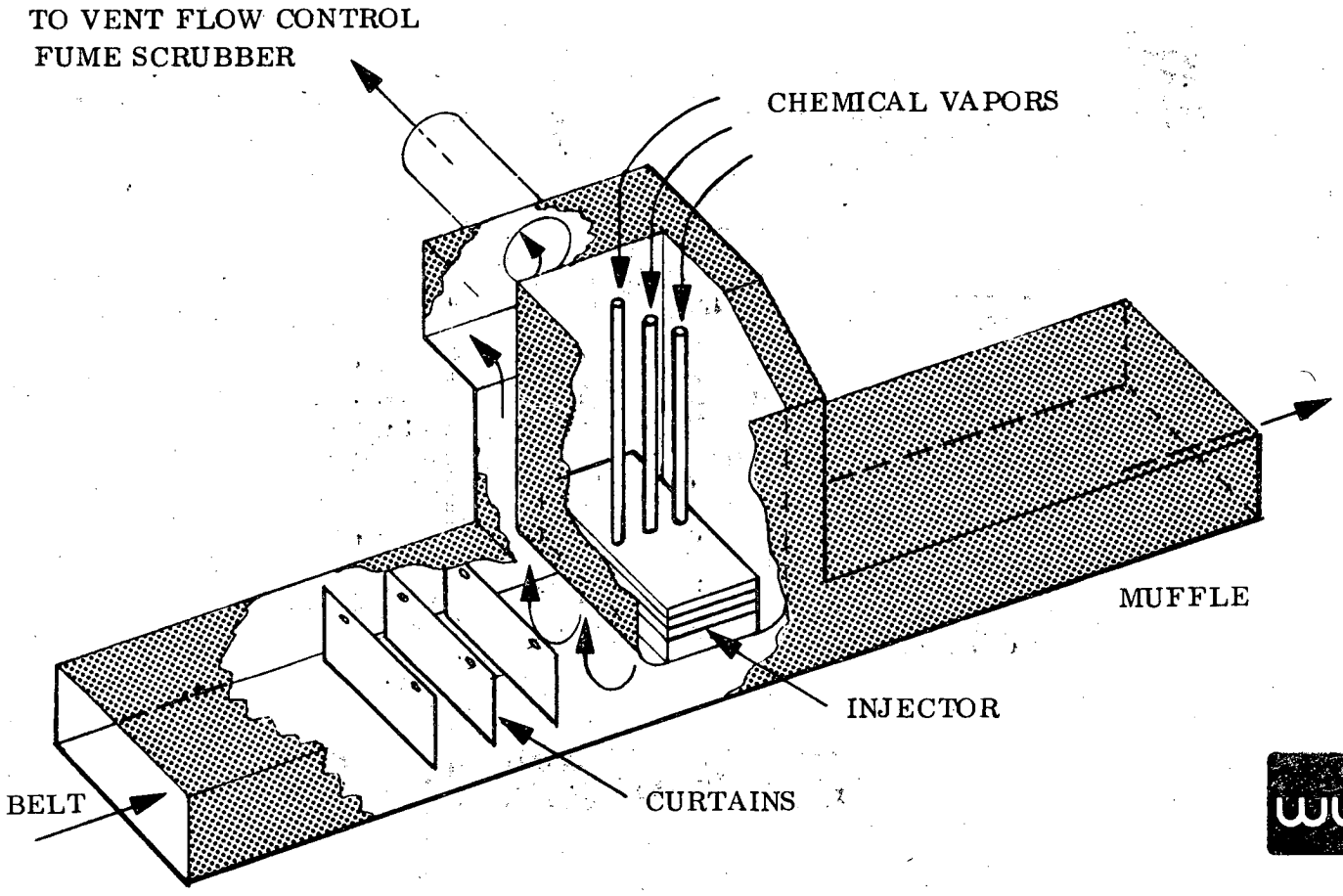

1332

CVD CHAMBER DETAIL

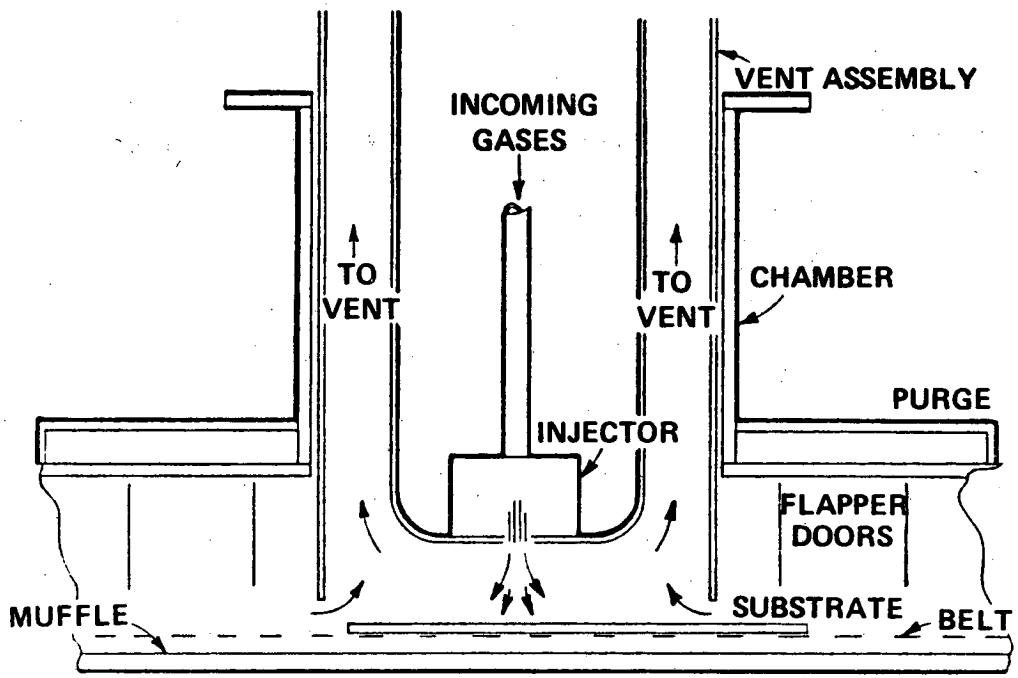

1333

INJECTOR DESIGN PRINCIPLE (TUBE)

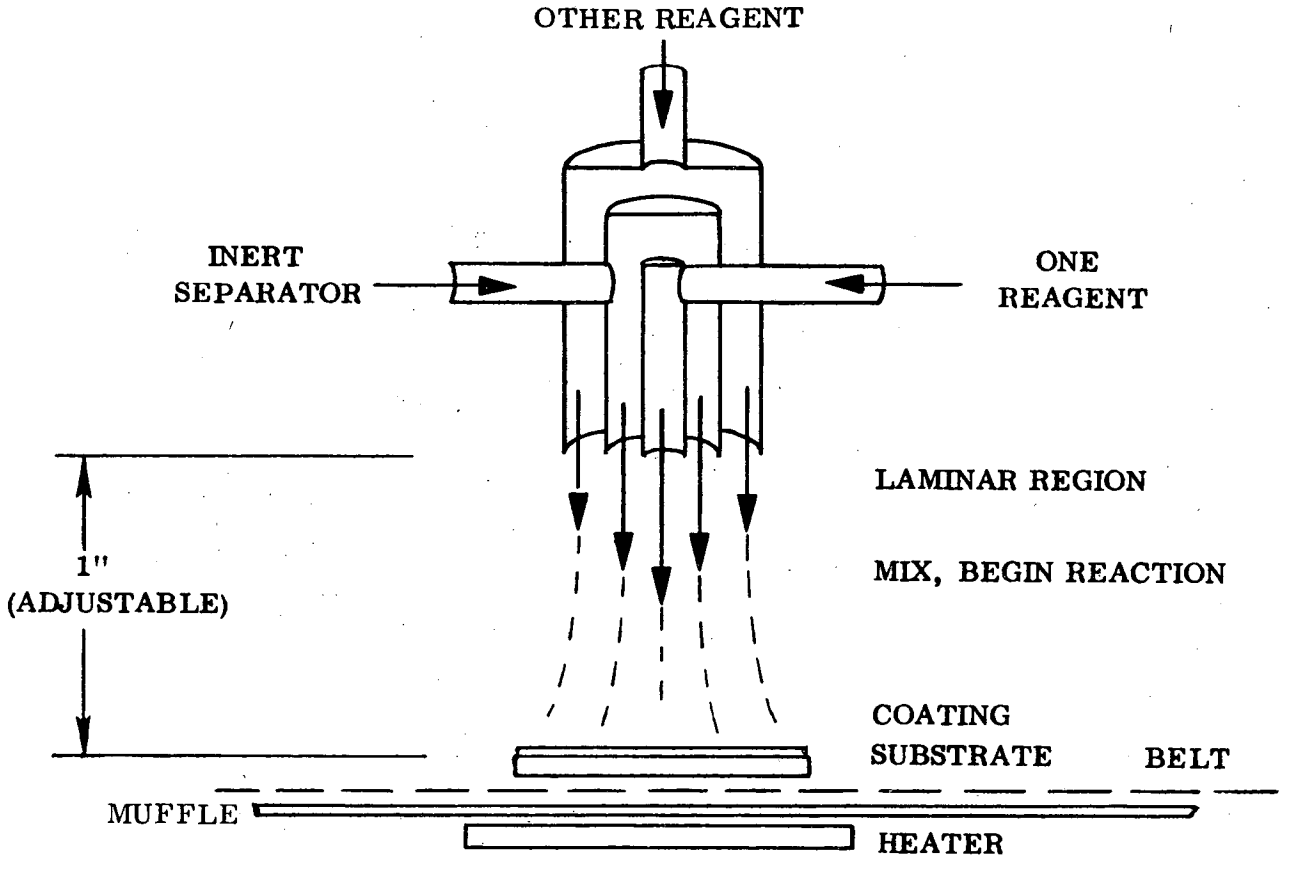

1334

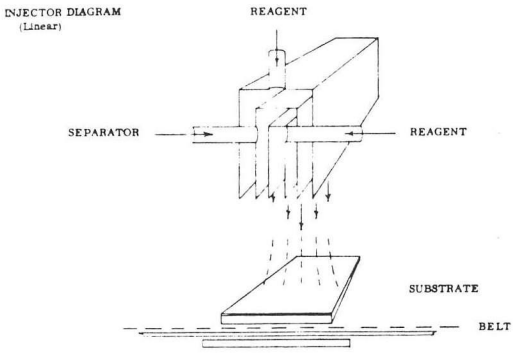

Fig. 9 Injector Design Principle (Slit)

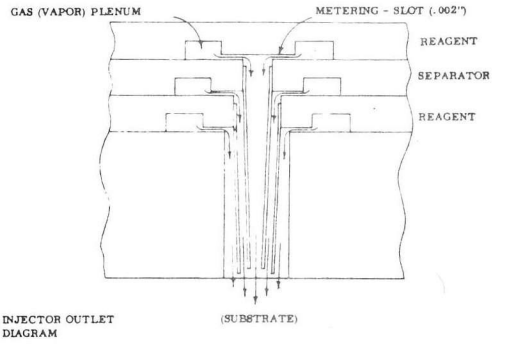

Fig. 10 Injector Metering Structure

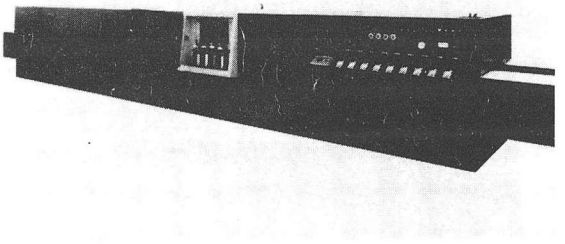

Fig. 11 Production Model Tin Oxide Coating Furnace (10685-1)

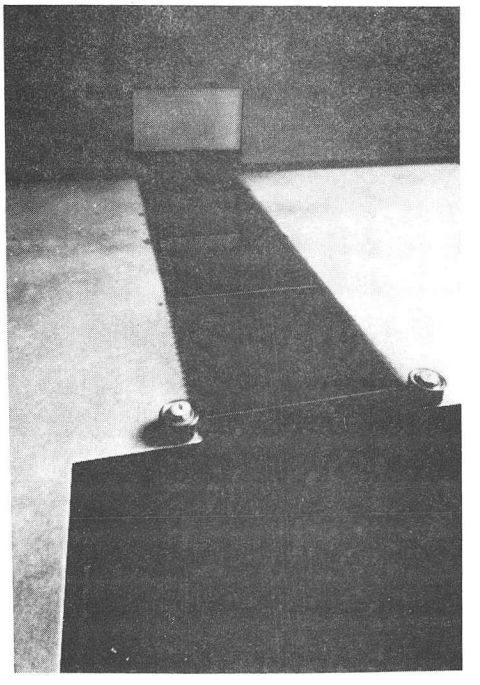

Fig. 12 Tin Oxide Coated Glass Exiting Furnace (10826-1)

INJECTOR DESIGN PRINCIPLE (SLIT)

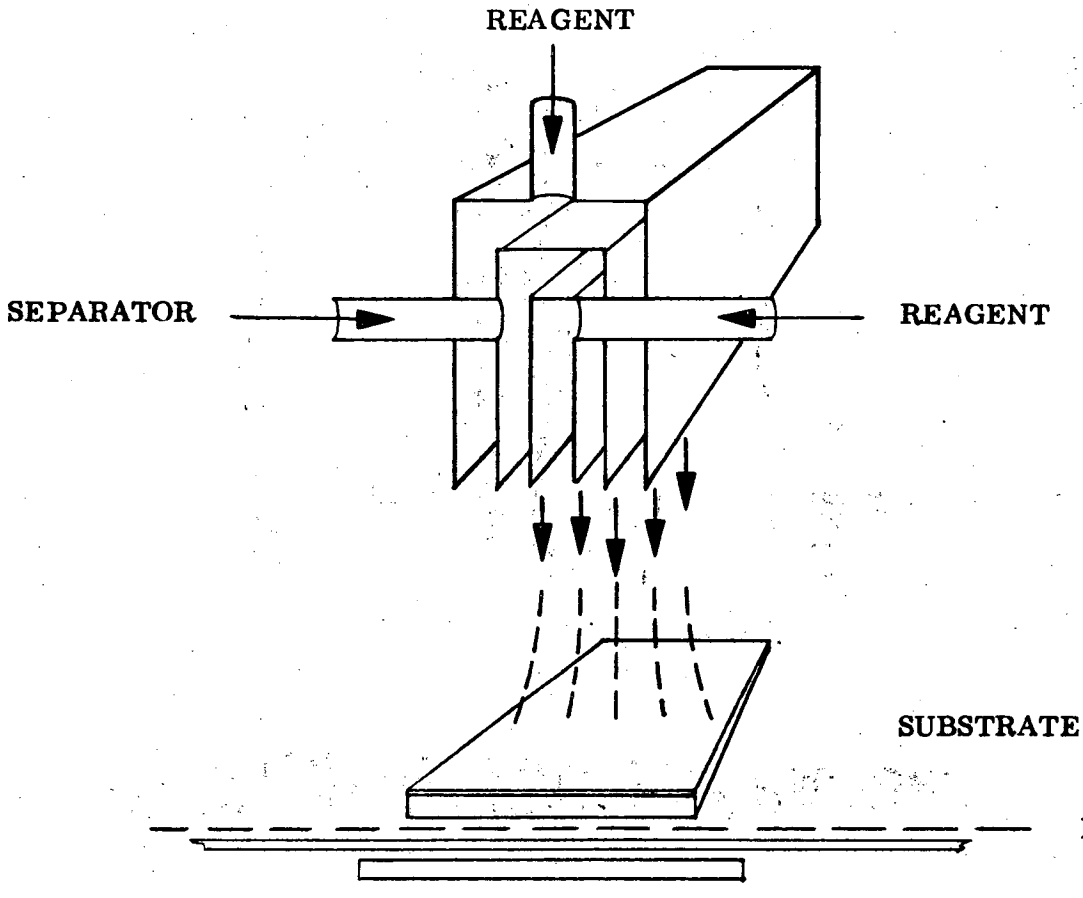

1335

INJECTOR METERING STRUCTURE

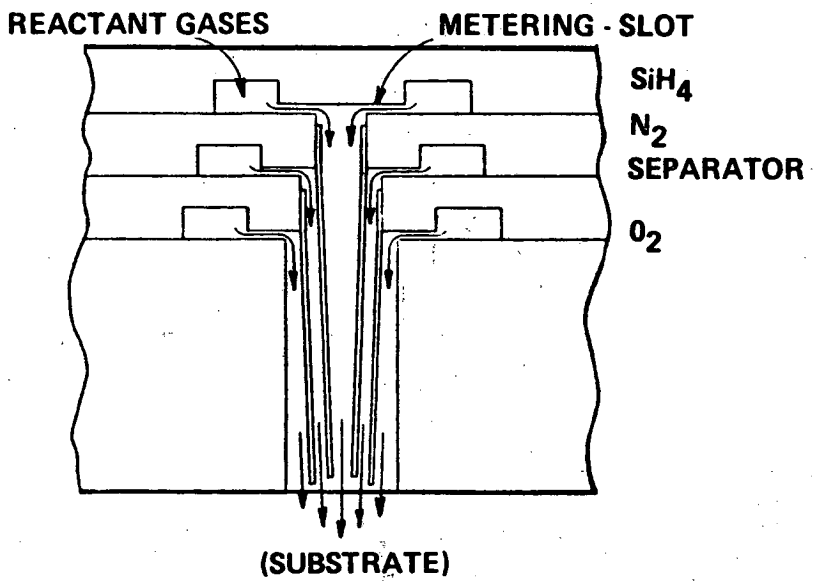

1336

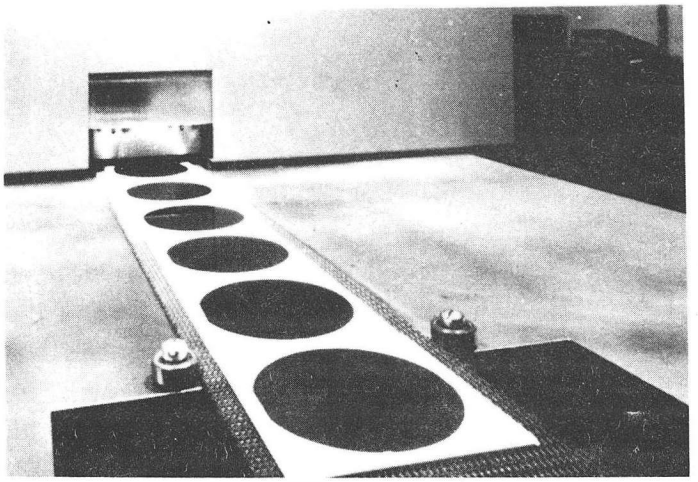

Fig. 13 Coated Semiconductor Wafers Exiting Furnace (10201-1)

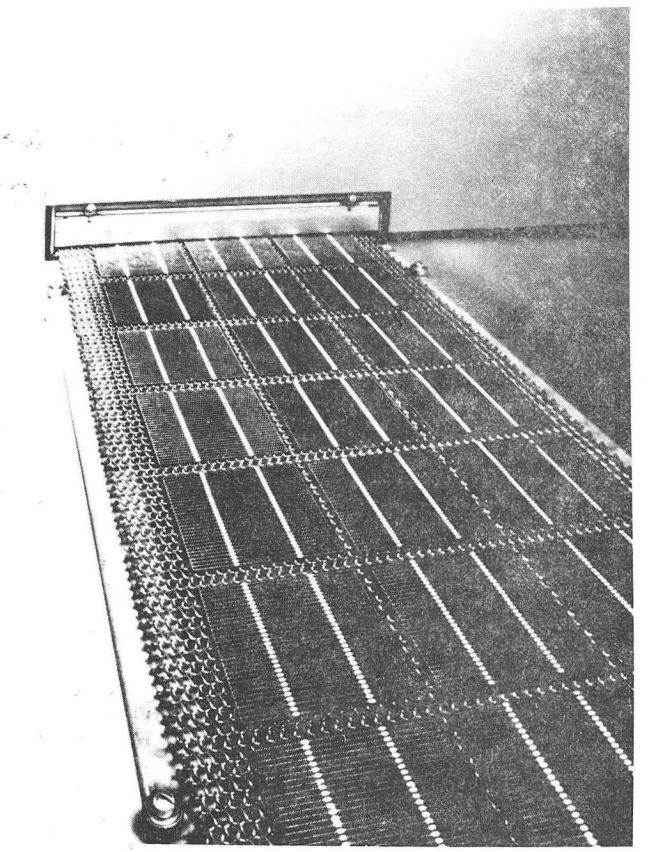

Fig. 14 Titanium Dioxide Coated Solar Cells Exiting Furnace. (10981-2)

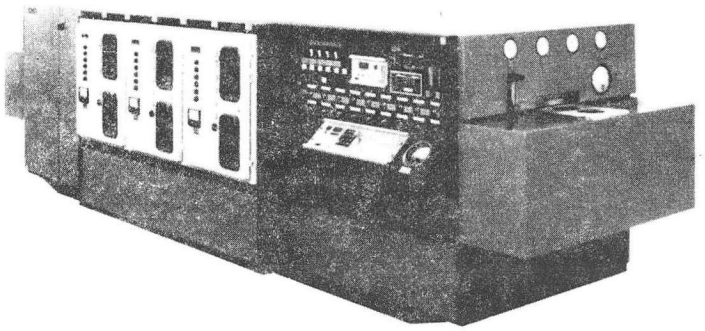

Fig. 15 Three Stage Semiconductor Production Model Conveyorized APCVD (11486-1)

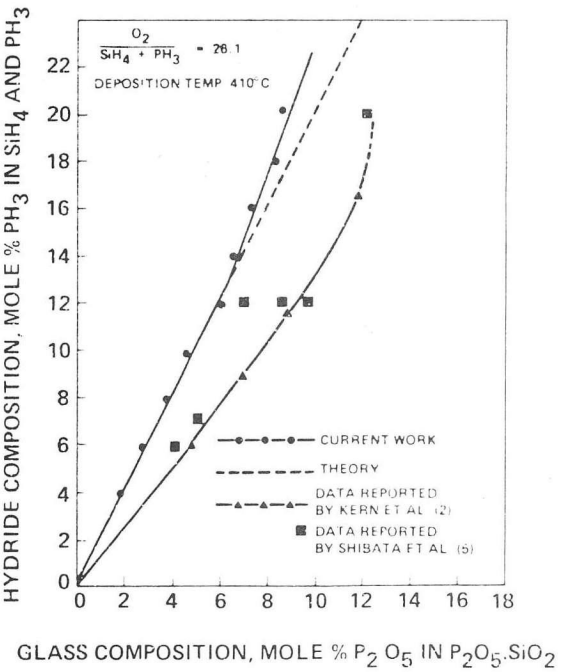

Fig. 16 Graph Vapor Composition vs. Coating Composition (P-doped SiO_2)

VAPOR COMPOSITION
vs.
COATING COMPOSITION (P-DOPED SiO_2)

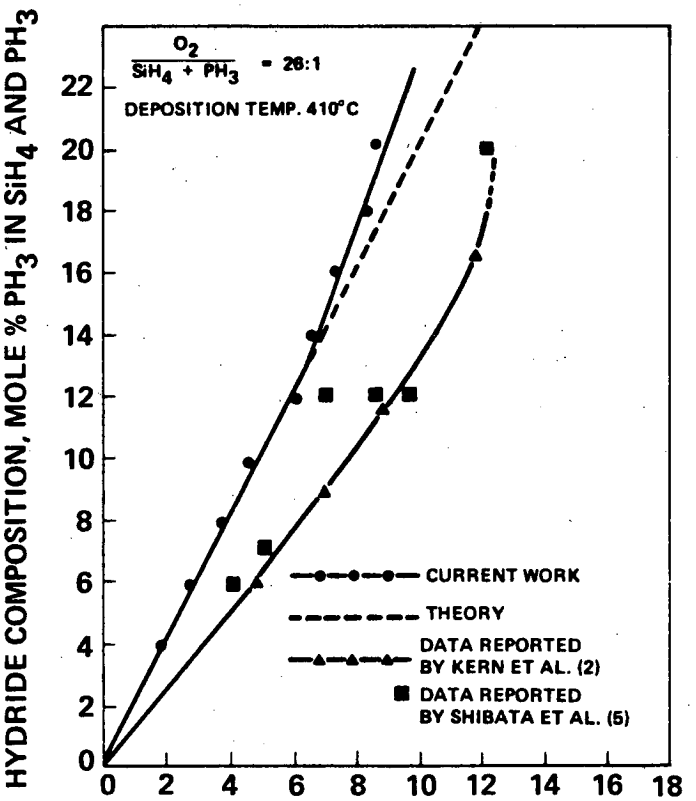

1337

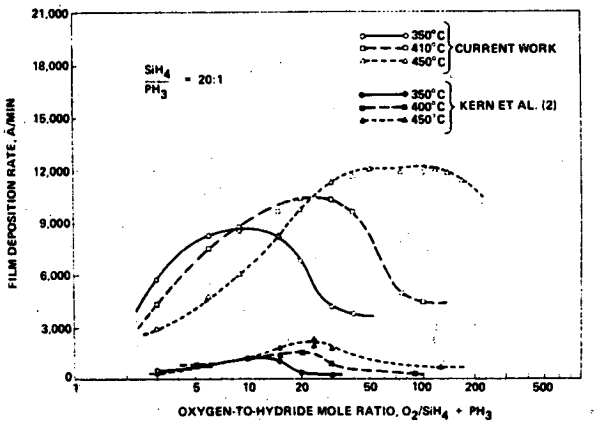

Fig. 17 Graph Oxygen vs. Coating Results (SiO_2)

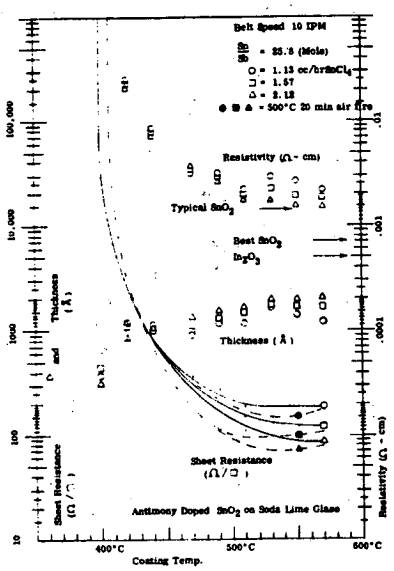

Fig. 18 Graph Temperature vs. Coating Results (Sb-doped SnO_2)

OXYGEN vs. COATING RESULTS (SiO_2)

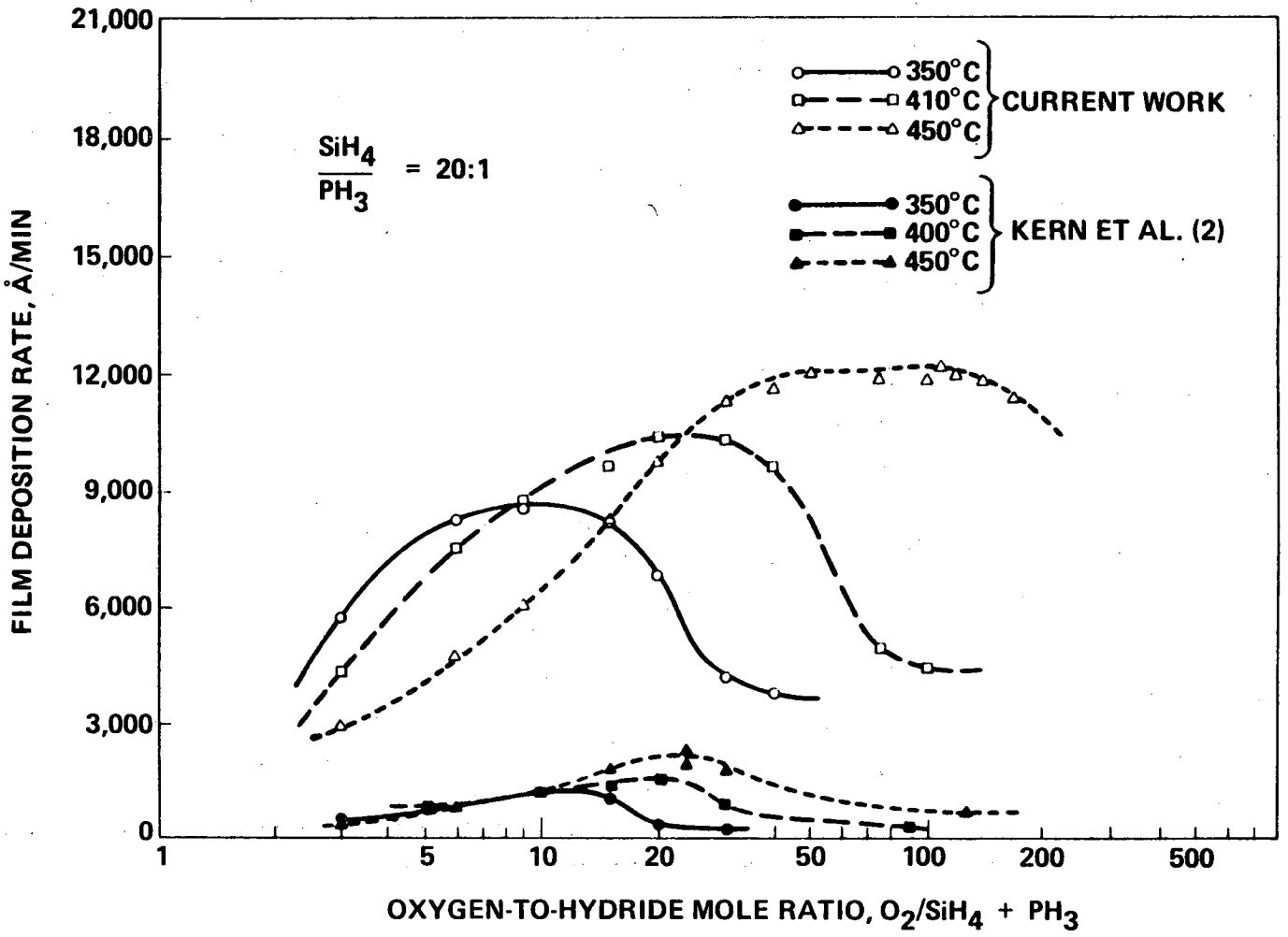

1338

TEMPERATURE vs. COATING RESULTS (Sb-DOPED SnO_2)

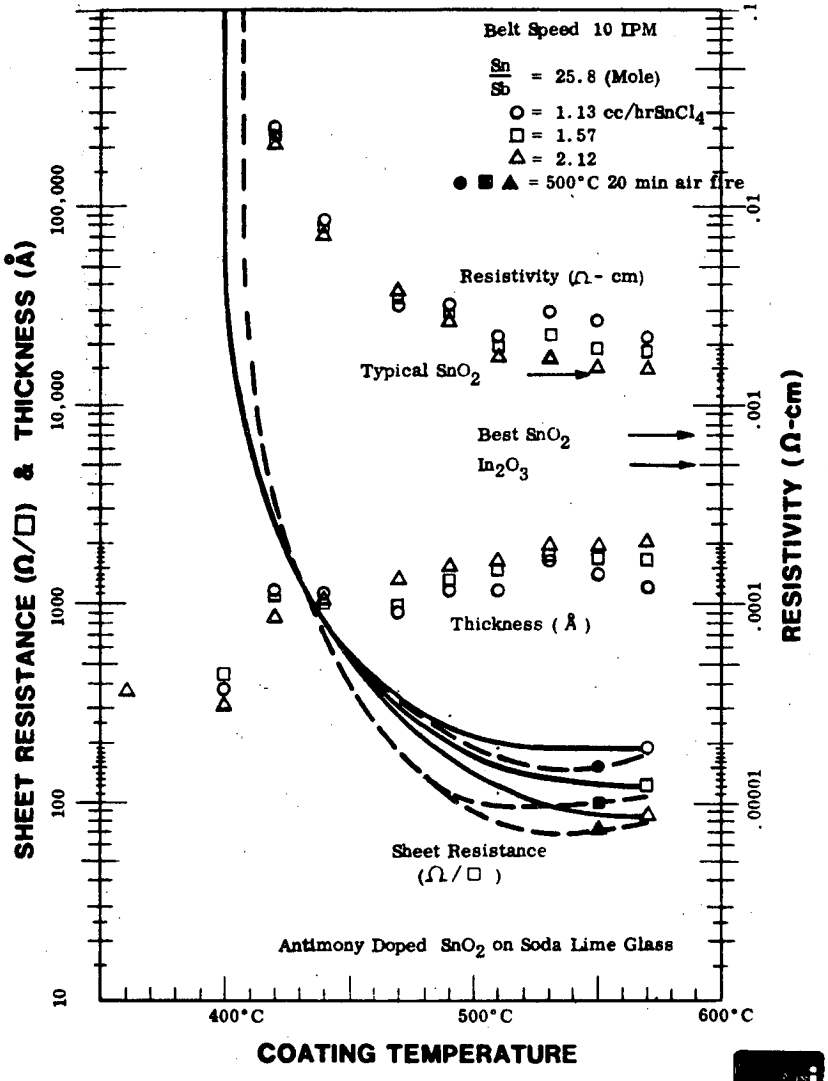

1339

Vacuum roll coating equipment

Ernst K. Hartwig
Leybold-Heraeus GmbH, Roll Coating Division, Wilhelm-Rohn-Strasse 25
D-6450 Hanau 1, Federal Republic of Germany

Abstract

Vacuum roll coating equipment is built for an increasingly large number of different products for various applications. A variety of technical solutions with regard to the main functional construction groups allow the coating equipment to be taylored according to the given requirements of special products. With a system of interchangeable groups it is possible to compose specialised vacuum roll coating equipment.

Introduction

Thin film technology applied to rolled flexible web materials is called High Vacuum Roll Coating. High vacuum roll coating is most important for industrial high volume application.

Among the numerous reasons why the thin film vacuum coating process continues to gain such popularity, two of them are of great importance for web-shaped materials:

- The same or almost identical properties can be obtained by vacuum coating a material - as with material in solid form - with much less material consumption.
- Thin film vacuum coated materials have useful properties which the same materials in solid form do not possess.

These two factors are the main economical and technical reasons why such a large number of vacuum coated products are now entering the market. It therefore must be distinguished between two groups of products:

- Substitutes
- Completely new products

Because of its high volume application, one source of new roll coating products may be thin film products, up to now based on non-flexible carriers. This may be is one important reason why a paper about roll coating equipment should be placed in this Conference.

Product applications

The following products are made of high vacuum coated web-shaped material:

Decorative products	Metallized paper	Metallized Fabrics
Hot stamping films	Labels, especially for	Curtains
Reflective road signs	beer, champagne, wine	Overcoats
Labels	and liquor bottles	Jackets
Packaging (paper, film laminates)		Shoes
Garlands	Cigarette bundling tissue	Gloves
Metallic yarn (Lurex)	Electro-sensitive paper	Insulated drapery
Metallic wall coverings		Tents and sleeping bags

Functional products	Special products
Thin film capacitors	Evaporated window films - monolayer and multilayer
Food packaging	Sputtered window films - monolayer and multilayer
Coffee packaging	Conductive transparent films
Wall insulation	High barrier products (oxygen, water vapour)
Aircraft wall insulation	Reproductive materials
Cryogenic insulation	Magnetic tapes
Flexible duct work insulation	Optical application (not window films)
Light reflectors (copying machines)	
Solar energy reflectors	
Cable wrappings	
Insulated blankets	
Wound dressing	

Basic design of roll coating equiment and process engineering concept

Most complex equipment and process descriptions have a very limited period of validity. Research, development and experience cause changes to the equipment for known products almost as often as new product requirements create the need for change.

Despite this constantly changing state-of-the-art, there exists an unchangeable basic design for all vacuum roll coaters which consists of the following three main construction elements:

- A source which holds the coating material and causes its transfer to a base material.
- A holding and transport system for the base material.
- A vacuum to enable the process.

In roll coating, the flexible base material on which the coating is deposited is a web. The material is exposed to the source for coating under vacuum whilst moving.

There are numerous technical solutions available to be incorporated into a plant, the selection and combination of which is depending on the particular purpose required.

The detailed specifications of a plant are determined by:

- The coating material, its properties and the thickness of the coat to be applied.
- The number of coats to be applied in one cycle.
- One-side or two-side coating.
- The kind of substrate, its thickness, width and length.
- The required output.
- Economical considerations.

Processing sequence

Production of coated film in a high vacuum roll coating plant proceeds in the following stages:

- Fitting the roll of substrate into the transportation, guiding and winding system.
- Evacuating the chamber in which the coating process takes place.
- Activating the coating source or sources.
- Starting the winding system which conveys the substrate past the coating source or sources.
- Evaporation and condensation of the coating material on the substrate as a thin film.
- Breaking the vacuum and cooling.
- Changing the roll of film (in semi-continuous plants) or maintenance of the plant (in the case of continuous air-to-air plants).

The following sections describe the existing possibilities of variation. A roll coating plant of modular design can be adapted optimally for the manufacture of a certain product.

Roller arrangement, film guidance and winding system

The overall design of a plant in respect of its roller arrangement, film guidance and winding system is decisively influenced by the question of whether the plant is to be operated continuously or semi-continuously. Which form of operation is chosen depends not only on technical considerations, but is influenced to a great extent also by economical aspects.

Semi-continuous operation

In a roll coating plant designed for semi-continuous operation, the roll of substrate is situated inside the vacuum chamber. Here the roll is unwound, exposed to a source and re-

wound again under vacuum. The working cycle consists of four steps which are:

- Pumpdown
- Evaporation
- Venting and cooling
- Re-charging

The working cycle chart, Figure 1, illustrates the relationship between these four different states. The higher the percentage of time spent on evaporating, the greater is the plant efficiency or productivity. With regard to the substitute this means: The efficiency is increasing with the increasing roll diameter (limited) and decreasing with the thickness of the web.

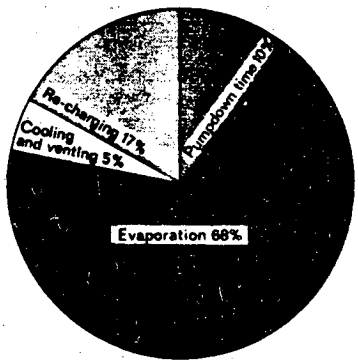

Figure 1. Example for a working cycle.

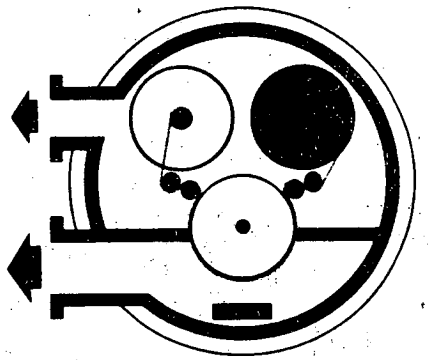

Figure 2. Schematical diagram of a semi-continuous plant.

Semi-continuous roll coating is the process preferred at the moment, as it has a great number of important advantages in comparison with other processes:

- High flexibility of the system for processing various base materials and products.
- Very favourable winding conditions, no air-telescoping on high speed, low tension rewinding.
- Ideal dust-free and scratch-free winding conditions for freshly-applied, sensitive coats.
- Technical and economical superiority with thin films or less than 90 µm.

Continuous operation with air-to-air plants

In those roll coating plants that operate continuously, the roll of substrate and the one on which the coated film is wound are situated outside the vacuum chamber. The substrate must therefore enter and leave the vacuum chamber through locks. The air-to-air plants, Figure 3, closely reach the ideal of 100 % utilization of the operating time for coating purposes. They are designed in such a way that the working cycle is interrupted only when maintenance is required. There are, however, still being difficulties experienced at the moment in realizing this concept.

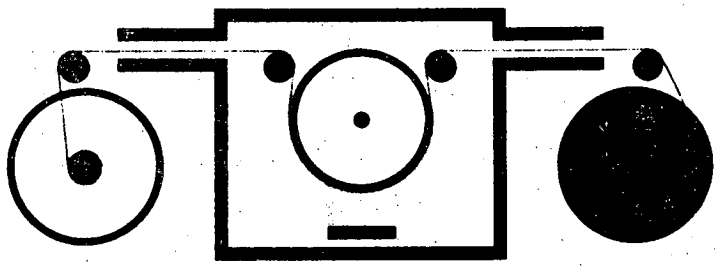

Figure 3. Schematical diagram of an air-to-air plant.

The latest plants running at high speeds require sophisticated lock systems and a flying splice winding system which allows roll changing without stop. The design of such plants is, of course, considerably more complicated. The gain this system is offering is much lower than its price increase justifies in comparison to semi-continuous plants.

The key to the technical success of air-to-air plants can be found in the lock system which must be capable of transporting the film material into the vacuum chamber for coating and out again afterwards without damage. A further source of numerous problems is the maintenance of the thermal evaporation sources during long term continuous operation. Extensive efforts are being made for solving these problems.

Coating materials and substrates

Practically all metals, many of their oxides and alloys and also a considerable number of other elements and compounds are suitable for deposition as thin layers on substrates in a vacuum coating process.

The criteria for the selection of a coating material are its price, its availability and the nature of the coating process itself, i.e. whether it will be complicated or not.

The majority of all the roll coating plants built up to now operate with aluminium as coating material. Vacuum-deposited aluminium has good electrical properties, good reflection properties, as well as decorative appearance. It adheres to the substrate well, has a relatively low melting point and a good corrosion behaviour.

Aluminium is available in wire form and is therefore well-suited for continuous feeding. Its price is relatively low, and the world's reserves of aluminium are larger than those of other metals. The coating costs are lower than for any other metal, with the exception of zinc.

Aluminium can be expected to remain the most widely used coating material for many years. The shares of other materials already used for roll coating will, however, increase in future, as the field of application is growing steadily. Metals in question are nickel, cobalt, chromium, steel, tin, indium, zinc, titanium, as well as their alloys and oxides.

As a substrate, the industry offers a number of plastic films for high vacuum roll coating, in particular polyester, polypropylene, polyethylene, nylon and polycarbonate films. Selected papers and the classical material cellophane usually require precoating and make greater demands on the pump set of a roll coating plant.

Coating processes

Depending on the way solid material is transformed into vapours, one differentiates between:

- Thermal evaporation and
- Cathode sputtering

Regardless of the type of coating process being used, advantage is taken of the possibility of mixing vapours or dust of various materials or reacting the coating material of a source with gases fed to it separately, e.g. oxygen to obtain oxides. This kind of roll coating is called

- Reactive coating process

and is also dealt with in this paper.

Thermal evaporation

The energy required for the evaporation of solid materials or powders may be supplied in a number of ways:

- By heat radiation (oven). Heat sources, such as electric heating elements, heat vessels containing the coating material. The fitting of reflecting and insulating shields transform this system into an oven.

- By resistance heating. Electric conductive boats are heated directly by current passage.

- By inductive heating. The coating material inside a crucible is melted and evaporated by an induction coil surrounding it.

- By electron beam gun. The surface of the coating material is melted and evaporated by bombardment with electrons.

The solid and powder materials are either evaporated from the melt or sublimated directly from the solid form. The evaporation of alloys from a melt is limited, because their components will evaporate in different quantities at various temperatures. Certain compounds will also dissociate during evaporation and may therefore be used under certain conditions, only. The various sources used for thermal evaporation are shown in Figure 4.

Radiation-heated evaporation source

In this form of thermal evaporation, metals with low melting points are first melted and then evaporated. The energy is supplied by heat radiation.

The coating material is situated in boats made of a material with a considerably higher melting point then the one of the coating material itself. The evaporation source contains one or more boats. The material is fed into it in batches. After one or several working cycles being concluded, the boats are filled up or exchanged for new boats containing pre-melted material.

A radiation heated evaporation source is thermally retarted and requires an extensive heating-up period before gaining thermal stability which then, however, remains very stable. Such a source is not suitable wherever fast control is needed.

This oven is the classical evaporation source for zink and other materials with a low melting point. Its employment is limited by the thermal stability of the boats and shields in comparison to substrates with higher melting points. With regard to other evaporation sources, the efficiency rate of a well-designed oven is very high.

Resistance-heated evaporation source

The elements of this system are boats built of intermetallic bars which are provided with cavities. They are heated as a resistor by current. The coating material is fed continuously as a wire.

The entire evaporation system consists of a number of equidistantly arranged boats. The power is supplied individually for each boat by individually controlled power supplies.

All power supplies are activated and controlled by an integrated master system.

The wire feed system supplies the same amount of wire to all boats. This is the most important basis for a constant and uniform evaporation rate of the entire system.

For aluminium, this evaporation system presently offers the most advanced technology adaptable for high thickness and high uniformity coating, as well as for solar control film requirements.

The same boat may be used for different metalls, too, mainly with reduced efficiency. The range of application of these boats is limited by the thermal stability of the semi-conductive material and the surface-wetting properties of the metal.

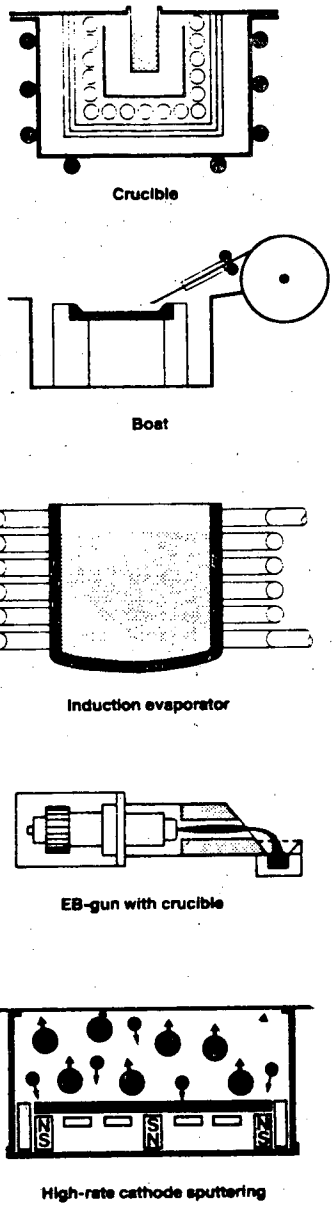

Figure 4. Schematical diagram of different evaporation sources.

Induction-heated evaporation source

In this process, a crucible is induction-heated, melting the coating material and evaporating it. The evaporation system consists of a number of induction-heated crucibles, the size of which and their distance from each other permit variation to a certain extent.

The material is usually fed batchwise in the shape of granules or small pieces. In semi-continuous operation, the size of the roll of substrate is limited. For air-to-air plants not continuously fed evaporation sources are unsuitable.

The induction-heated evaporator can be employed for a wide range of melting points and is therefore suitable for many coating materials. For many years it was therefore the most popular evaporation source, particularly in the USA. The induction-heated evaporator is thermally slower than evaporation boats, because its crucible contains a considerably larger quantity of metal.

For the evaporation of aluminium, the induction-heated evaporator is inadequate in comparison with the modern, sophisticated one using boats, with regard to the uniformity in film thickness, its maintenance and the cleanliness obtainable for the system.

Electron beam gun

Melting and evaporating materials with an electron beam is the most versatile and technically sophisticated method of all evaporation processes. Only cathode sputtering can offer similar or even more versatile application concerning the evaporation of various materials.

The energy is directly supplied to the surface of the coating material by electron beam. The great advantage of this type of evaporation is the direct and speedy supply of energy to the particular evaporation position.

The material is evaporated from ceramic or metal crucibles, the latter, for example made of copper, being usually water-cooled.

In a high vacuum roll coating plant, there are one or more electron beam guns needed for the evaporation system, depending on the width of the substrate. The web width suitable for coating by means of electron beam guns ranges between 200 and 300 mm. By using an oscillating electron beam in a technique called Jumping Beam Process evaporation of two different materials from two separate crucibles is possible in any ratio. This technique is used, for example, for coating alloys.

The coating material may either be supplied in batches by topping up the crucibles or continuously by wire feed or by vertical insertion of a metal rod, the surface of which is evaporated directly.

The electron beam gun can be used for the evaporation of a wide range of metals with a relatively high melting point and for a number of non-metallic materials, like SiO or SiO_2.

The equipment essential and its investment costs are equal to the ones of an induction-heated evaporator or may be slightly higher.

Cathode Sputtering

Nowadays, cathode sputtering is increasingly used in high vacuum roll coating, apart from the thermal evaporation processes.

Evaporation is the change of the state of a material - for instance a metal - by supplying it with heat until it transforms from solid state into liquid state and then into vapours which are then transferred and deposited.

Sputtering is the displacement of particles from a solid surface by ion bombardment and the precipitation and deposition of such particles onto a second surface. Depending on whether the ion bombardment is induced by a direct voltage - as in the case of many metals - or by a RF-voltage - as in the case of many semi-conductors and insulators - one speaks of DC or RF sputtering.

Many years ago it was found that in a suitably dimensioned and aligned magnetic field the number of particles transferred may be increased and the accompanying loss in heat reduced. This magnetic field may be applied both to the DC energized cathodes and the RF energized cathodes. This technique is called High Rate Sputtering or Magnetron Sputtering.

Sputter technology has been employed to a fairly great extent for a number of years in stationary (batch) plants to coat optical and electronical products.

Fundamentally speaking, the sputter technique is just as suitable for the coating of a moving web. Sputter electrodes ensure the greatest uniformity of film thickness among all coating techniques. Sputtered films have a finer, more compact structure, i.e. a smoother surface, and therefore better barrier properties.

The material efficiency and the operational reliability of the material source is higher for sputtering than with all other coating techniques. It is possible to sputter with various materials simultaneously, thus producing multi-layer coats.

The specific rates of the sputtering electrodes are much lower than those of all evaporation sources, such as resistance heated boats or electron beam guns. Among all sputtering electrodes the specific rate of the magnetron cathode is the largest.

Reactive coating process

For coating metallic oxides, the metallic substance is transformed in its gas phase into an oxide, a nitride or another compound by subjecting it to a reactive atmosphere.

The advantage of applying this technique to the sputtering process is that the technically less difficult DC sputtering can be employed when a metallic target is used. In this way, for example, coats of bismuth oxide, tin oxide, tin-indium oxide or titanium oxide are obtained. Reactive processes are also used for thermal evaporation. By evaporating, for example, silicon in an oxygen atmosphere, silicon dioxide us obtained.

In non-reactive processes, the coating rates are largely determined by the power of the evaporator or the cathode. In reactive processes additional problems may occur within the gas supply and the reaction between the reactive gas and the target. The result of this is a lower evaporation rate and a more difficult process control in comparison with the non-reactive sputtering.

Winding systems

There are some significant differences between winding systems of continuous and semi-continuous plants. Since the winding system of a semi-continuous plant is within the vacuum under operation and is exposed to the vapours of the coating material, special demands are made on the design:

- The winding system must be as compact as possible to keep the size of the vacuum chamber small.
- The winding system must not release any gases, vapours or fluids which may have any adverse effects on the vacuum. This requirement represents particular problems, for example, how to lubricate the bearings.
- The winding system possesses an air side and a vacuum side. The drives, gears and in some cases also the belt or chain transmission systems are situated outside the vacuum chamber connected with vacuum-tight leadthroughs.

For air-to-air and for semi-continuous roll coating, the following is of importance:

During the coating process, the substrate is exposed to heat. In order to prevent thermal damage from being caused, the substrate is passed over a chill roll, thus keeping it smooth and compensating the heat generated and transferred during the coating process. In most cases the web layes on a so-called coating drum whilst being exposed to the coating source. This drum is chilled.

The degree of cooling required for the chill roll depends on the kind and thickness of the substrate and the type of coating to be applied. In many cases, water is a sufficient cooling agent.

For the processing of very thin films, refrigeration equipment needs to be used for constantly cooling the chill roll down to -30°C or even lower. When such refrigeration equipment is being used, then the chill roll must be brought to room temperature before flooding the vacuum chamber to prevent condensation of water vapours.

When working with extremely thin films, special devices are engaged to ensure good contact with the coating roll. For example, an additional drive is being used between the coating roll and the take-up roll to ensure good thermal contact between the substrate and the coating roll without influencing the rewinding tension.

The thinnest films available on the market at the moment are coated and rewound in LEYBOLD-HERAEUS capacitor film roll coating plants. Such films are currently 1.5 µm polyester, 1.7 µm polycarbonate and 4 µm polypropylene.

Drive system and tension control

In semi-continuous plants, the drive systems are used in a similar way than those fitted in non-vacuum winding units. It depends on the given speed range and the range of tension to be supplied to the web which particular drive system is to be selected. For thin plastic films of 12 microns or less, a three motor calculator controlled system is preferred which is controlled as follows:

Each drive is regulated by a thyristor control element. Special electric DC motors with a low inertia moment are being used, as they have excellent dynamic properties. By keeping the braking force of the unwind motor proportional to the diameter of the feedstock roll, the web is unrolled from the feed roll with a constant tension. Each particular diameter is individually calculated from the rotation rates of the unwind roll and coating drum. The diameter of the coating drum remains unchanged. Should and additional drive be needed to the ones mentioned above in order to obtain better contact and for tension separation, it can be integrated into the described system.

Single and multi-chamber systems

A further possibility of varying plant design is to subdivide the vacuum chamber into two or more separate compartments. Different vacuum conditions can prevail in each of those. They are frequently evacuated by separate pump sets. There are a number or reasons for such a subdivision of the vacuum chamber, including:

- Two or more coating stations without any cross-contamination being allowed.
- Generating and holding the more expensive high vacuum in the coating area, only.
- Pumpdown on higher pressure with higher efficiency wherever possible, for instance in the winding area.

During the many years of development of web coating plants, models with one, two, three and four chambers have been built for one layer-one station coating. Advances in process development have, however, created a situation in which more than two chambers no longer appear to be necessary for general purpose use. The two chamber system, Figure 5, is now the preferred plant design for the production of high-quality coatings on plastic films. The two-chamber system is essential in the economical and also technically satisfactory aluminium coating of paper.

Two-side coating and multi-layer coating

Coating on both sides of the substrate is necessary for certain applications. Examples of these are plastic films and papers for various types of capacitors or polyester for high-quality metallic yarn.

In the case of thermal evaporation, such a web coating plant has two evaporation sources and two chill drums. The winding system of such a plant allows two modes of operation:

- One coating on either side of the web
- Two coatings on one side of the web

Two side coating is also possible when the web is passed twice through a plant with one evaporation source. However, one needs to operate two plants with one evaporation source each, if the same material throughput is to be obtained as with a plant having two evaporation sources.

The costs for a plant with two evaporation sources are, however, not twice as high, but only about 1.7 times higher than those of a plant with one evaporation source and comparable technical characteristics.

Further cost reductions result from lower installation, operation and maintenance costs. All in all, economic advantages could, however, only be achieved, if more than 60 percent of the output were coated on both sides.

The possibility of applying two coatings to one side of the substrate can be utilized to produce particularly thick coats in an economical way.

If two different coating sources are fitted and the web transport system is made reversible, one will already have a general purpose plant for the production of multi-layer coats.

To be able to deposit different materials which call for different vacuum conditions, the coating chambers must be separated from each other. In addition to this, it is also essential that a suitably arranged pumpset is installed to evacuate both chambers.

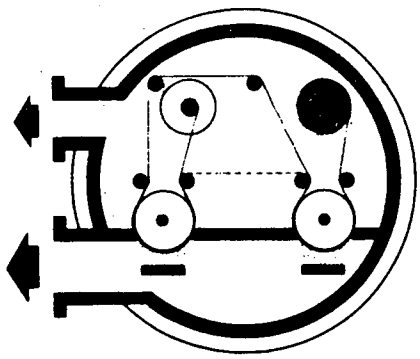

Figure 5. Schematical diagram of a plant for two-side coating.

Different arrangements - sputter roll coater

The first known commercial web sputtering plant was built already over eight years ago for 20 inch-wide material. Since then more than ten additional web sputtering plants were built. The largest plant constructed to date is coating material over 80 inches wide and it is fitted with several high-rate cathodes.

As a result of the differences between thermal evaporation sources and sputter sources, the design of a sputter roll coater varies significantly from a conventional roll coater working with thermal evaporation sources.

The unique design of the web sputtering plants is due to two distinct characteristics of the sputtering electrodes:

1. They do not operate with liquid metals. Their surface, therefore, does not need to be arranged horizontally.

2. Sputtering electrodes have a relatively low specific sputtering rate. To improve throughput rates, the material target area must be as large as possible.

In a typical sputtering plant the web is allowed to pass over a chill roll of large diameter, where it is exposed to as many sputtering cathodes as may possibly be arranged around the drum, as shown in Figure 6. The length of the cathodes in the web direction is largly determined by the magnetic field configeration of the cathode.

This design has to be changed, if different materials are coated in one run, and especially, if reactive and non-reactive coating will be done in one run. Chamber subdivision may also be essential again.

In addition, by altering the design of a sputtering plant extensively, most effective processes may be created.

Sputter roll coating is a very young technology. It is just in the beginning of a period of development and diversification.

The start of this technique has so far proven to be very successful and most promising for the future. This at least is true more generally for the entire field of High Vacuum Roll Coating.

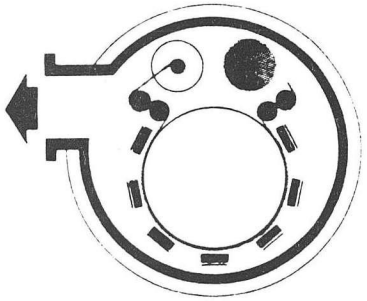

Figure 6. Schematical diagram of a cathode sputtering plant.

There are a lot of new products which have not been created until now. There are many products which could be better or cheaper by substituting a material with a thin film.

And last but not least, there are thin film products manufactured in batch coaters today which will be modified to a product one of these days which may be made in large quantities and with high efficiency in a HIGH VACUUM ROLL COATER.

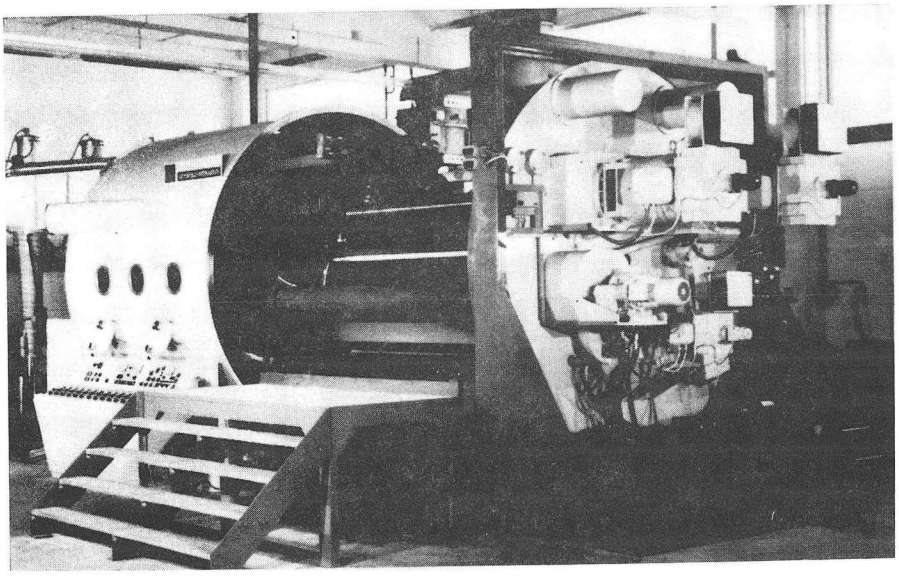

Continuous coating of indium tin oxide onto large area flexible substrates

W. C. Kittler, Jr., I. T. Ritchie
Sierracin/Intrex Products, 20500 Plummer Street, Chatsworth, California 91311

Abstract

A process is described for the continuous coating of rolls of flexible material up to 36" wide with a transparent electrically conductive layer of indium tin oxide. These coatings are produced by either direct sputtering or by reactive magnetron sputtering from a metal alloy target. The latter process is preferred from a cost standpoint. Coatings are available with visible light transmittances and electrical resistances ranging from greater than 0.8 and less than 100Ω/□ to 0.9 and greater than 1MΩ/□ respectively. A variety of substrates, such as polyester, Teflon, Kapton, polycarbonate can be coated. Uses of these coatings range from use in transparent touch panels to static drains and heat mirrors. Several of these applications are discussed briefly.

Introduction

Thin films which are transparent to visible radiation and are electrically conducting find widespread application in such diverse technological areas as energy conservation, information storage and as display electrodes.

Historically, noble metals (usually gold or silver) which are sufficiently thin to be partially transparent have been employed for this purpose. However, there are several disadvantages associated with their use, including high cost and limited light transmittance. Suitably doped wide band gap semiconductors have more recently become available and have begun to replace metal coatings in many applications. Reviews of transparent conducting coatings have recently been given by Vossen[1] and Haacke[2]. In general, these wide band gap semiconductors are less costly, environmentally stable (since most are oxides) and have a greater light transmittance than metal coatings. Until recently, these coatings have been deposited onto glass or semiconductor substrates which are capable of withstanding the high deposition, or post deposition annealing temperatures which have been necessary to obtain suitably low electrical resistances.

In this paper, we describe a deposition process for the continuous coating of flexible polymer substrates at room temperature, with indium tin oxide using reactive magnetron sputtering. Substrates such as polyester, polycarbonate, Teflon and Kapton up to 36" wide and 4000' long can be coated. This capability greatly reduces the cost and increases the number of potential applications of these coatings.

Sierracin/Intrex ® has been producing transparent, electrically conducting gold coatings on polymer substrates for over ten years, and sees the development of similar indium tin oxide (ITO) coatings as an important advance in this technology[3].

Equipment

Continuous coating

The continuous coating of a flexible substrate has many advantages over batch coating; the principal advantage is the possibility of incorporating closed loop control into the deposition system. Sensors to determine coating properties can be placed downstream of the deposition station and measurements of these properties are used to maintain the desired deposition conditions. It is difficult to incorporate such feedback control into batch coating systems.

A 250 cu. ft. vacuum chamber which is also used to e-beam deposit semitransparent gold films on polymer substrates, has been modified as shown schematically in Figure 1 for the production of ITO coatings. Initial experiments were run with a laboratory scale coater which could coat film 6" wide. The results showed that it was indeed possible to produce satisfactory ITO films without having to heat the substrate or post deposition anneal. Neither operation is in general feasible with polymer films.

Process parameters

There are many process parameters which can influence the quality of ITO coatings on film. The most important of these are listed below:

- Substrate quality; polymer film can be coated without outgassing or other pretreament. However, most polymers require a pretreatment step to remove absorbed gas or need to be coated with a solvent based or vacuum deposited coating.
- Total sputtering pressure.
- Power delivered to sputtering target.
- Reactive gas pressure and flow rate.
- Film and chamber outgassing during processing.
- Film transport speed.
- Target state.
- Degree of vacuum.

These latter two parameters will affect the amount of leader film lost in startup unti a coating is produced with the desired properties.

The properties of the coating which are to be controlled are its thickness, light transmittances and electrical resistance. If it is to be used for thermal radiation contro the infrared emittance also needs to be monitored. For low resistance films (less than $\sim 200\Omega/\square$), there is an approximate inverse linear relationship between electrical resistance and infrared emittance[4]. The deposition rate of the coating is determined by both sputtering power and film speed. Electrical resistance and light transmittance are defined by coating thickness and film stoichiometry.

Coating equipment

Reactive magnetron sputtering was chosen as the deposition technique as it provides a linear source which offers high deposition rates, good rate stability and great control over coating properties. A 42" long magnetron source is disposed in the vacuum chamber as shown in Figure 1, with a gas inlet manifold running along its length. Total system pressure is measured with a capacitive manometer and gasses are bled into the chamber via servo driven needle valves and flow meters. Coating resistance and transmittance monitors are placed downstream of the sputtering target. A microcomputer is linked to all these components as shown in Figure 2.

This provides for data acquisition as well as deposition control. The simplest form of control is to hold film speed, deposition power and total pressure constant, while varying the oxygen partial pressure to produce films with the desired electrical resistances. If a good initial value is chosen the light transmittance will have a reasonably high and predictable value. More complicated control programs have been developed, however which control oxygen flow as a function of trends (averaged over $\sim$10s) in resistance and transmittance.

Results

ITO coatings are routinely produced onto 36" wide film up to 4000' long at film speeds of 2 to 20 fpm.

Figure 3 shows typical visible light transmittance as a function of sheet resistance for coated film. These coatings have nominally the same stoichiometry and the resistance is varied by changing the film thickness. The electrical transport parameters of a typical $300\Omega/\square$ film, which may be used as a transparent electrode, are given in Table 1. The mobility is unusually high for ITO films, but the carrier concentration is unusally low. The coatings are normally deposited at 3.0μm total pressure, under slight compressive stress, as this tends to give better adhesion and strength[5]. However, for thinner ($<50\mu$m) or less stiff substrates, such as Teflon®, the coatings should be deposited without stress to avoid substrate distortion.

Applications

The most sophisticated applications of transparent conductors such as ITO are those which require a high optical transmission and a very low resistance. For example, transparent electrodes for photovoltaic devices, need a high transmission ($\sim$0.80) to maximize short circuit current and a low electrical resistance ($<20\Omega/\square$) is required to minimize the series resistance of the cell. Heat mirror coatings also require a sufficiently low electrical resistance ($\sim 20\Omega/\square$) to have a high infrared reflectance[4,6]. The visible transmittance and infrared reflectance of such a coating on polyester film is shown in Figure 4. Roll coating must be used for these solar energy applications to be cost effective.

Other electrode applications where the sheet resistance requirements are not as critical include the use of such coatings in liquid crystal and electroluminescent display devices. Here a resistance of $200\text{-}500\Omega/\square$ is usually sufficient.

One of the more interesting applications of ITO coatings on polymer substrates is

their use in transparent membrane switches, such as the Transflex® panels. Two sheets of ITO coated plastic are patterned with parallel lines of ITO and positioned orthogonally with respect to each other, separated by a small gap, as shown in Figure 5. Application of pressure to one surface causes an electrical contact to be made and thus, the assembly is able to act as a transparent keyboard, which may be positioned over a video, or other display device. Analog versions of this panel may also be fabricated.

Other applications of ITO coated plastic include use as a ground plane in an updatable microfiche system and as a static drain on satellite thermal control blankets.

Conclusion

A procedure has been described to deposit low resistivity indium tin oxide coatings onto flexible polymer substrates using closed loop control of the process. The important electrical and optical properties of these coatings have been measured and several applications discussed.

Acknowledgements

The authors would like to acknowledge useful discussions and support from J. Fenn and the assistance of the Sierracin Research Department in design and construction of the coater.

References

1. Vossen, J. L., Phys. Thin Films, Vol. 9, pp. 1. 1977.
2. Haacke, G., Annual Review of Material Sciences, Vol. 7, pp. 73. 1977.
3 Roll coating of ITO is also being investigated by Teijin Ltd., Japan and M.I. Ridge et al, Thin Solid Films, Vol. 80, pp. 31. 1981.
4. Frank, G. et al, Thin Solid Films, Vol. 77, pp. 107. 1981.
5. Thornton, J. A. and Penfold, A. S., "Thin Film Processes", Chap. II-2, Vossen, J. L. and Eds, W. Kern, Academic Press, N.Y. 1978.
6. See for example, O.P. Agnihotri and B. K. Gupta, "Solar Selective Surfaces", John Wiley & Sons, Inc. 1981.

TABLE 1

Coating	Indium Tin Oxide
Thickness	50nm
Resistance	300 Ω /□
Resistivity	1.5×10^{-3} Ω cm
Hall Mobility	60 $cm^2 v^{-1} s^{-1}$
Carrier Concentration	7×10^{19} cm^{-3}

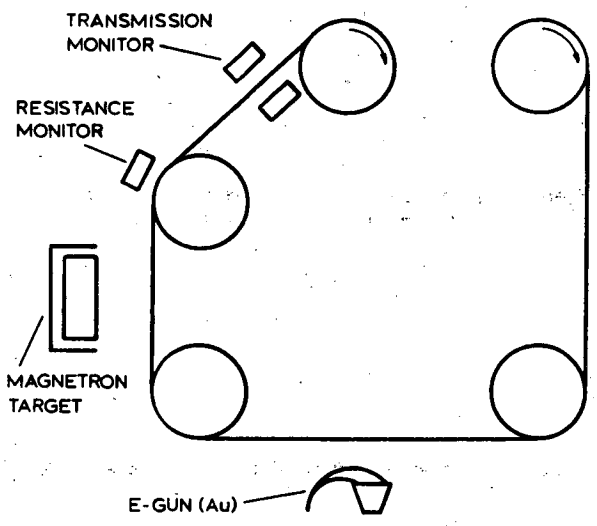

Figure 1
Schematic of Deposition Chamber Fixturing

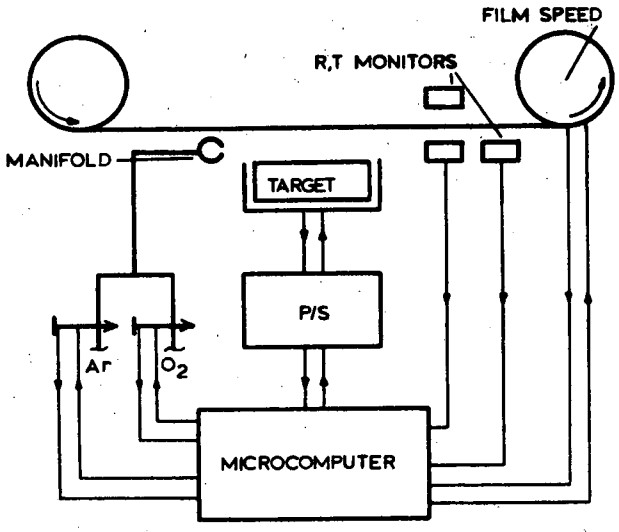

Figure 2
Schematic of Deposition Control Circuitry

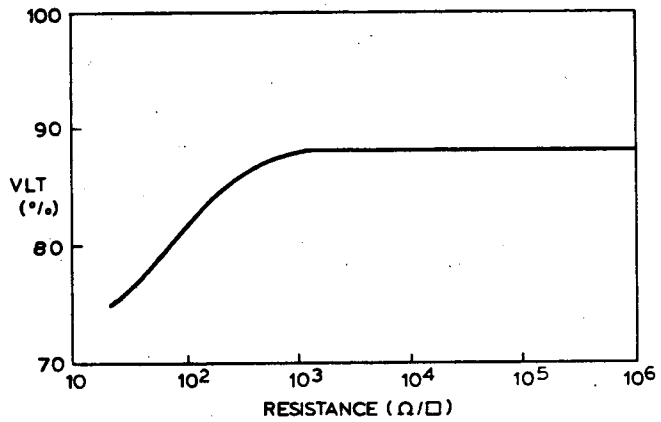

Figure 3
Visible Light Transmittance as a Function of Film Resistance

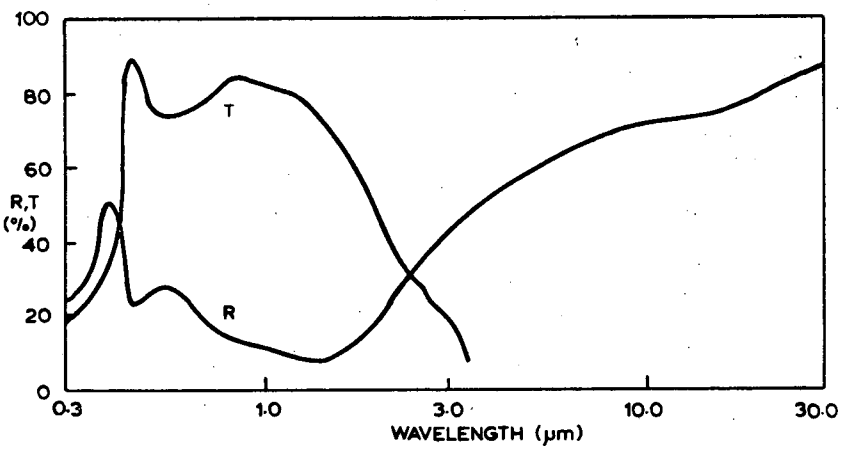

Figure 4
Transmittance and Reflectance of a 20 Ω/□ ITO Coating on Polyester

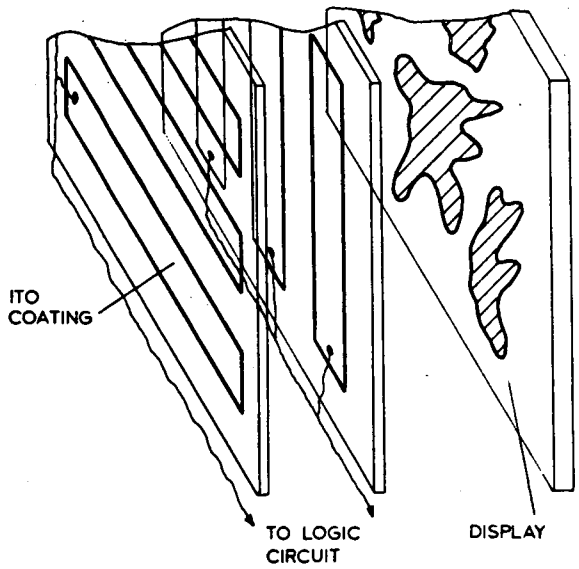

Figure 5
Schematic of a Transparent Membrane Switch

New techniques for roll coating of optical thin film

Martin I. Ridge, Ronald P. Howson, Charles A. Bishop
Department of Physics, University of Technology, Loughborough LE11 3TU, United Kingdom

Abstract

Methods of deposition have been developed which are adapted for the vacuum roll-to-roll coating of plastic with optical thin films. Planar magnetron sputtering and low pressure plasma assisted CVD are shown to be peculiarly fitted for this application. The construction of such an apparatus is described and examples of indium and indium-tin oxide films made by these techniques are given.

Introduction

In recent years it has become apparent that many optical thin film structures are about to be required in large area quantities, particularly in the field of solar energy conversion and conservation. Historically, vacuum aluminising plastic and paper for the packaging markets has been the major outlet for the volume roll-to-roll coating industry and relatively simple technologies have been adequate to meet the design specification laid down by these customers. Many producers of aluminised plastic have, in the last few years, refined their product in order that it might be marketed as a solar control film to reduce the load on air conditioning plant in the summer months and it is apparent that there are several other thin film coatings under intensive development which will have similar large area markets; in particular visually transparent, heat reflecting film for energy conservation in a domestic environment and highly reflecting films for solar furnace plant. These films, especially the former, require much more sophisticated technologies as they are based upon either very closely controlled dielectric and metallic film thicknesses or upon the particular condensate stoichiometries produced by reactive deposition processes. However, for such products to be cost effective in application it is still necessary to produce the coating at a high rate, particularly as the capital cost of such manufacturing plant is so high. For these reasons the conventional evaporation source is replaced by the magnetron sputtering source which is ideally suited for the high rate, well controlled reactive deposition ofmany elemental and metal alloy oxide films.

As an experimental technique, roll-to-roll coating offers the unique facility of continuously monitoring a coated substrate whilst various process parameters are varied. For a balanced dynamic system such as high rate reactive deposition when the oxygen partial pressure or flow rate must be matched against the target sputter yield there is no other technique that allows for rapid optimisation of the process variables. The problem of having to work at the relatively high partial pressures of contaminants associated with vacuum roll-to-roll coating is obviated by the high condensation rates employed, such that the ratio of the rates of arrival of condensate to contaminant species is as high, or higher, than if the system were to be at higher vacuum and the lower growth rates associated with r.f. sputter deposition or ion beam sputtering were used.

Given the commercial interest in coatings hitherto produced on a laboratory scale under high vacuum, low deposition rate condition, and the experimental capability of this apparatus we have designed and built such an equipment, Figure 1.

Experimental

The machine is capable of winding up to 300m of 100 mm wide plastic, usually of 50 um thick polyethylene tetephthalate, ICI Melinex*, at speeds of up to 13m $min.^{-1}$. The drives to each of the three rollers (wind-on (3), wind-off (4) and main drum (2), Figure 1.) are transmitted into the vacuum by ferrofluidic drives and the tension in the film and the speed with which it is passed over the main drum controlled electronically. The plastic is prevented from slipping over the surface of the main drum, resulting in a loss of position index, by pinch rollers (5) and is loaded onto the equipment from the manufacturers cardboard core using a fourth driven roller (1). The water cooled platten (6) upon which the roll-to-roll mechanics are assembled is insulated from the earthed vacuum chamber by a PTFE spacer, to allow an r.f. potential to be applied to the apparatus in order that a second discharge may be struck independently of the magnetron source, thus facilitating the controlled ion bombardment of the substrate - the r.f. ion plating technique. This feature was incorporated to allow for the continuation of our previously reported work[1] which clearly demonstrated the advantageous effects of such an auxiliary discharge when

*Trademark

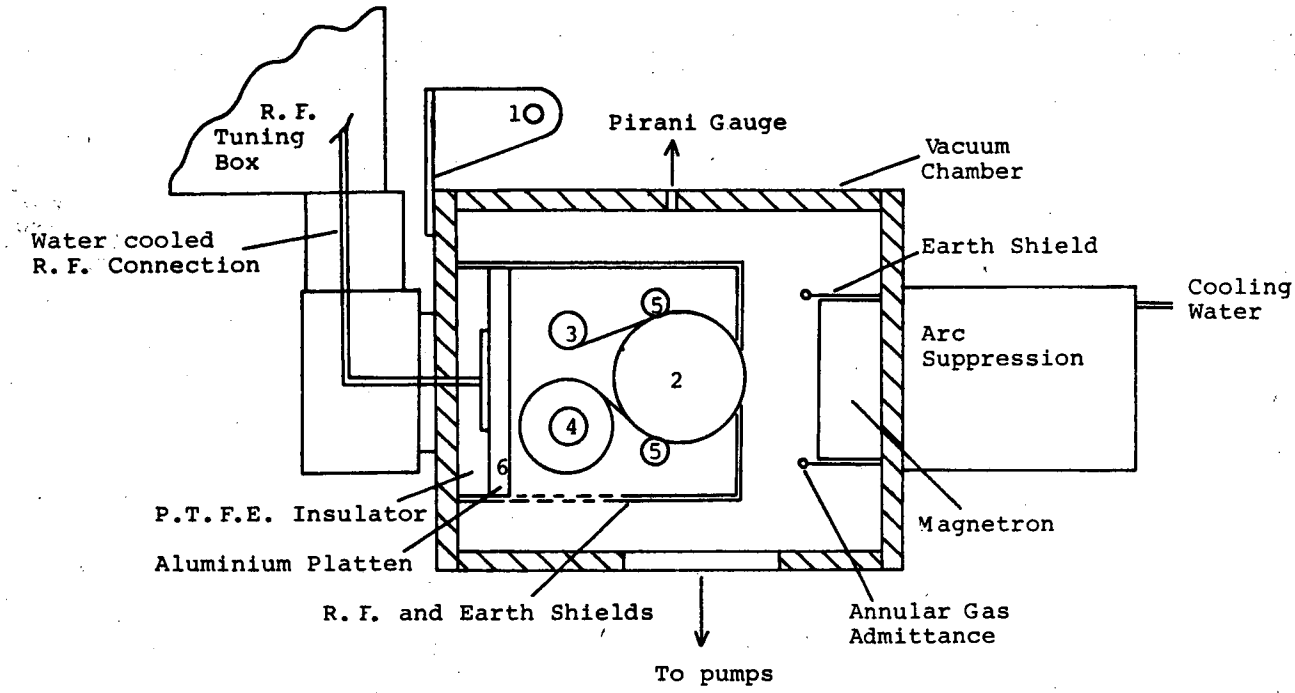

Figure 1: The roll-to-roll coating apparatus detail and vacuum system showing the magnetron source in position

depositing transparent conducting coatings onto glass substrates. In addition we have reported previously work on the low pressure plasma assisted chemical vapour deposition (CVD) of the oxides of Ge, Si, Ti, Sn and In[2] and on the preparation of indium oxide by evaporation, doped with fluorine introduced as CF_4 and decomposed in an r.f. discharge at the substrate[3], all of which took place at room temperatures and consequently lent itself to further investigation upon plastic substrates.

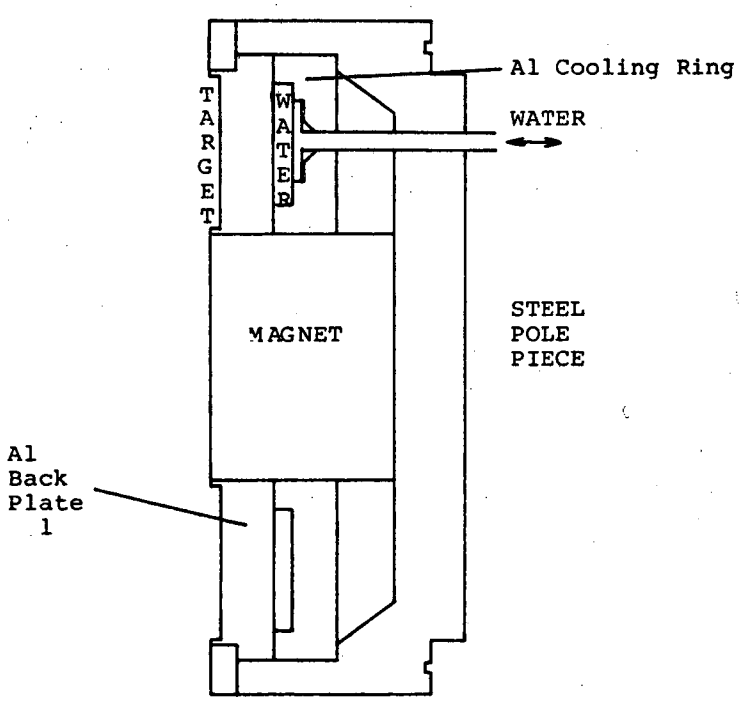

Figure 2: Magnetron source detail.

In order that this discharge could be maintained only in the region where deposition was required to take place, concentric shields were positioned about the roller system; the inner of the two was connected to the rollers and held at the r.f. potential, the outer shield, spaced from the inner such that at all points the distance between the two was less than the dark space corresponding to an r.f. potential of up to 1.5 kW (peak) at 13.56 MHz in a residual gas pressure of up to 10 mTorr, was earthed. Apertures of 60 x 80 mm allowed for condensation of material on the plastic passing over the surface of the main drum facing the magnetron source and simultaneous ion bombardment by the concomitant r.f. discharge. The r.f. potential was generated by a 2 kW 13.56 MHz Plasma Therm HFS200D automatically tuned machine and fed to the roller system by a water cooled connection to the rear of the aluminium platten[6].

The shields were otherwise solid except for a region beneath the wind-off roller (4) where mesh was used to facilitate the pumping of desorbing gases.

The magnetron source is shown schematically in Figure 2 and was designed for the high rate sputtering of low melting point elements and alloys, in particular In, In/Sn and Cd/Sn. The cathode was eroded only in an annular region where the electric and magnetic fields were orthogonal, since gas scattering led to a net deposition on areas of the cathode outside this intense toroidal plasma, and consequently target material was formed into an annular aluminium back plate (1) in Figure 2, to correspond with the dimensions of this region of maximum erosion. By carefully wetting the aluminium surface, indium and indium-tin alloy could be cast into such a mould and a metallurgical bond achieved between the two, thus assuring that there were no thermal boundaries to impede the flow of heat from the target surface to the water cooling behind the aluminium backing plate. In this manner it was possible to sputter with input power densities in the annular erosion region of up to 100 Wcm^{-2} into indium cathodes 7 mm thick, which is approaching an input density limited by the thermal conductivity of the indium cathode material. Due to the magnetic plasma confinement of the magnetron source and the resultant annular erosion profile there is inevitably a non-uniform target utilisation and material wastage. With this cathode roughly 80% by weight of the annular target was used before replacement was necessary and with low melting point elements and alloys this residue was easily recycled. Power of up to 4 kW was supplied to the magnetron from d.c. motor generators and the current electronically regulated to within 0.05%. Typical operating conditions at 5 mT of an Ar/O_2 mixture using an indium cathode were 450 V at 8A. Auger analysis of such films revealed no impurities. Gases were premixed and introduced in an annular fashion about the substrate as shown in Figure 1. Flow rates and total system pressure were automatically regulated by a Vacuum General Type 78-7 system in conjunction with a Consolidated Vacuum Corporation Inc. Type GP.310 Pirani Gauge. With this equipment the system could be maintained to within 0.05% of the desired pressure of between 4 and 5 mT and this corresponded to gas throughputs of around 200 x 10^{-5} Torr $m^3.s^{-1}$ using conventional diffusion and rotary pumps. A separately pumped Edwards High Vacuum EQ50 mass spectrometer was used to continuously monitor the partial pressures within the sputtering chamber and enabled the quantity of reactive gas during, for example, metal oxide deposition to be maintained constant over long periods of time when otherwise time varying desorption from within the chamber (due to thermal drift and altered surface state resulting from coating build-up) would lead to an uncontrolled reaction environment. As our prime interest was in transparent, highly conducting metal and metal alloy oxide films an in situ monitor was installed to give constant readout of the resistance of coated film passing between two contacts.

Results

The equipment has been used to deposit coatings of indium tin oxide and indium oxide. In Figure 3 we show the variation of sheet resistance and magnetron voltage, at constant current, of indium tin oxide films for increasing oxygen mass flow, from the region where the condensateis metallic through to the highly transparent oxides. In this experiment the total system pressure was held constant and the Ar/O_2 ratio of the admitted gas varied. It can be seen that transparent (absorption coefficients 0.2 x 10^6 m^{-1}) conducting (resistivity $10^{-5}\Omega$ m) indium-tin oxide films are obtained only in a very narrow range of oxygen mass flow and that the slope of the curve within this region is extremely high. A similar magnetron voltage behaviour to that described by Schiller et al.[4] when preparing TiO_2 is seen in this region, ascribed to the changing ratio of area of target coated with oxide to area of metallic target. In Figure 4 we show a more detailed plot of results obtained when working only in the region of transparent, conducting deposits, and from the abscissa it is apparent that oxygen partial pressure control to within about 5 x 10^{-5} Torr, or 1% appears to be required in order that films of highest conductivity might be continuously produced. This result is, as reported previously,[5] in good agreement with Fan et al.[6] The hysteresis in Figure 4 for the plots of increasing and decreasing oxygen mass flows is again a consequence of the target surface condition and history and has been examined in detail by Schiller et al.[7] The consequence of applying an r.f. potential is also indicated in Figure 4, where it is seen that a small amount of r.f. power (50W) renders transparent an otherwise opaque metallic deposit. This is a clear demonstration of the 'plasma activation' concept in that the reactivity of the reactive gas and condensate are obviously enhanced. These films, prepared at 3A, 1.2 kW with substrates moving at 0.25 m/min.$^{-1}$ are in the range 50 to 90 nm thick, (corresponding to specific growth rates of up to 400 $nm.min^{-1}$ $kW_{d.c.}^{-1}$) measured using a Gaertner ellipsometer with very careful preparation of the sample rear surface and care in specimen orientation to take into consideration the high degree of birefringence present in the plastic substrates. Very similar results have been obtained with indium oxide deposits and we have deposited films with sheet resistances of less than $25\Omega_{\square}^{-1}$ (resistivities down to 4 x $10^{-6}\Omega$ m) at between 400 and 600 $nm.min^{-1}kW_{d.c.}^{-1}$ having Hall mobilities of up to 45 $cm^2 V^{-1}.s^{-1}$. Such a transparent conductor has an infra-red emissivity at 8 to 14 um of between 0.25 and 0.30 and the application of such heat reflecting film is discussed most fully by Howson et al.

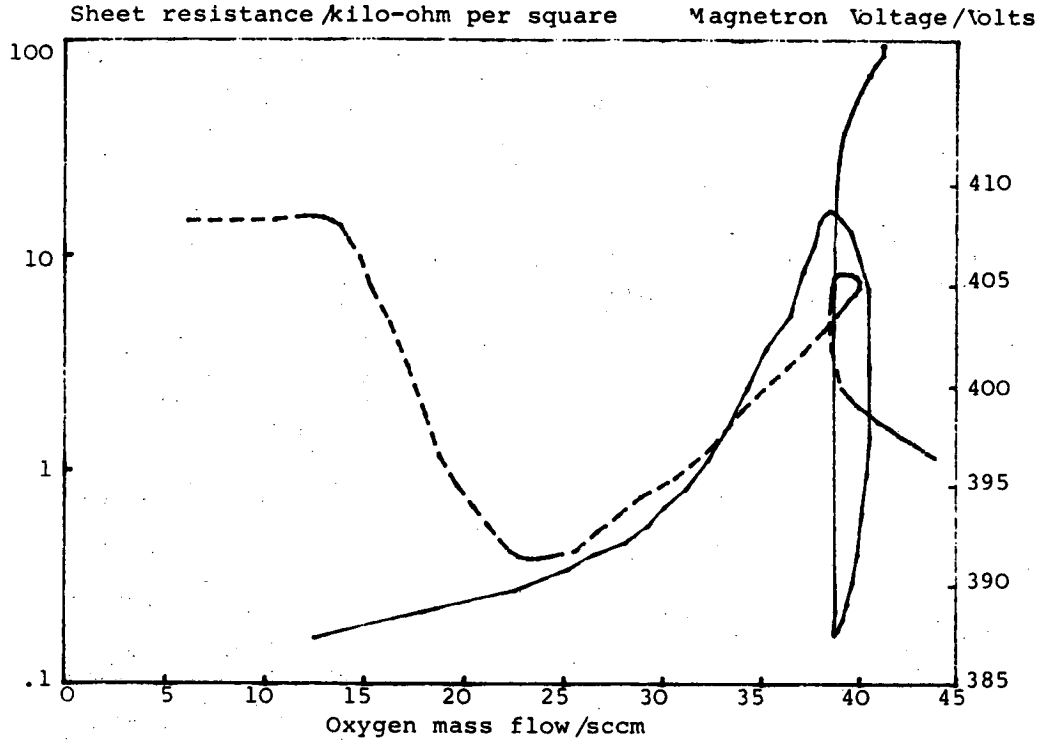

Figure 3:

Sheet resistance and magnetron voltage vs oxygen mass flow rate for an In-10% Sn film prepared with magnetron conditions of 3A, 1.2 kW and 3.5 mTorr at a film speed of 0.25 $m.min^{-1}$ ——— sheet resistance; -------- magnetron voltage.

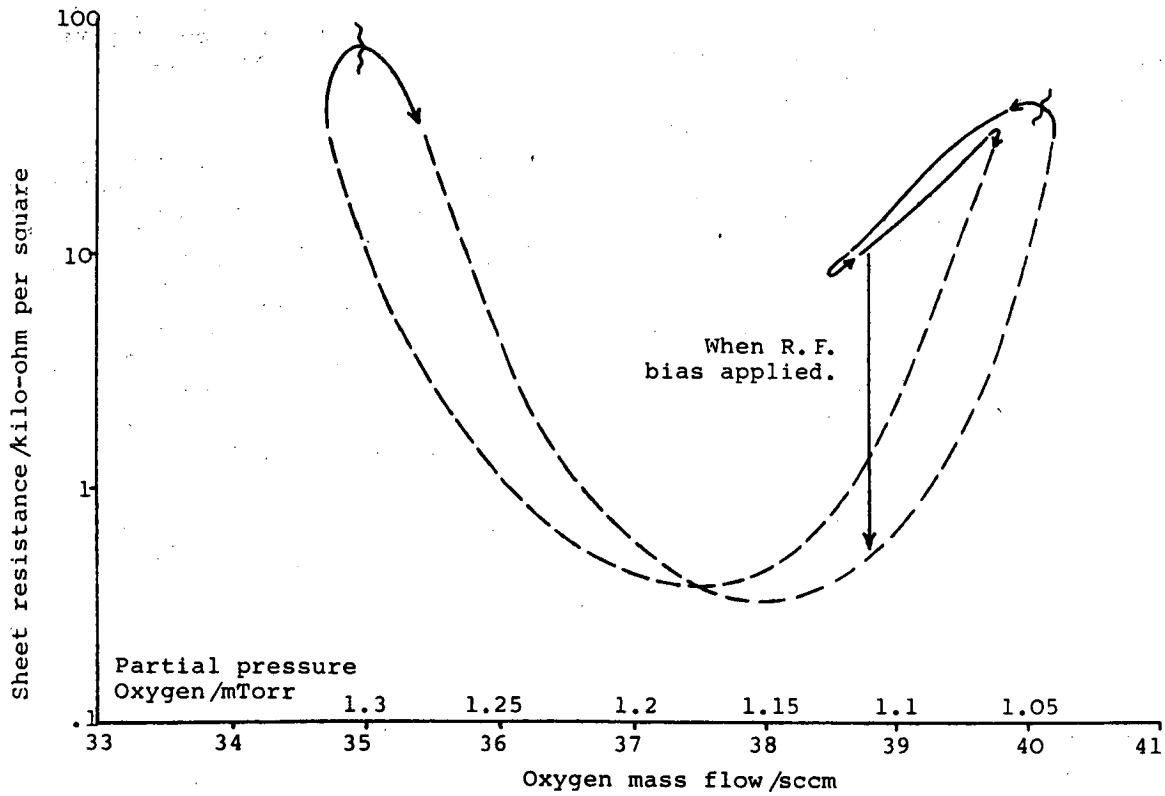

Figure 4: Sheet resistance vs. oxygen mass flow rate for an In-10% Sn film prepared with no r.f. bias with magnetron conditions of 3A, 1.2 kW and 3.5 mTorr and a plastic speed of 0.25 $m.min^{-1}$: -------, oxide; ———, metallic.

in another paper in these proceedings.[8] By increasing the magnetron current to 8A, 3.7 kW such films have been produced at speeds of 0.25 m.min.$^{-1}$; however, at this rate of deposition it was found that the oxygen partial pressure in the system had to be maintained to within about 2.5 x 10^{-5} Torr, or 0.5% for deposits of optimum conductivity. It is interesting to note that at this rate of deposition the consumption of oxygen rose from about 25 scm^{3}min^{-1} without the discharge to about 75 scm^{3}min^{-1} during film growth. By continuously monitoring the sheet resistance and subsequently measuring the resistivity and the emissivity of the sample, the graph shown in Figure 5 was obtained which demonstrates that by controlling the resistance of the film measured in situ we can control the emissivity of the coating, and in general, the lower the measured resistance the lower the emissivity and the higher is the infra-red reflectivity.

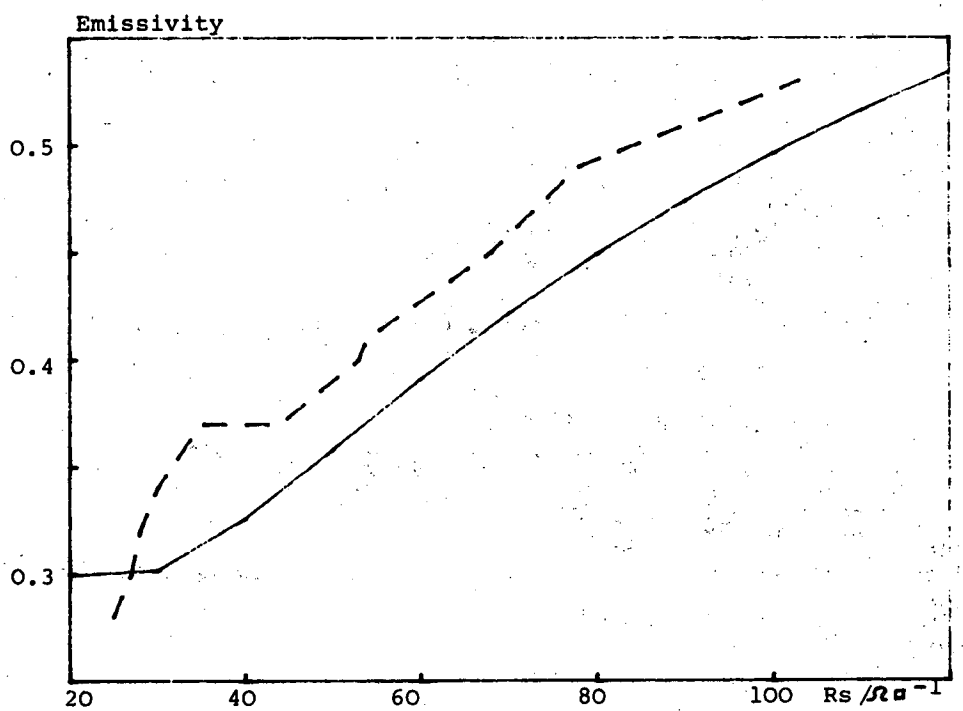

Figure 5: Emissivity of indium oxide films deposited onto 50 um PET substrates at 8A, 3.7 kW as a function of the sheet resistivity; -------- experimental; ——— theoretical (using Hall coefficients taken from a 27Ω□$^{-1}$ film; n = 2.1 x 10^{26}cm^{-3}, u = 30 cm^{2}v^{-1}s^{-1}).

Also on Figure 5 is a computer generated plot based upon the theory of Drude and it can be seen that there is good agreement between the two, bearing in mind the assumption made in this program that the Hall parameters were constant with film thickness, which is almost certainly not the case, and that the data was acquired from a film at the (low emissivity) end of the experimental data, where the two curves cross. (This point is also amplified by Howson et al.[8]).

Conclusion

A roll-to-roll apparatus has been constructed and used to coat moving plastic substrates with transparent conducting heat reflecting films of indium-tin and indium oxides. Using precise control of the various sputtering parameters, continuous production at 0.25 m.min^{-1} from one 3.7 kW magnetron source of transparent film (absorption coefficient 0.2 x 10^6m^{-1}) of high conductivity (4 x 10^{-6}Ωm) having infra-red emissivities of below 0.3 has been achieved. The radio frequency bias has, in accordance with our previous work, been shown to have a significant influence upon the nature of the growing film.

References

1. Howson R.P., Avaritsiotis J.N., Ridge M.I., Bishop C.A.,
Properties of conducting transparent oxide films produced by ion plating onto room temperature substrates.
App. Phys. Lett. 35(2), 15 July, 1979, p. 161.

2. Turner P, Howson R.P., Bishop C.A.,
Optical thin films obtained by plasma-induced chemical vapour deposition (CVD).
Thin Solid Films 83 (1981) 253.

3. Avaritsiotis J.N., Howson R.P.,
Fluorine doping of In_2O_3 film employing ion-plating techniques.
Thin Solid Films 80 (1981) 63.

4. Schiller S, Beister G, Schneider S, Sieber W.
Features of and in situ measurements on absorbing TiO_2 films produced by reactive d.c. magnetron sputtering.
Proceedings of the International Conference on Metallurgical Coatings, San Diego, California, U.S.A. April 21-25 1980, Vol 1, p.475.

5. Ridge M.I., Stenlake M, Howson R.P., Bishop C.A.,
The application of ion-plating to the continuous coating of flexible plastic sheet.
Thin Solid Films 80 (1981) 31.

6. Fan J.C.C.,
Production of Sn-doped In_2O_3 (ITO) film at low deposition temperatures by ion-beam sputtering.
Appl. Phys. Lett., 34(8) 15 April 1979, 515.

7. Schiller S, Heisig V, Steinfelder K, Strumpfel J.,
Using the d.c. magnetron for the reactive deposition of oxides.
Proceedings of the International Conference on Ion Plating and Allied Techniques, London, U.K., July, 1979, p.211.

8. Howson R.P., Ridge M.I.,
Heat mirrors on plastic sheet using transparent oxide conducting coatings.
These proceedings.

TECHNICAL INFORMATION DEPARTMENT
LAWRENCE BERKELEY LABORATORY
UNIVERSITY OF CALIFORNIA
BERKELEY, CALIFORNIA 94720